



National Library
of Canada

Acquisitions and
Bibliographic Services Branch

395 Wellington Street
Ottawa, Ontario
K1A 0N4

Bibliothèque nationale
du Canada

Direction des acquisitions et
des services bibliographiques

395, rue Wellington
Ottawa (Ontario)
K1A 0N4

Your file - Votre référence

Our file - Notre référence

NOTICE

The quality of this microform is heavily dependent upon the quality of the original thesis submitted for microfilming. Every effort has been made to ensure the highest quality of reproduction possible.

If pages are missing, contact the university which granted the degree.

Some pages may have indistinct print especially if the original pages were typed with a poor typewriter ribbon or if the university sent us an inferior photocopy.

Reproduction in full or in part of this microform is governed by the Canadian Copyright Act, R.S.C. 1970, c. C-30, and subsequent amendments.

AVIS

La qualité de cette microforme dépend grandement de la qualité de la thèse soumise au microfilmage. Nous avons tout fait pour assurer une qualité supérieure de reproduction.

S'il manque des pages, veuillez communiquer avec l'université qui a conféré le grade.

La qualité d'impression de certaines pages peut laisser à désirer, surtout si les pages originales ont été dactylographiées à l'aide d'un ruban usé ou si l'université nous a fait parvenir une photocopie de qualité inférieure.

La reproduction, même partielle, de cette microforme est soumise à la Loi canadienne sur le droit d'auteur, SRC 1970, c. C-30, et ses amendements subséquents.

Canada

UNIVERSITY OF ALBERTA

Modeling of Drug Binding and Partitioning in the Liver

by

Tina J. Larson



A thesis submitted to the Faculty of Graduate Studies and Research in partial fulfillment of the requirements for the degree of Master of Science.

DEPARTMENT OF: Chemical Engineering

Edmonton, Alberta

Fall, 1994



National Library
of Canada

Acquisitions and
Bibliographic Services Branch

395 Wellington Street
Ottawa, Ontario
K1A 0N4

Bibliothèque nationale
du Canada

Direction des acquisitions et
des services bibliographiques

395, rue Wellington
Ottawa (Ontario)
K1A 0N4

Your file / Votre référence

Our file / Notre référence

The author has granted an irrevocable non-exclusive licence allowing the National Library of Canada to reproduce, loan, distribute or sell copies of his/her thesis by any means and in any form or format, making this thesis available to interested persons.

L'auteur a accordé une licence irrévocable et non exclusive permettant à la Bibliothèque nationale du Canada de reproduire, prêter, distribuer ou vendre des copies de sa thèse de quelque manière et sous quelque forme que ce soit pour mettre des exemplaires de cette thèse à la disposition des personnes intéressées.

The author retains ownership of the copyright in his/her thesis. Neither the thesis nor substantial extracts from it may be printed or otherwise reproduced without his/her permission.

L'auteur conserve la propriété du droit d'auteur qui protège sa thèse. Ni la thèse ni des extraits substantiels de celle-ci ne doivent être imprimés ou autrement reproduits sans son autorisation.

ISBN 0-315-95065-X

Canada

Name Tina Larson

Dissertation Abstracts International is arranged by broad, general subject categories. Please select the one subject which most nearly describes the content of your dissertation. Enter the corresponding four-digit code in the spaces provided.

Biomedical Engineering

SUBJECT TERM

0541

SUBJECT CODE

U·M·I

Subject Categories

THE HUMANITIES AND SOCIAL SCIENCES

COMMUNICATIONS AND THE ARTS

Architecture 0729
Art History 0377
Cinema 0900
Dance 0378
Fine Arts 0357
Information Science 0723
Journalism 0391
Library Science 0399
Mass Communications 0768
Music 0413
Speech Communication 0459
Theater 0465

EDUCATION

General 0515
Administration 0514
Adult and Continuing 0516
Agricultural 0517
Art 0273
Bilingual and Multicultural 0282
Business 0688
Community College 0275
Curriculum and Instruction 0727
Early Childhood 0518
Elementary 0524
Finance 0277
Guidance and Counseling 0519
Health 0680
Higher 0745
History of 0520
Home Economics 0278
Industrial 0521
Language and Literature 0279
Mathematics 0280
Music 0522
Philosophy of 0998
Physical 0523

Psychology 0525
Reading 0535
Religious 0527
Sciences 0714
Secondary 0533
Social Sciences 0534
Sociology of 0340
Special 0529
Teacher Training 0530
Technology 0710
Tests and Measurements 0288
Vocational 0747

LANGUAGE, LITERATURE AND LINGUISTICS

Language
General 0679
Ancient 0289
Linguistics 0290
Modern 0291
Literature
General 0401
Classical 0294
Comparative 0295
Medieval 0297
Modern 0298
African 0316
American 0591
Asian 0305
Canadian (English) 0352
Canadian (French) 0355
English 0593
Germanic 0311
Latin American 0312
Middle Eastern 0315
Romance 0313
Slavic and East European 0314

PHILOSOPHY, RELIGION AND THEOLOGY

Philosophy 0422
Religion
General 0318
Biblical Studies 0321
Clergy 0319
History of 0320
Philosophy of 0322
Theology 0469

SOCIAL SCIENCES

American Studies 0323
Anthropology
Archaeology 0324
Cultural 0326
Physical 0327
Business Administration
General 0310
Accounting 0272
Banking 0770
Management 0454
Marketing 0338
Canadian Studies 0385
Economics
General 0501
Agricultural 0503
Commerce-Business 0505
Finance 0508
History 0509
Labor 0510
Theory 0511
Folklore 0358
Geography 0366
Gerontology 0351
History
General 0578

Ancient 0579
Medieval 0581
Modern 0582
Black 0328
African 0331
Asia, Australia and Oceania 0332
Canadian 0334
European 0335
Latin American 0336
Middle Eastern 0333
United States 0337
History of Science 0585
Law 0398
Political Science
General 0615
International Law and Relations 0616
Public Administration 0617
Recreation 0814
Social Work 0452
Sociology
General 0626
Criminology and Penology 0627
Demography 0938
Ethnic and Racial Studies 0631
Individual and Family Studies 0628
Industrial and Labor Relations 0629
Public and Social Welfare 0630
Social Structure and Development 0700
Theory and Methods 0344
Transportation 0709
Urban and Regional Planning 0999
Women's Studies 0453

THE SCIENCES AND ENGINEERING

BIOLOGICAL SCIENCES

Agriculture
General 0473
Agronomy 0285
Animal Culture and Nutrition 0475
Animal Pathology 0476
Food Science and Technology 0359
Forestry and Wildlife 0478
Plant Culture 0479
Plant Pathology 0480
Plant Physiology 0817
Range Management 0777
Wood Technology 0746

Biology

General 0306
Anatomy 0287
Biostatistics 0308
Botany 0309
Cell 0379
Ecology 0329
Entomology 0353
Genetics 0369
Limnology 0793
Microbiology 0410
Molecular 0307
Neuroscience 0317
Oceanography 0416
Physiology 0433
Radiation 0821
Veterinary Science 0778
Zoology 0472

Biophysics
General 0786
Medical 0760

EARTH SCIENCES

Biogeochemistry 0425
Geochemistry 0996

Geodesy 0370
Geology 0372
Geophysics 0373
Hydrology 0388
Mineralogy 0411
Paleobotany 0345
Paleoecology 0426
Paleontology 0418
Paleozoology 0985
Palynology 0427
Physical Geography 0368
Physical Oceanography 0415

HEALTH AND ENVIRONMENTAL SCIENCES

Environmental Sciences 0768
Health Sciences
General 0566
Audiology 0300
Chemotherapy 0992
Dentistry 0567
Education 0350
Hospital Management 0769
Human Development 0758
Immunology 0982
Medicine and Surgery 0564
Mental Health 0347
Nursing 0569
Nutrition 0570
Obstetrics and Gynecology 0380
Occupational Health and Therapy 0354
Ophthalmology 0381
Pathology 0571
Pharmacology 0419
Pharmacy 0572
Physical Therapy 0382
Public Health 0573
Radiology 0574
Recreation 0575

Speech Pathology 0460
Toxicology 0383
Home Economics 0386

PHYSICAL SCIENCES

Pure Sciences

Chemistry
General 0485
Agricultural 0749
Analytical 0486
Biochemistry 0487
Inorganic 0488
Nuclear 0738
Organic 0490
Pharmaceutical 0491
Physical 0494
Polymer 0495
Radiation 0754
Mathematics 0405
Physics
General 0605
Acoustics 0986
Astronomy and Astrophysics 0606
Atmospheric Science 0608
Atomic 0748
Electronics and Electricity 0607
Elementary Particles and High Energy 0798
Fluid and Plasma 0759
Molecular 0609
Nuclear 0610
Optics 0752
Radiation 0756
Solid State 0611
Statistics 0463

Applied Sciences

Applied Mechanics 0346
Computer Science 0984

Engineering

General 0537
Aerospace 0538
Agricultural 0539
Automotive 0540
Biomedical 0541
Chemical 0542
Civil 0543
Electronics and Electrical 0544
Heat and Thermodynamics 0348
Hydraulic 0545
Industrial 0546
Marine 0547
Materials Science 0794
Mechanical 0548
Metallurgy 0743
Mining 0551
Nuclear 0552
Packaging 0549
Petroleum 0765
Sanitary and Municipal 0554
System Science 0790
Geotechnology 0428
Operations Research 0796
Plastics Technology 0795
Textile Technology 0994

PSYCHOLOGY

General 0621
Behavioral 0384
Clinical 0622
Developmental 0620
Experimental 0623
Industrial 0624
Personality 0625
Physiological 0989
Psychobiology 0349
Psychometrics 0632
Social 0451



UNIVERSITY OF ALBERTA

RELEASE FORM

NAME OF AUTHOR: Tina J. Larson

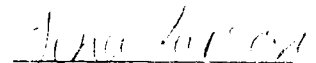
TITLE OF THESIS: Modeling of Drug Binding and Partitioning in the Liver

DEGREE: Master of Science

YEAR THIS DEGREE WAS GRANTED: 1994

Permission is hereby granted to the University of Alberta Library to reproduce single copies of this thesis and to lend or sell such copies for private, scholarly or scientific research purposes only.

The author reserves all other publication and other rights in association with the copyright in the thesis, and except as hereinbefore provided neither the thesis nor any substantial portion thereof may be printed or otherwise reproduced in any material form whatever without the author's prior written permission.



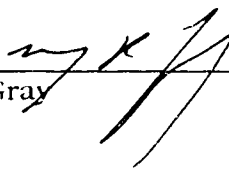
Tina Larson
9409-64 Ave.
Grande Prairie, AB
T8W 1B4

Date: Oct 7 1994

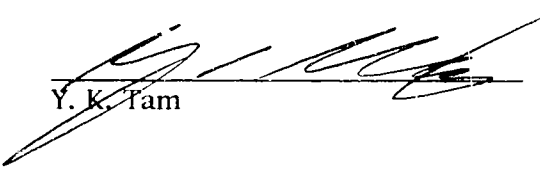
UNIVERSITY OF ALBERTA

FACULTY OF GRADUATE STUDIES AND RESEARCH

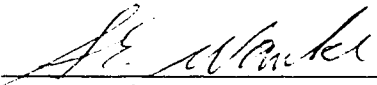
The undersigned certify that they have read, and recommend to the Faculty of Graduate Studies and Research for acceptance, a thesis entitled Modeling of Drug Binding and Partitioning in the Liver submitted by Tina J. Larson in partial fulfillment of the requirements for the degree of Master of Science.



M. R. Gray



Y. K. Tam



S. E. Wanke

Oct 7, 1974

ABSTRACT

Rat livers were utilized in this study to obtain experimental data on the metabolism of diltiazem. This highly lipophilic heart drug was perfused in isolated rat livers at concentrations ranging from 0.663 to 51.16 μM . This data along with data obtained by Hussain et al. (1984) was used to construct a mathematical model to describe the importance of binding and partitioning of diltiazem in the liver.

The data obtained was best described qualitatively by a three compartment model. The first compartment represents the sinusoids and the flow of material through the vasculature of the liver. The second and third compartments are in parallel to each other and represent the partitioning and binding of drug to liver tissues respectively. The partitioning of the drug was considered a linear phenomenon. Binding, however, requires a specific binding site, most likely a liver protein, and was best described by a Langmuir adsorption model.

Computer simulations of the mathematical model were completed using Matlab (1993) to determine optimized parameters to describe each experiment. The estimated partition coefficients for diltiazem and metabolites ranged from 95.27 to 463.5 and 1.466 to 28.81 respectively. These values show the lipophilic properties of the drug and metabolites as well as the increased polarity of the metabolites. The metabolic rate constant ranged from 0.1198 to 52.38 min^{-1} and was generally inversely dependent on diltiazem inlet concentration. The metabolic rate constant was much lower than the partition rate constants in the range of 30 to 50 μM inlet diltiazem concentration, indicating that metabolism was the rate limiting step in drug elimination. The estimated

number of binding sites in the liver ranged from 57.62 to 309.7 $\mu\text{mol/g}$ liver confirming that the number of binding sites was very large.

The model was successful at describing the experimental data except at early influx times. This is due to the estimation of the metabolic rate as a constant. The model thus over-predicts the diltiazem concentration profile when minor pathways have not yet been saturated and the metabolic rate is dramatically underestimated.

ACKNOWLEDGEMENTS

I would like to thank everyone who has helped me to achieve the almost impossible goal of completing this thesis and obtaining the M.Sc. degree. Without the love and support of those who were important in my life this goal would never have been accomplished.

THANKS!!

To Soheir: Your help in the lab was invaluable to completing my research! THANKS!

To Dr. Tam: For the essential pharmaceutical and physiological knowledge and background. THANKS!

To the Pharmacokinetics Research Group: For the friendship, support, knowledge, and understanding. Your determination in research is contagious. THANKS!

To Dr. Gray: For the guidance and support that was always available. Your insight was amazing and your support never failing. THANKS!

To the Chemical Engineering Students: For the friendship, support, and empathy. Your camaraderie will be sorely missed. THANKS!

To my family: For always being my background support system when times were tough. Your enormous support and love is never failing. THANKS!

To Brad: For putting up with me and being there when I needed you. You have encouraged me to always achieve my goals and gave me a shoulder to cry on. THANKS!

TABLE OF CONTENTS

Chapter		Page
1	INTRODUCTION	1
2	LITERATURE REVIEW	3
	2.1 Basic Liver Physiology and Drug Metabolism	3
	2.2 Properties and Metabolic Pathways of Diltiazem	9
	2.3 Liver Models	13
	2.4 Liver Models for Drug Binding and Partitioning	21
3	EXPERIMENTAL METHODS AND MATERIALS	26
	3.1 Liver Perfusion	26
	3.2 HPLC Analysis	27
	3.3 Radioisotope Analysis	31
4	RESULTS AND DISCUSSION	33
	4.1 Qualitative Features of Diltiazem Modeling	33
	4.2 Development of Model Equations	45
	4.3 Numerical Methods	50
	4.4 Simulation Results	51
5	CONCLUSIONS AND FURTHER WORK	56
6	REFERENCES	58
	Appendix A - Experimental Data	60
	Appendix B - HPLC Standard Curves	62
	Appendix C - Experimental Concentration Data	68
	Appendix D - Matlab m-files	89
	Appendix E - Simulation Results	94

LIST OF TABLES

	Page
Table 3.1 Typical HPLC retention times.	28
Table 3.2 Results of tracer purity test.	31
Table 4.1 Conventional pharmacokinetic parameters.	36
Table 4.2 Sum of squared residuals.	53
Table 4.3 Three compartment optimization parameters.	53
Table 4.4 Three compartment optimization parameters for total measured metabolites.	54
Table 4.5 Three compartment optimization parameters for binding.	54

LIST OF FIGURES

	Page
Figure 2.1 Schematic diagram of the gastrointestinal system and liver adapted from Shargel et al. (1993).	6
Figure 2.2 Schematic diagram of liver structure adapted from Saville et al. (1992b).	7
Figure 2.3 Representation of the network of blood vessels and sinusoids in the liver based on a micrograph of a polymer cast of the liver by Motta et al. (1978). The black areas are tissue and the remainder is sinusoids. PVb is the portal vein and HAb is the hepatic artery.	8
Figure 2.4 Proposed metabolic pathways of diltiazem in humans taken from Hussain et al. (1992). (MA = <i>N</i> -demethyldiltiazem, M1 = deacetyldiltiazem, M2 = <i>N</i> -demethyldeacetyldiltiazem, M4 = <i>O</i> -demethyldeacetyldiltiazem, M6 = <i>N,O</i> -didemethyldeacetyldiltiazem, M1-NO = deacetyldiltiazem <i>N</i> -oxide, M4-NO = <i>O</i> -demethyldiltiazem <i>N</i> -oxide)	12
Figure 2.5 Schematic diagram of the nonparametric models adapted from Levenspiel (1972).	15
Figure 2.6 Schematic diagram of the homogeneous models adapted from Fogler (1992).	17
Figure 2.7 Schematic diagrams of the heterogeneous models adapted from Saville et al. (1992b).	19
Figure 2.8 Compartmental model for binding and transport proposed by Weisiger (1985).	23
Figure 3.1 Typical chromatogram of a sample containing internal standard and 1500 ng/mL of diltiazem and its metabolites.	29
Figure 3.2 Typical standard curve for diltiazem. The coefficient of determination, $r^2=0.9954$. The calibration equation was calculated to be: DZ concentration = $34.45 + 4132 * \frac{\text{Peak Response}}{\text{Internal Standard Area}}$	30
Figure 3.3 Radiolabelled diltiazem, cis-(+)-[<i>N</i> -methyl- ^3H]-. (* = tritium label)	32

	Page
Figure 4.1 Outlet concentration of diltiazem and five of its metabolites for Rat #7 obtained by infusing 37.71 μ M diltiazem for 60 minutes followed by a 60 minute washout period.	34
Figure 4.2 Outlet concentration of diltiazem, DZ, total measured metabolites, M, and total radioactive species, H3, for Rat #7 obtained by infusing 37.71 μ M diltiazem with a radiolabelled tracer for 60 minutes followed by a 60 minute washout period. The total radioactive species concentration was obtained by a scintillation counter whereas the diltiazem and metabolite concentrations were obtained by HPLC.	35
Figure 4.3 Typical diltiazem concentration profile from a perfused rat liver describing the phases of diltiazem metabolism.	38
Figure 4.4 Time to reach steady state vs. diltiazem outlet concentration. Experimental data taken from Hussain et al. (1994).	40
Figure 4.5 Normalized washout profiles of six different radioactive experiments.	41
Figure 4.6 Schematic diagram depicting a simplified hepatocyte.	43
Figure 4.7 Schematic diagram of a three compartment model for diltiazem metabolism.	44
Figure 4.8 Compartmental model of Langmuir adsorption model.	46
Figure 4.9 Three compartment model proposed for diltiazem metabolism.	48
Figure 4.10 Experimental (x) and simulated (—) concentration profiles for diltiazem and experimental (*) and simulated (- -) concentration profiles for total metabolites in the effluent of an isolated liver from Rat #7 with inlet diltiazem concentration of 37.71 μ M.	52

NOMENCLATURE

SYMBOL	DEFINITION
A	albumin concentration in the blood
C	concentration
C_1	concentration in the sinusoids
$C_{1,DZ}$	concentration of diltiazem in the sinusoids
$C_{1,M}$	concentration of metabolites in the sinusoids
$C_{1,DZ,sim}$	simulated concentration of diltiazem in the sinusoids
$C_{1,M,sim}$	simulated concentration of metabolites in the sinusoids
$C_{2,DZ}$	concentration of diltiazem in the tissues
$C_{2,M}$	concentration of metabolites in the tissues
C_2, C_{Ct}, C_t	concentration in the liver tissue
$C_{DZ,exp}$	experimental concentration of diltiazem in the sinusoids
$C_{M,exp}$	experimental concentration of metabolites in the sinusoids
$C_{out,ss}$	steady state outlet concentration
C_{in}	inlet concentration
Cl	clearance
Cl_h	hepatic clearance
C_{si}	unbound drug concentration in the sinusoids
$C_{i,s}$	concentration at the interface between the tissue and the sinusoids
D_{IX}	axial diffusion coefficient
D_{IR}	radial diffusion coefficient
E_{ss}	steady state extraction ratio
i	compartment number
I.D.	internal diameter

SYMBOL	DEFINITION
k_1, k_{12}	rate constant for cellular uptake
k_2, k_{21}	rate constant for cellular release
$k_{12,DZ}$	rate constant for cellular uptake of diltiazem
$k_{21,DZ}$	rate constant for cellular release of diltiazem
$k_{12,M}$	rate constant for cellular uptake of metabolites
$k_{21,M}$	rate constant for cellular release of metabolites
k_3, k_m	rate constant for metabolism
$k_{m,DZ}$	rate constant for metabolism of diltiazem
$k_{f,M}$	rate constant of formation of metabolites
k_b, k_{13}	rate constant for binding
k_{dis}, k_{31}	rate constant for dissociation of binding complex
K_p	partition coefficient
$K_{p,DZ}$	partition coefficient for diltiazem
$K_{p,M}$	partition coefficient for metabolites
k_R	kinetic rate constant for reaction
l	axial length of the liver
n, n_3	number of filled binding sites
$n_{3,DZ}$	number of binding sites filled with diltiazem
$n_{3,M}$	number of filled binding sites filled with metabolites
N	number of compartments
N	number of experimental data points
n_{sat}, n_3^{sat}	total number of binding sites available
P	tissue permeability
Q	volumetric flow rate
r	radial distance

SYMBOL	DEFINITION
r_c	radius of the capillary or sinusoid
R_j	rate of reaction of component j
SSR	sum of squared residuals
SSR_{TOT}	total sum of squared residuals
SSR_{DZ}	sum of squared residuals for diltiazem simulation
SSR_M	sum of squared residuals for metabolite simulation
t	time
t_{ss}	time to steady state
u	flow velocity through the sinusoids
V_1, V_{SI}	volume of the sinusoids
V_2, V_{CI}	volume of the liver tissue
V_d	volume of distribution
V_i	volume of compartment i
V_L	total volume of the liver
x	axial distance

GREEK SYMBOLS

ν_L	mixing parameter
---------	------------------

GLOSSARY

agina: spasmodic, choking or suffocating pain. Used almost exclusively to denote angina pectoris (Dorland's Med. Dict., 1982).

agina pectoris: paroxysmal pain in the chest, usually due to interference with the supply of oxygen to the heart muscle (Dorland's Med. Dict., 1982).

clearance: a measure of drug elimination from the body in terms of volume of body fluid cleared of drug per unit time (Shargel et al., 1993).

conduction cell (of the heart): cells which carry the electrical impulses causing contraction of the muscle cells. These cells are also part of the pacemaker system of the heart (DeCoursey, 1974).

coronary: of or relating to the heart or its blood vessels (New Merriam-Webster Dict., 1989).

elimination: the irreversible removal of drug from the body by all routes of elimination. The two major routes of elimination are excretion, mainly through urine, and metabolism, mainly through hepatic enzymatic reactions (Shargel et al., 1993).

extraction ratio: the amount of drug removed from the blood as a fraction of the inlet drug concentration.

hepatic clearance: the volume of body fluid cleared of drug by the liver per unit time (Shargel et al., 1993).

hypertension: persistently high arterial blood pressure (Dorland's Med. Dict., 1982).

myocardial cells: muscle cells of the heart.

pharmacokinetics: the kinetic study of drug metabolism including drug absorption, distribution, and elimination (Shargel et al., 1993).

sacroplasmic reticulum: a network of channels within the muscle fiber which regulates the calcium ion concentration surrounding the contractile fibers of the muscle (Stryer, 1988).

smooth muscle cells: muscles that are involved with organs of the body which contract involuntarily, i.e. intestinal walls (DeCoursey, 1974).

supraventricular: situated or occurring above the ventricles, especially in an atrium or atrioventricular node (Dorland's Med. Dict., 1982).

tachycardia: abnormally rapid heart rate (Dorland's Med. Dict., 1982).

vascular: referring to many blood vessels (DeCoursey, 1974).

volume of distribution: a factor that must be taken into account in estimating the amount of drug in the body from the concentration of drug found in the sampling compartment. The volume of distribution can also be considered as the apparent volume in which the drug is dissolved. It does not have a true physiologic meaning in terms of an anatomic space (Shargel et al., 1993).

CHAPTER 1 - INTRODUCTION

The liver is the primary site in the body for metabolism of many drugs. Chemical reactor models can be applied to the liver to describe mathematically the physiological processes which are occurring. The basic processes involved in drug metabolism include flow through the liver capillary network, mass transfer between the capillaries and liver tissue, enzyme reactions within the liver cells, and binding of drug to proteins in the blood and liver tissue.

The drug of interest in this study is diltiazem, which is often used in the treatment of heart patients. This drug is lipophilic and is rapidly eliminated from the blood by the liver. Due to the lipophilicity of the drug, it is known to partition from the blood into the lipid bilayer of the liver cells quite readily (Saville et al., 1992a). It was suggested by Hussain et al. (1994) that this process is complicated by tight nonlinear protein binding of the drug and metabolites to liver tissues. A model for the metabolism of diltiazem is desired to fully understand the mechanisms involved. This model must account for the most important processes involved: lipid partitioning, enzyme reaction, and protein binding to liver tissue. In this study a three compartment model is proposed to describe the concentration profile of diltiazem and its metabolites in the liver.

Rat livers were used to collect experimental data on diltiazem metabolism. The livers were surgically removed and connected to a perfusion system to simulate physiological conditions in the rat. Diltiazem was perfused until steady state conditions were achieved. The drug perfusion was then stopped and the liver washed until all drug and metabolites were removed.

The time-dependent kinetics of diltiazem in an isolated rat liver was

investigated by Hussain et al. (1994). These results as well as the experimental results obtained in this study will be utilized to develop a mathematical model for diltiazem metabolism. The proposed model must be consistent with the known properties of diltiazem and with hepatic physiology and have the ability to describe the experimental data. Due to the large interindividual variation observed with the pharmacokinetic parameters diltiazem (Chaffman et al., 1985, Hermann et al., 1985) it is difficult to obtain results that are consistent for describing its metabolism. However, a model that describes the data will provide insight to the mechanisms involved.

CHAPTER 2 - LITERATURE SURVEY

The liver is the primary organ in the body for metabolism of drugs. This is accomplished by the following series of steps:

1. Drug enters the liver through the net flow of blood into the vascular network.
2. The drug is taken up from the vascular network into the liver cells.
3. Drug is eliminated by enzyme-mediated reactions within the liver cells.
4. Metabolic products and unconverted substrate are released from the liver cells back into the blood stream.
5. The drug or metabolites may bind to proteins in the blood or liver tissue.

The major purpose of a liver model is to predict the liver outlet concentration in response to transient changes in drug concentration, blood flow, and metabolic activity. This is accomplished by mathematically describing each step of the drug elimination and accounting for the dominant physiology and physical processes that are occurring. A model can then provide insight into the nature and function of the liver.

2.1 Basic Liver Physiology and Drug Metabolism

The liver is an extremely complex and important organ in the body. It has five major functions in the human body (Decoursey, 1974):

1. Removal of blood degradation products which consist of worn out red blood cells and foreign solid materials.

2. Manufacturing plasma proteins and blood clotting factors for the circulatory system.
3. Producing bile acids to aid in digestion of fats.
4. Storage and regulation of glucose levels in the blood.
5. Detoxifying endogenous and exogenous poisons in the blood by metabolism or conjugation.

The last function listed above is the function of interest in pharmacokinetics. The liver interacts with a drug in the blood in the same way as a toxin and attempts to eliminate it from circulation through enzymatic reactions.

The enzyme reactions, or biotransformations, of drugs which occur in the liver can be divided into two major types of reactions, phase I and phase II reactions (Shargel et al., 1993). Most biotransformations usually result in a metabolite which is more polar than the parent drug. This allows the compound to be eliminated from the body more quickly than the parent drug. Phase I reactions are known as asynthetic reactions which introduce or expose a functional group on the drug compound. These reactions usually occur first and include oxidation, reduction, or hydrolysis of the parent drug. Phase II reactions follow phase I reactions and are conjugation reactions which use conjugating reagents. These reagents are derived from compounds involved in protein, carbohydrate, and fat metabolism. In the presence of the appropriate transferase enzyme, these reagents are combined with the drug to give metabolites such as sulfates and glucuronides. Liver enzyme reactions constitute the major route of drug transformation in the body leading to excretion through the kidneys.

The liver consists of a large right and left lobe that merge in the middle. It is located in the blood circulation path between the gastrointestinal tract and spleen and the inferior vena cava leading to the heart as illustrated in

Figure 2.1. The liver is highly perfused, receiving blood from both the hepatic artery and hepatic portal vein. The hepatic artery supplies approximately 25% of the blood, but carries approximately 80% of the oxygen supply. The large hepatic portal vein collects blood from various segments of the gastrointestinal tract and supplies the remaining 75% of the blood and many required nutrients to the liver (Shargel et al., 1993). The terminal branches of the hepatic artery and the portal vein fuse within the liver and mix within smaller blood vessels known as sinusoids as shown schematically in Figure 2.2. The blood leaves the liver by the hepatic artery which empties into the inferior vena cava. The liver also secretes bile acids within the lobes that flow through a network of channels eventually emptying into a common bile duct and stored in the gall bladder.

The cells which make up the liver tissues are called hepatocytes or parenchymal cells. A mono-layer of these cells are present for each sinusoid. The main liver enzymes for drug transformation are located in these cells and thus is where most drug metabolism occurs. Endothelial cells line the sinusoids and contain fenestrae of various sizes. These fenestrae allow only dissolved substances to pass through to the endothelial space of Disse before entering the hepatocytes (Saville et al., 1992). Kupffer cells are also found within the sinusoids and are responsible for engulfing worn out red blood cells and foreign solid material in the circulatory system (Shargel et al., 1993). The blood vessels of the liver comprise approximately 15% of the total liver volume and the remaining 85% is primarily liver tissue (Shargel et al., 1993). The bile ducts are less than 1 to 2% of the total liver volume and are usually included in the cellular portion of the liver.

Figure 2.3 illustrates that the liver is a continuous network of highly interconnected blood vessels. It is very unlikely that blood will pass directly

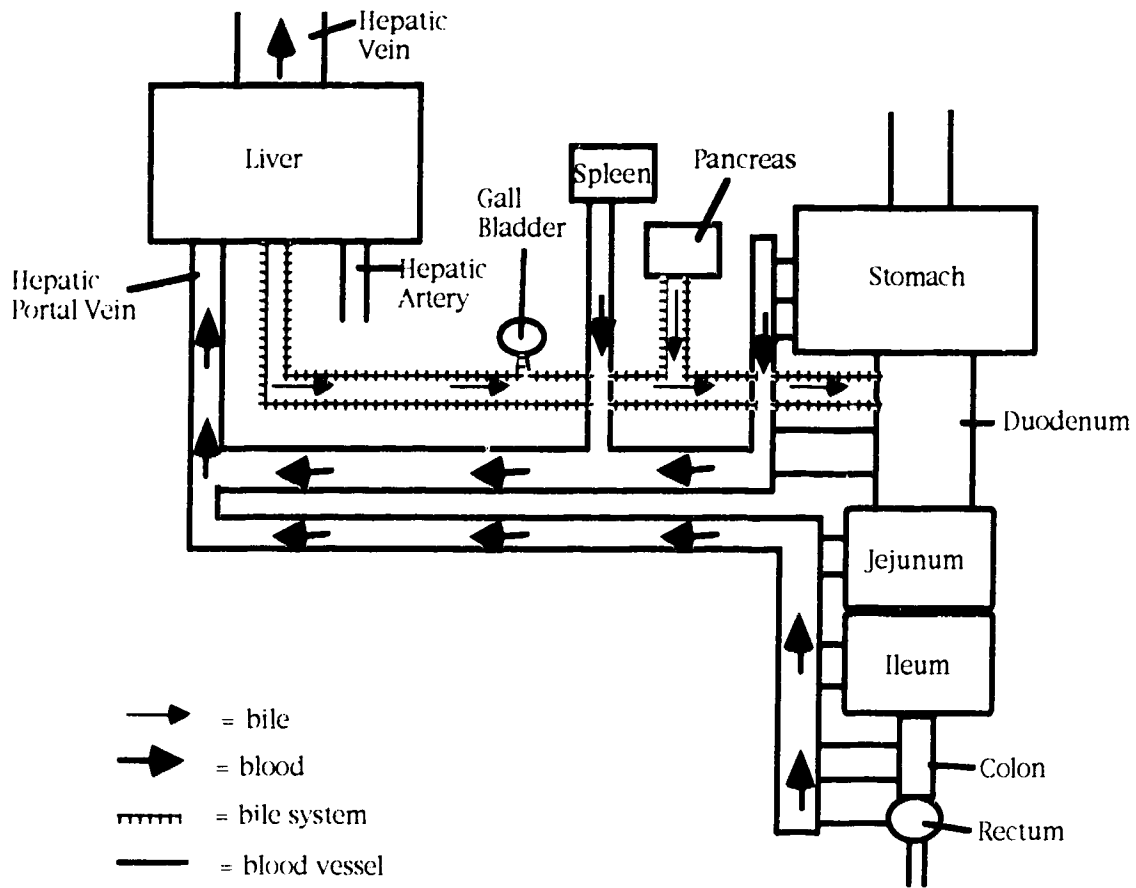


Figure 2.1 Schematic diagram of the gastrointestinal system and liver adapted from Shargel et al. (1993).

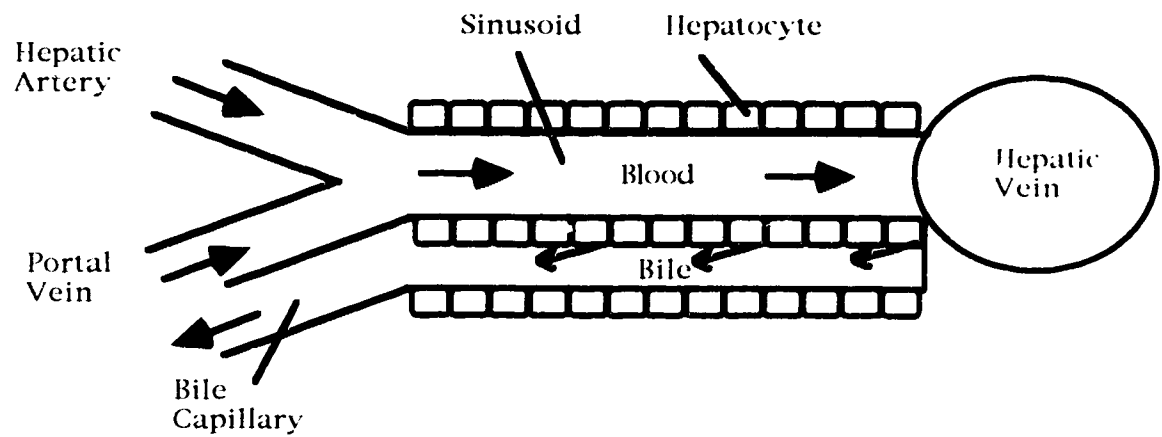


Figure 2.2 Schematic diagram of liver structure adapted from Saville et al. (1992b).

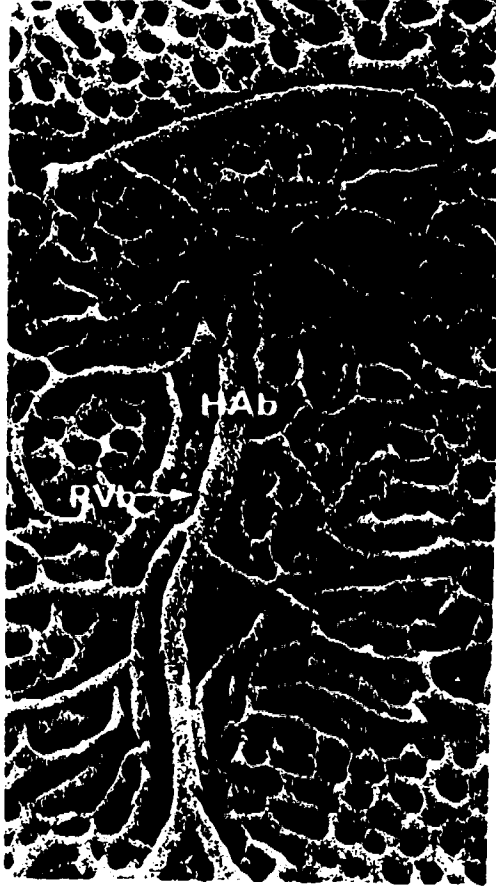


Figure 2.3 Representation of the network of blood vessels and sinusoids in the liver based on a micrograph of a polymer cast of the liver by Motta et al. (1978). The black areas are tissue and the remainder is sinusoids. PVb is the portal vein and HAb is the hepatic artery.

from the inlet to outlet or follow a simple or predictable path. Numerous fluid flow studies in the liver have been reviewed by Saville et al. (1992b). From this review four conclusions were made:

1. Flow reversal within a sinusoid has been observed.
2. Adjacent sinusoids may have counter current flow.
3. Transient back flow into adjacent sinusoids can occur.
4. A volume of blood may follow any path through the liver depending only upon the local pressure gradients that exist at that moment.

Therefore, the blood distribution in the liver changes from moment to moment and mixing is quite extensive. Due to the time-dependent distribution of blood flow in the organ, it is apparent that a complete model to describe the flow in the vasculature of the liver is extremely complex. Thus a time and spatially averaged model is more appropriate to describe the flow of blood.

2.2 Properties and Metabolic Pathways of Diltiazem

Diltiazem belongs to a very important class of cardiovascular drugs known as calcium channel blocking agents. These drugs inhibit the transmembrane influx of calcium ions in myocardial and vascular smooth muscle cells (AHFS Drug Info., 1991). Calcium ions are important in the excitation-contraction coupling processes in these muscle cells (Chaffman et al., 1985) and the discharge of electrical pulses in the specialized conduction cells of the heart (AHFS Drug Info., 1991). The membranes of these cells contain channels that are selective for calcium ions and carry a slow inward current. It is thought that diltiazem inhibits the ion-control gating mechanism of these channels and/or interferes with the release of calcium from its storage in the sarcoplasmic reticulum (AHFS Drug Info., 1991).

Diltiazem is therefore able to inhibit the contractile processes of myocardial and vascular smooth muscle cells. This physiological action is useful in the treatment of many different cardiovascular diseases such as supraventricular tachycardia (Hermann et al., 1985), unstable angina, hypertension, stable angina, and angina due to coronary artery spasm (Chaffman et al., 1985). It is reported that a plasma concentration of at least 100 µg/L is required to produce therapeutic results (Chaffman et al., 1985).

Diltiazem is a benzothiazepine derivative with the chemical name of *cis*-(+)-3-acetoxy-5-[2-(dimethylamino)ethyl]-2,3-dihydro-2-(4-methoxyphenyl)-1,5-benzothiazepin-4(5H)-one (Hermann et al., 1985). It is a highly lipophilic drug with an octanol/water partition coefficient of 200 (Hermann et al., 1985) and an octanol/buffer partition ratio of 158 at a pH of 7.4 (Chaffman et al., 1985). High lipophilicity leads to a high distribution of the drug in the tissues and organs of the body since they generally have a higher lipid content than the blood.

It was also found that 78 to 87% of the diltiazem found in the blood is bound to plasma proteins (Chaffman et al., 1985). Of the bound fraction, 35 to 40% is bound to albumin and the remainder to α_1 -acid glycoproteins and various gammaglobulins. Studies have also shown that diltiazem binds to lipoproteins quite extensively and this binding is not associated with surface apoproteins but with either the phospholipids or the neutral lipid core (Kwong et al., 1985). Hussain et al. (1994) studied the reversible and irreversible binding of diltiazem to liver tissue using radiolabelled drug. Their study showed that diltiazem is quite tightly bound to liver proteins.

It is very important to distinguish between the binding and partitioning properties of diltiazem. Binding is a phenomenon which requires a specific receptor site that the drug molecule must come in contact with.

These receptor sites for drugs are usually proteins found either in the blood or tissue. These proteins are distinctly different from the metabolic proteins which are responsible for drug transformations. Binding to metabolic proteins does occur, however this binding capacity is not large enough to give the extent of macroscopic binding which occurs in the liver. Partitioning is a phase equilibrium phenomenon which require the drug to diffuse from an aqueous phase to a lipid phase. Since both partitioning and binding removes diltiazem from the blood, it is very difficult to distinguish between these two phenomena.

Volume of distribution, V_d , is a measurement which describes the extent of distribution of a drug in the body. This measurement is a combination of both binding and partitioning. For diltiazem the volume of distribution is reported to be between 3 to 8 L/kg (Hermann et al., 1985). This very high value is in good agreement with its lipophilic properties and high binding capacity. The large range of this value indicates that there is a wide interindividual variability in the extent of binding and partitioning of diltiazem in the body.

Diltiazem is extensively metabolized with a mean total clearance, Cl , of 11.5 to 21.3 mL/kg/min in man, predominantly due to liver metabolism (Chaffman et al., 1985). The major phase I metabolic pathways in humans are *N*-dealkylation and deacetylation (Chaffman et al., 1985). Hussain et al. (1992) have proposed a metabolic network for the metabolism of diltiazem in humans based on a review of many studies. This network is shown in Figure 2.4, where not only *N*-dealkylation and deacetylation occur but also a minor pathway of *N*-oxidation. Pharmacological studies have indicated that two of the diltiazem metabolites have pharmacologic activity. The deacetyl metabolite, M1, and the

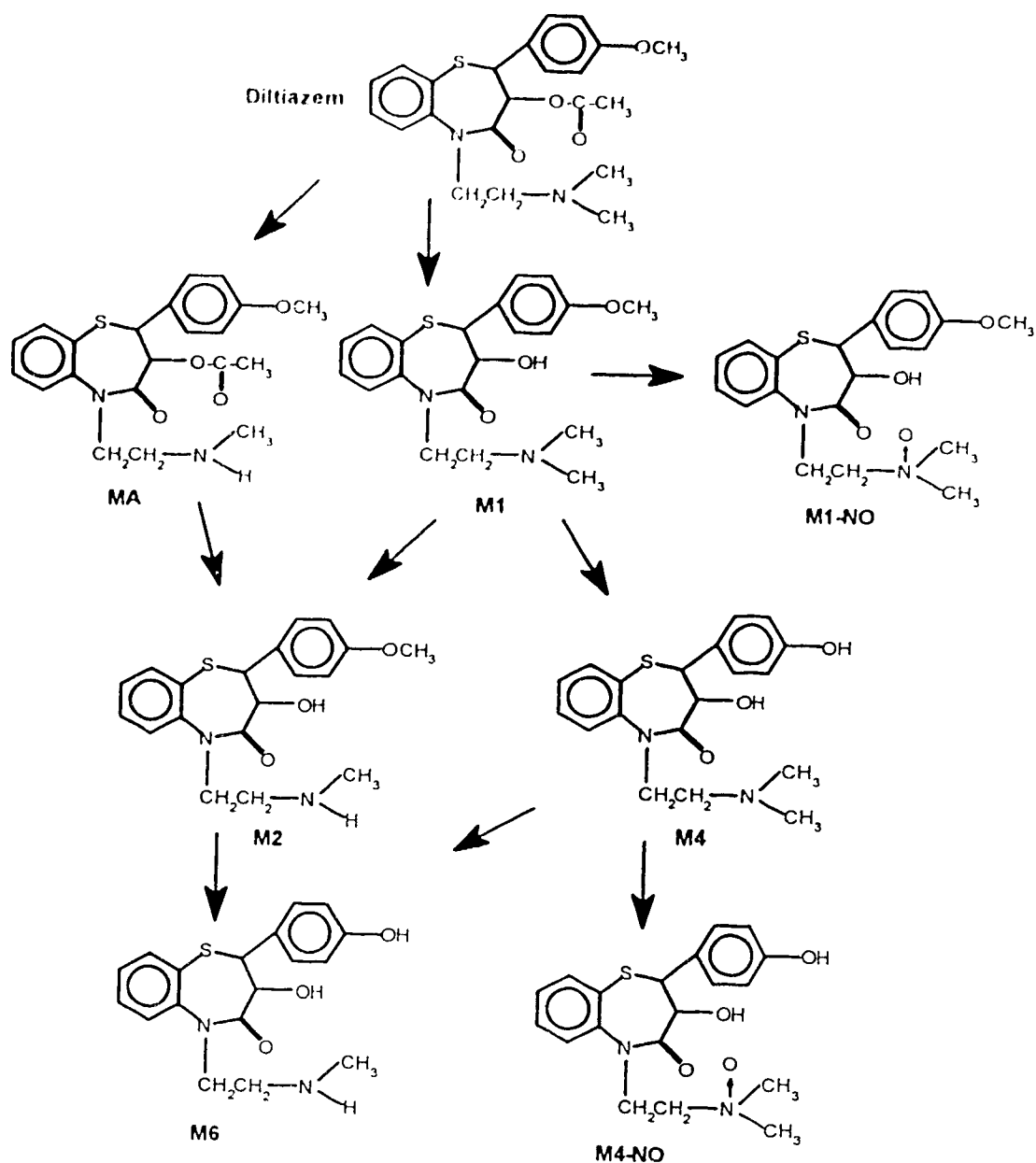


Figure 2.4 Proposed metabolic pathways of diltiazem in humans taken from Hussain et al. (1992). (MA = *N*-demethyldiltiazem, M1 = deacetyldiltiazem, M2 = *N*-demethyldeacetyldiltiazem, M4 = *O*-demethyldeacetyldiltiazem, M6 = *N,O*-didemethyldeacetyldiltiazem, M1-NO = deacetyldiltiazem *N*-oxide, M4-NO = *O*-demethyldeacetyldiltiazem *N*-oxide)

N-monodemethyl metabolite, MA, have approximately 50% and 20% of the potency of diltiazem respectively (Chaffman et al., 1985).

Large interindividual variation has been observed when studying the pharmacokinetics of diltiazem. With a single dose study, a three-fold variation in parameters has been reported (Chaffman et al., 1985). However, plasma levels of diltiazem during chronic treatment can show a ten-fold variability (Hermann et al., 1985). This variability is thought to arise from the interindividual variability in metabolism (Chaffman et al., 1985). However, Kwong et al. (1985) proposed that the high variability may be due to highly variable plasma levels of the major diltiazem binders including lipoproteins and α_1 -acid glycoproteins.

2.3 Liver Models

In order for a liver model to provide insight as well as be useful it must meet the following criteria:

1. The model should accurately represent the physiological and physical processes that are occurring in the liver. The parameters should mathematically describe these processes and not just be curve fitting parameters.
2. The model should be broadly applicable to a wide variety of compounds and metabolic products.
3. The model should contain a minimum number of parameters so that it may be used in a predictive fashion and reduce data requirements.

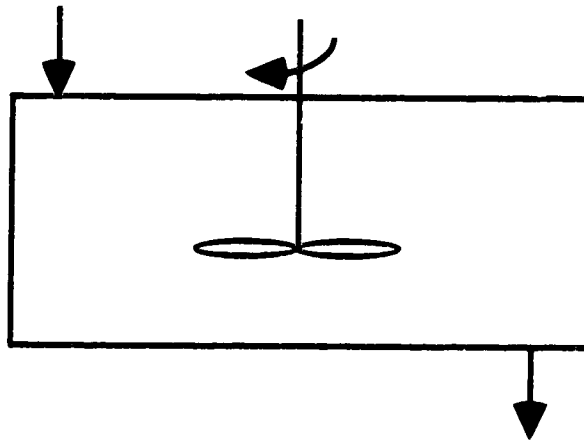
A complete liver model, incorporating all aspects of physiology, would be too complex mathematically, therefore it is often necessary to make some approximations of the liver physiology and blood flow.

Liver models may be classified based on the complexity of the model and the types of approximations made. Nonparametric models have no parameters for mixing within the blood vessels of the liver or mass transfer between the blood and liver cells. Homogeneous mixing models describe the extent of the intrahepatic mixing, but do not explicitly account for mass transfer between the cells and the blood. Heterogeneous models contain parameters for mass transfer between the cells and blood as well as for the extent of mixing. Many liver models have been recently reviewed by Saville et al. (1992b) and many conclusions from this work are summarized in the following paragraphs.

The classical nonparametric models are the well stirred model and the parallel tube model. These models both incorporate a means to describe substrate concentration in the liver by assuming an extreme in mixing profile coupled with a reaction term. The well stirred model assumes that compounds are equally and instantaneously distributed throughout the entire liver. Thus no concentration gradients exist within the liver and it may be considered a homogeneous continuous stirred tank reactor as shown in Figure 2.5 a). The outlet concentration profile of a substrate exiting the liver is therefore given by:

$$\frac{dC}{dt} = \frac{Q(C_{in} - C)}{V_L} - R_j \quad 2.1$$

where C is the concentration of the substrate in the liver, t is time, C_{in} is the inlet concentration, Q is the volumetric flow rate through the liver sinusoids, V_L is the total volume of the liver, and R_j is the rate of reaction of component j . On the other extreme, the parallel tube model assumes plug flow of blood through a single unbranched hepatic tube which yields an exponential concentration gradient across the liver. Therefore, the liver is considered homogeneous and flow is unidirectional as in a plug flow reactor depicted in



a) well stirred model



b) parallel tube model

Figure 2.5 Schematic diagram of the nonparametric models adapted from Levenspiel (1972).

Figure 2.5 b). The resulting equation describing the steady-state concentration in the liver for this model is:

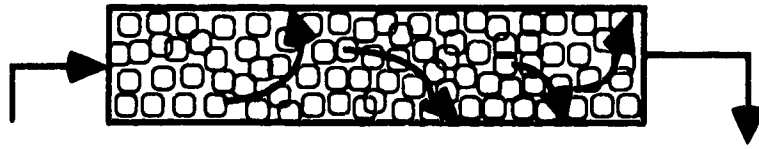
$$\frac{dC}{dV_L} = -\frac{R_j}{Q} \quad 2.2$$

A key advantage of the well stirred model is that the solution is mathematically simple and easily applied to the prediction of drug and metabolite levels in the liver. The parallel tube model requires the solution of a partial differential equation if the time-dependent behavior is studied and thus is more complex mathematically. The major drawback of the nonparametric models is that they are not physiological models nor can they predict the metabolism of materials which are limited by mass transfer into the liver cells.

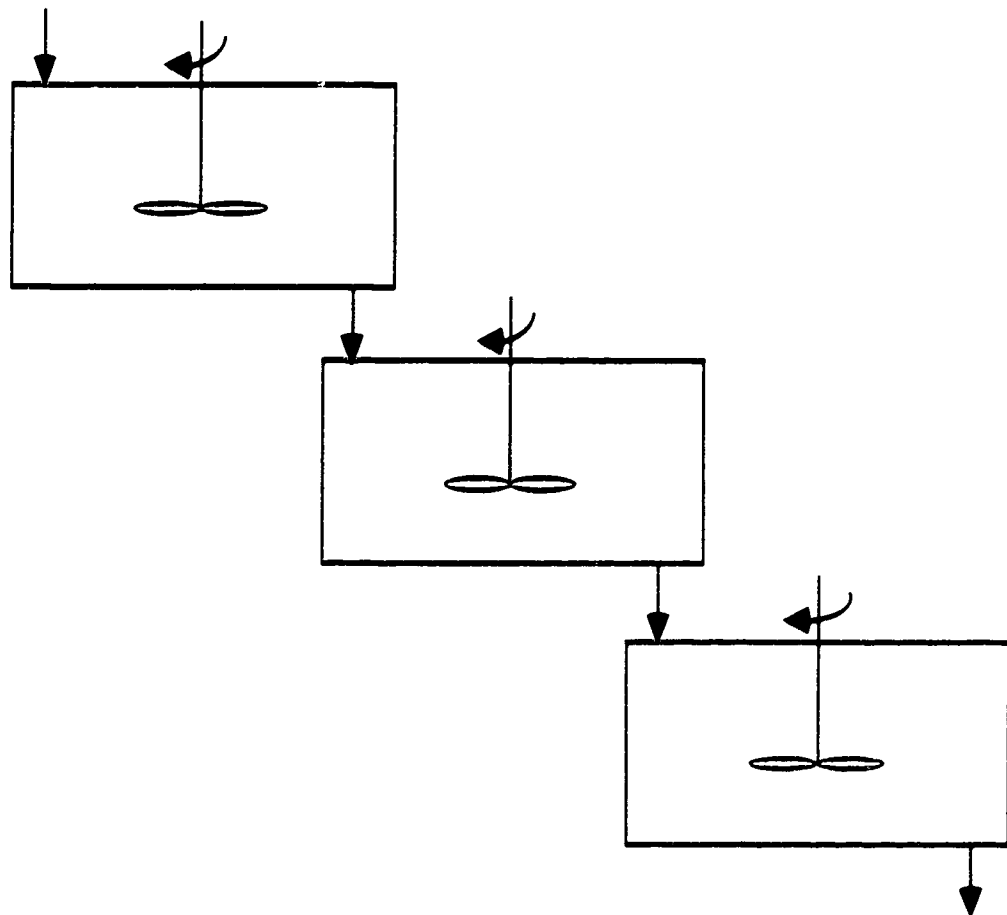
Homogeneous mixing models attempt to describe the extent of mixing between the extremes of the well stirred and the parallel tube models. Two such models have been proposed for liver modeling are the axial dispersion model and the series compartment model as illustrated in Figure 2.6. The axial dispersion model assumes that the liver is a packed bed in which different degrees of axial mixing can occur. The full range of mixing phenomenon can be simulated by adjusting a mixing parameter, v_L , in the equation below:

$$\frac{\partial C}{\partial t} = v_L \frac{\partial^2 C}{\partial x^2} - u \frac{\partial C}{\partial x} - k_R C \quad 2.3$$

In this equation x is the axial distance through the liver, u is the flow velocity through the sinusoids, and k_R is the kinetic rate constant for reaction. The series compartment model is also known as the tanks-in-series model. The liver is assumed to be a sequence of well-mixed compartments connected in series. The number of compartments, N , is not indicative of liver physiology but is an arbitrary parameter used to correlate the extent of mixing. This



a) axial dispersion model



b) series compartment model

Figure 2.6 Schematic diagram of the homogeneous models adapted from Fogler (1992).

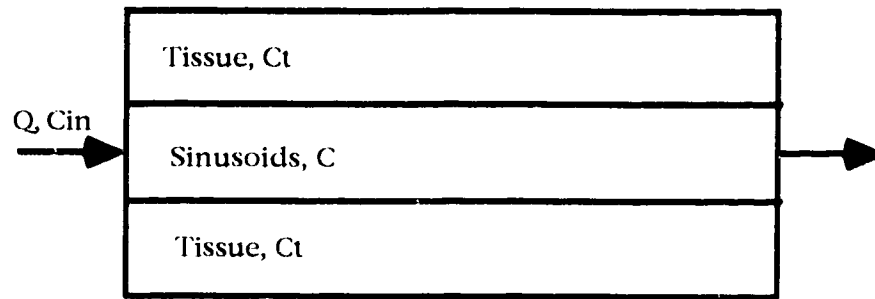
model is also capable of describing the full range of mixing behavior. When N is one the well stirred model equation is obtained and when N is greater than 30 the parallel tube model is applicable. The concentration profile for this model is thus:

$$\frac{dC_i}{dt} = \frac{Q(C_{i-1} - C_i)}{V_i} - k_R C_i \quad 2.4$$

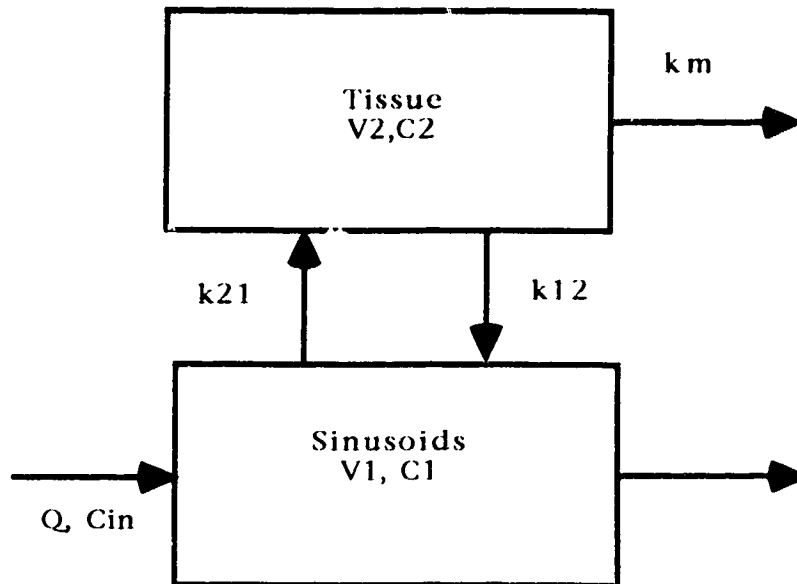
where i is the compartment number and V_i is the volume of compartment i calculated by dividing the total liver volume by the number of compartments, N .

The axial dispersion model suffers from mathematical complexity. It requires the solution of a partial differential equation with two boundary conditions. The model only has a sound theoretical basis if the dispersion parameter, defined as v_L/uL , where L is the axial length of the liver, is less than 0.15. For most compounds the dispersion parameter in the liver has been found to be between 0.2 and 0.5. Hence, for the flow and mixing conditions observed in the liver, the model does not have a sound theoretical basis, but provides only an empirical method for analyzing drug elimination by the liver. The simplicity of the series compartment model has made it an attractive model for describing complex flow and reaction and, for the liver, provides the same type of empirical modeling as the axial dispersion model. The primary limitation of the model is that it does not explicitly include physiological phenomena in the liver such as variable transit times through the sinusoids, saturable binding, or the effects of mass transfer into tissue.

Two heterogeneous models that have found to be very useful in liver modeling are the tubular and compartmental models illustrated in Figure 2.7. The tubular model assumes the liver is a single, straight hepatic tube surrounded by a concentric tissue compartment. Within the tissue, both axial



a) tubular model



b) compartmental model

Figure 2.7 Schematic diagrams of the heterogeneous models adapted from Saville et al. (1992b).

and radial diffusion can occur. This model is an extension of the axial dispersion model. The compartmental model is used when the time scale for mass transfer is much larger than the time for mixing in the sinusoids. The flow of materials is restricted to the sinusoids and materials gain access to the tissue compartment by mass transfer. Complete mixing is assumed within each compartment.

The model equations for the tubular model are found below.

$$\text{Sinusoids:} \quad \frac{\partial C}{\partial t} = -u \frac{\partial C}{\partial x} - 2\pi r_c P(C - C_{t,s}) \quad 2.5$$

$$\text{Tissue:} \quad \frac{\partial C_t}{\partial t} = D_{TX} \frac{\partial^2 C_t}{\partial x^2} + \frac{D_{TR}}{r} \frac{\partial}{\partial r} \left(r \frac{\partial C}{\partial t} \right) \quad 2.6$$

The radius of the sinusoid is symbolized as r_c , P is the tissue permeability, $C_{t,s}$ is the concentration at the interface between the tissue and the sinusoids, C_t is the concentration in the tissue, r is the radial distance, and D_{TX} and D_{TR} are the coefficients for axial and radial diffusion respectively. This model is based on net rates of diffusion and neglects physiological effects such as bypassing, variable blood flow velocities in a network of sinusoids, transient back flow and no provision is made for chemical reaction of the substance. The equations are mathematically complex and require numerical solutions to obtain a concentration profile. In order to estimate the tissue diffusion coefficients D_{TR} and D_{TX} , accurate tissue concentrations must be known. These measurements are virtually impossible to obtain and thus only approximations can be made.

In the compartmental model, each compartment is described by an ordinary differential equation. The model equations for the compartmental model illustrated in Figure 2.7 are found below.

$$\text{Sinusoids:} \quad V_1 \frac{dC_1}{dt} = QC_{in} - QC_1 - V_1 k_{12} C_1 + V_2 k_{21} C_2 \quad 2.7$$

$$\text{Tissue:} \quad V_2 \frac{dC_2}{dt} = V_1 k_{12} C_1 - V_2 k_{21} C_2 - V_2 k_m C_2 \quad 2.8$$

The volume of the sinusoids and tissue are given by V_1 and V_2 respectively, C_{in} is the inlet concentration of drug, C_1 and C_2 are the concentration of the drug in the sinusoids and tissue respectively, k_m is the rate constant for metabolism of the drug, and k_{12} and k_{21} are the rate constants for cellular uptake and release respectively.

A broad spectrum of conditions can be handled by a compartmental model, suggesting that it would be applicable to a variety of compounds and physiological conditions. The model accounts for the heterogeneous nature of the organ, combining cellular uptake and release with intracellular reaction. The model is relatively simple mathematically, consisting of a set of ordinary differential equations which may be easily integrated to predict intracellular and sinusoidal levels of a drug and its metabolites. The primary limitation of the model is that it does not explicitly account for the processes that control intrahepatic mixing.

2.4 Liver Models for Drug Binding and Partitioning

Binding of drugs is analogous to chemisorption in that drugs only bind to certain binding molecules or sites, which are usually protein molecules. Thus most drug binding models incorporate a Langmuir type model to account for drug binding. Much of the work on drug binding has been focused on binding of drugs to albumin in blood, which can significantly alter the concentration of free drug available in plasma since drug that is bound cannot be utilized at the site of action nor can it be metabolized. Weisiger (1985) developed a compartmental model which describes drug metabolism in the

liver combined with mass transfer between the sinusoids and tissue and the dynamic exchange between bound and free drug in plasma. This model is illustrated in Figure 2.8 and the model equations are as follows:

Unbound drug in sinusoids:

$$V_{si} \frac{dC_{si}}{dt} = Q(C_{s,i-1} - C_{si}) - (k_1 + k_b\Lambda)V_{si}C_{si} + k_2V_{ci}C_{ci} + k_{dis}V_{si}C_{sbi} \quad 2.9$$

Bound drug in sinusoids:

$$V_{si} \frac{dC_{sbi}}{dt} = Q(C_{sb,i-1} - C_{sbi}) - k_{dis}V_{si}C_{sbi} + k_b\Lambda V_{si}C_{si} \quad 2.10$$

Drug in tissue:

$$V_{ci} \frac{dC_{ci}}{dt} = k_1V_{si}C_{si} - (k_2 + k_3)V_{ci}C_{ci} \quad 2.11$$

where C_{si} is the unbound drug concentration in the sinusoids, C_{sbi} is the bound drug concentration in the sinusoids, C_{ci} is the tissue drug concentration, Λ is the albumin concentration in the blood, k_1 is the rate constant for cellular uptake, k_2 is the rate constant for release from the cells, k_3 is the rate constant for intracellular reaction, k_b is the rate constant for binding to albumin, k_{dis} is the rate constant for dissociation of the bound complex, and V_{si} and V_{ci} are the volume of individual sinusoidal and cellular compartments respectively and are equal to the total volume of the region divided by the total number of compartmental units, N .

This model is an extension of the series compartment model and can account for a wide variety of physiological conditions. Since the total albumin concentration far exceeds the concentration of bound drug, there is no need to account for the decrease in available sites as drug binds. This yields a linear system of equations that are mathematically simple and easily solved analytically.

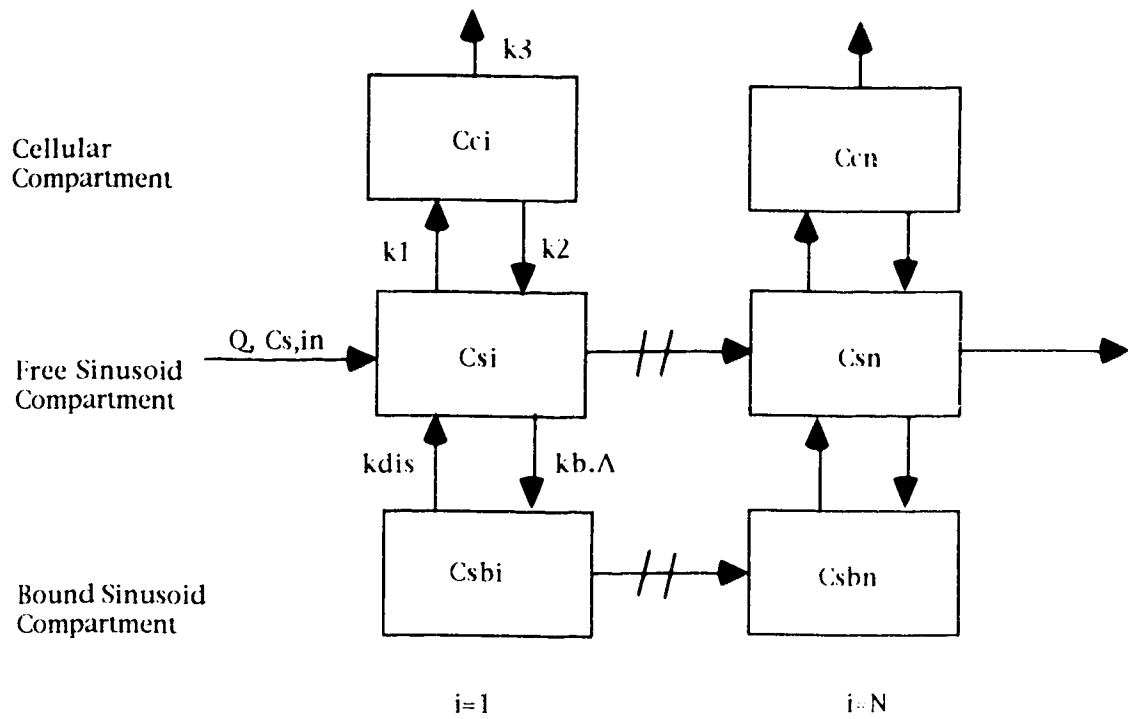


Figure 2.8 Compartmental model for binding and transport proposed by Weisiger (1985).

A revised form of Wesiger's model (1985) was developed by Saville et al. (1992a) to describe the kinetics of lidocaine and its metabolites in the liver. It was observed that for lipophilic compounds, distribution of the drug through the liver tissue requires 3 to 5 minutes to complete, whereas vascular mixing within the sinusoids was complete in approximately 20 seconds. Thus the time scale for distribution was significantly larger than the time for mixing and well stirred conditions would be appropriate. The model therefore required only one set of compartments to adequately describe experimental results. Since the experimental procedure utilized isolated perfused rat livers with a Krebs's buffer solution, the compartment for drug-albumin binding was not required. The final model was very similar to the compartmental model illustrated in Figure 2.7 with a modification in the rate constant for reaction, k_m , to account for the deactivation of metabolic enzymes upon initial exposure to lidocaine. Therefore, Saville et al. (1992a) concluded that transport of the drug into the tissue and deactivation of the metabolic enzymes control the transient response of the liver to infusion of lidocaine.

Parameter estimates revealed that the rates of transport of lidocaine were significantly higher than the rate of reaction, and therefore intracellular reaction was clearly the rate limiting step. The rate of uptake was consistently higher than the rate of release from the cells suggesting a high affinity for the cellular region of the liver. Therefore the experimentally observed long time to steady state was partly due to a partitioning effect. The liver tissue can act as a large reservoir for the drug and metabolites thus the distribution of drug into tissue can delay the onset of steady state. It was concluded that for lipophilic compounds, transport and reaction dominate over any processes within the sinusoids, and vascular

mixing and changes in flow should have a negligible effect on drug metabolism.

The important properties that control the metabolism of diltiazem are its lipophilicity and protein binding. These two properties must be included when attempting to model this drug. The work done previously by Weisiger (1985) and Saville et al. (1992a) provide a strong base to begin to understand the metabolism of diltiazem in the liver and mathematically model its behavior.

CHAPTER 3 - EXPERIMENTAL METHODS AND MATERIALS

3.1 Liver Perfusion

All experiments utilized rat livers isolated from male Sprague-Dawley rats, weighing between 226 - 281 g, supplied by Biosciences Animal Services, University of Alberta. The animals were housed in the Dentistry-Pharmacy animal facility for at least two days prior to an experiment. The liver isolation and perfusion methods used were described by Miller (1973) and Tam et al. (1987) with slight modifications.

The rats were anesthetized prior to surgery with methoxyflurane obtained from Pitman-Moore (Mississauga, Ont.). The liver was isolated by surgical cannulation of the hepatic and portal veins and the inferior vena cava. The portal vein was cannulated with an intravascular over-the-needle catheter, called a Quick-Cath, from Baxter Healthcare Corporation (Dearfield, Ill.). The liver was perfused with Krebs's bicarbonate buffer solution with a pH of 7.4. The buffer was oxygenated with carbogen gas consisting of a mixture of carbon dioxide and oxygen in a ratio of 5:95. The perfusion rate was kept constant during the experiment with a flow rate of 3 to 5 mL/(min·g liver). The perfusion apparatus and solution was maintained at 37°C by enclosing the equipment in a constant temperature controlled cabinet.

The general physical appearance of the liver, the consistency of perfusion pressure, and the consumption of oxygen by the liver were used as guides to its viability over the course of the experiment. Standard liver function tests for aspartate and alanine transferase levels in the perfusate effluent before and after the experiment, as well as the stability of diltiazem and metabolite levels at steady state confirmed liver viability during the

experiment. The results of liver function tests are shown in Table A.2 in Appendix A.

After surgery, the liver was allowed to equilibrate for approximately 20 minutes before drug infusion began. A mixture of radiolabelled and cold diltiazem was dissolved in Kreb's buffer solution and perfused until steady state was obtained. The liver was then washed with blank buffer until all drug and metabolites were removed. Rat and liver weights, inlet drug concentrations, and perfusion flow rates for each experiment are given in Table A.1 in Appendix A.

Samples of the effluent perfusate were taken during the drug perfusion and washout periods. Inlet samples were taken at various times during the perfusion of drug to guarantee a constant inlet concentration of diltiazem. All samples were collected on an ice bath and 25 μ L of 3 N hydrochloric acid was added to give a pH of approximately 5. These samples were then stored at -25°C and HPLC analysis was performed within two weeks. This was done to ensure the stability of diltiazem and its metabolites prior to analysis. At the end of the experiment the liver was blotted dry and its weight determined.

3.2 HPLC Analysis

Experimental samples were analyzed by high performance liquid chromatography, HPLC, to determine the concentration of diltiazem and five of its metabolites (M1, M2, M4, M6, and MA) using the procedure outlined by Hussain et al. (1992) with slight modifications. Cold Drug and metabolites were supplied by Nordic Merrell Dow Research (Laval, Que.). The HPLC instrumentation consisted of a Shimadzu LC-600 liquid chromatography pump, a SPD-6AV UV-VIS spectrophotometric detector, and a Waters WISP 710B

automatic injector. Separation of all six compounds was achieved using a 4 μ m Waters Novapak C₁₈ reversed phase cartridge column (10 cm x 8 mm I.D.). The optimum absorbance of the compounds was found at 214 nm. The internal standard used was benzylamphetazine. The mobile phase consisted of an aqueous solution containing 0.14% triethylamine and 0.045% H₃PO₄ mixed 67:33 (v/v) with acetonitrile and was pumped at a flow rate of 2.0 mL/min. Data acquisition and processing was accomplished with the Waters Baseline 810 Workstation on an IBM compatible computer.

Standard curves were constructed by injecting samples of diltiazem and its metabolites ranging in concentration from 100 to 2000 ng/mL and calculating the ratio of the area of each respective peak to the area of the internal standard. A chromatogram of a standard at 1500 ng/mL of diltiazem and its metabolites along with the internal standard is shown in Figure 3.1. Identification of each peak and its typical retention time is listed in Table 3.1. Each standard concentration was analyzed three times and linear regression was used to determine the best fit line through each set of standards. A typical standard curve for diltiazem is shown in Figure 3.2. Typical standard curves for the five remaining metabolites are shown in Appendix B. Quality control samples were prepared by an authorized person in the laboratory to establish the accuracy and precision of the assay. The quality control samples covered the range of concentrations of the standard curve.

Table 3.1 Typical HPLC retention times.

Compound	Retention Time min
M6	2.1
M4	3.1
M2	4.5
MA	7.7
M1	9.3
INTSTD	12.8
DZ	16.5

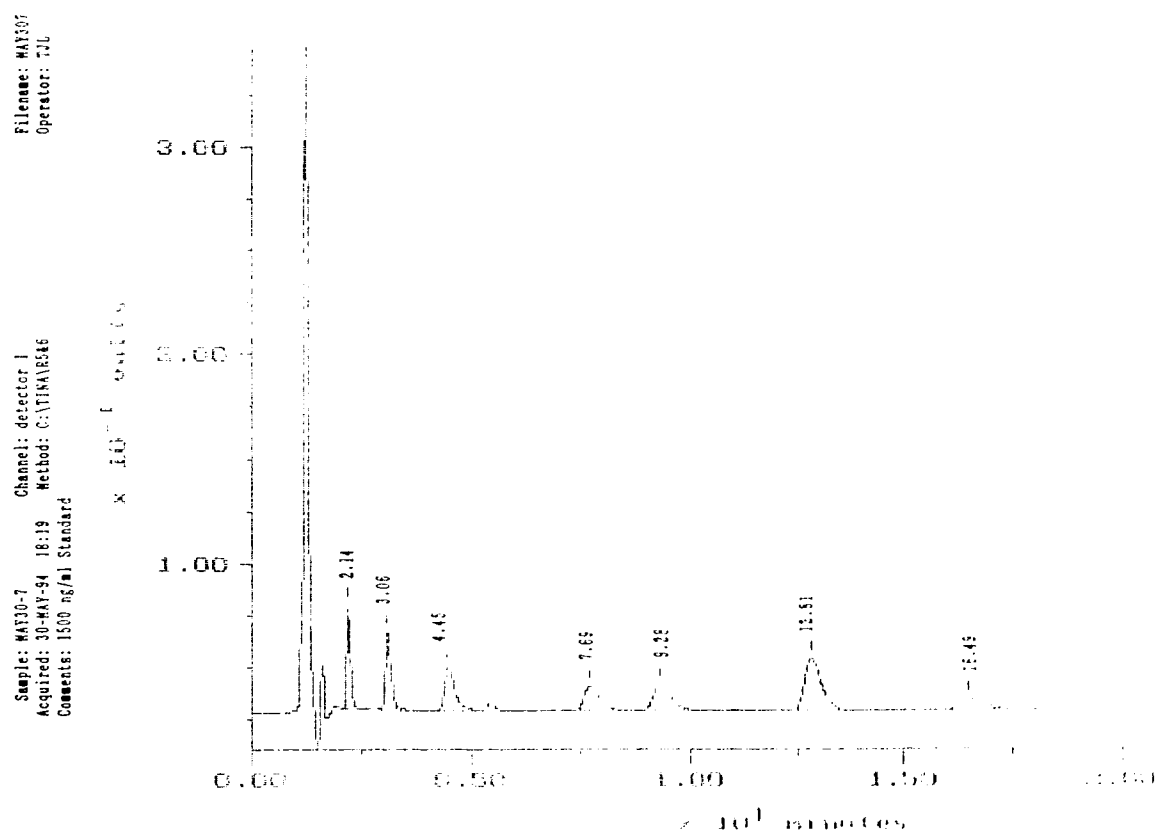


Figure 3.1 Typical chromatogram of a sample containing internal standard and 1500 ng/ml of diltiazem and its metabolites.

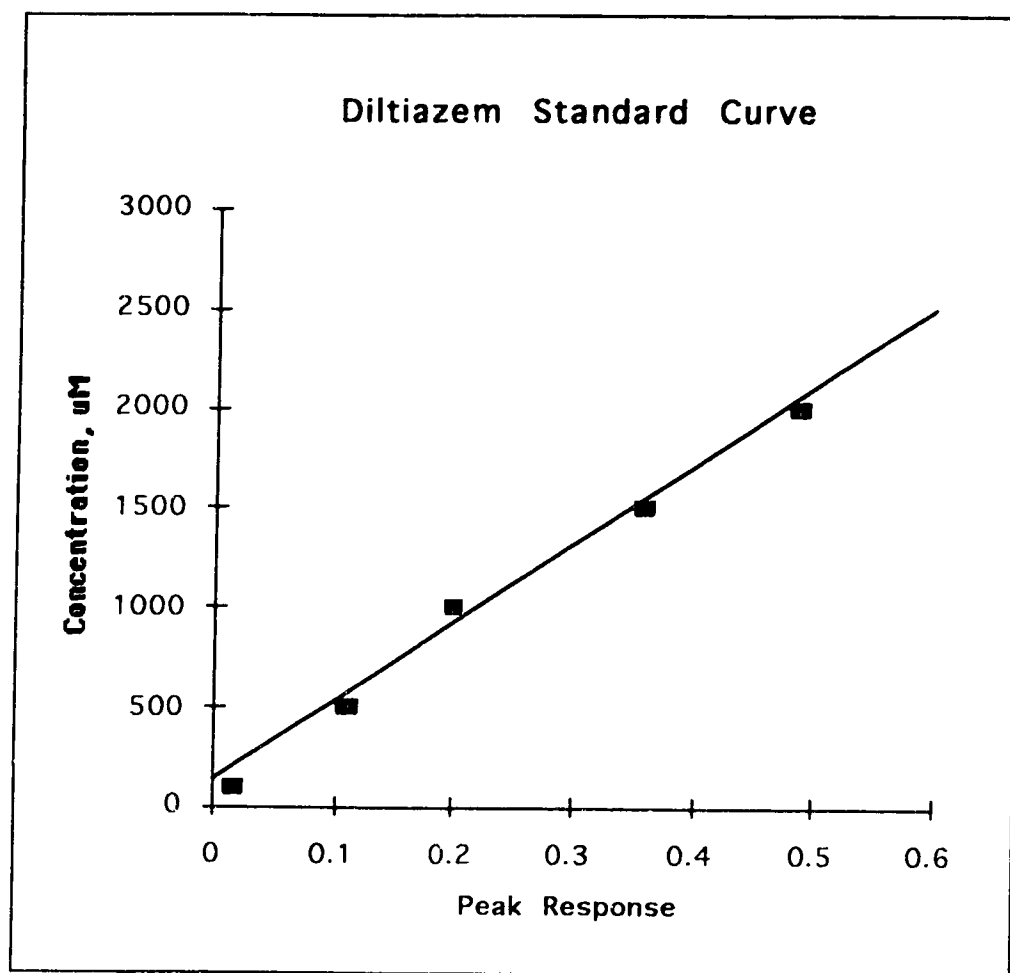


Figure 3.2 Typical standard curve for diltiazem. The coefficient of determination, $r^2=0.9954$. The calibration equation was calculated to be:
DZ concentration = $34.45 + 4132 * \text{Peak Response} * \text{Internal Standard Area}$

3.3 Radioisotope Analysis

The radiolabelled diltiazem tracer obtained from NEN Research Products, DuPont Canada Inc. (Markham, Ont.) is illustrated in Figure 3.3. It was a tritium label in the N-methyl position. Radioactive samples were prepared for analysis by adding 1.0 mL of effluent sample to 9.0 mL of scintillation fluor. The contents were then mixed for approximately 5 minutes. The radioactivity of each sample was then determined with a LKB Redirack Liquid Scintillation Counter corrected for tritium counting in decays per minute, dpm.

As a check of the purity of the tracer, a 5 mL solution containing concentrated amounts of unlabelled diltiazem and M1 was prepared with approximately 0.1 μ L of radioactive diltiazem tracer. A 100 μ L sample of this solution was injected to the HPLC and the diltiazem and M1 peaks were collected. These two samples along with a 100 μ L sample of the original solution were counted and the results are found in Table 3.2 below. This test proved, within experimental error, the tracer was in fact a diltiazem tracer.

Table 3.2 Results of tracer purity test.

<u>Sample</u>	<u>Counts dpm</u>
Blank	0.0
Original Solution	67647.9
DZ Peak	64290.8
M1 Peak	494.8

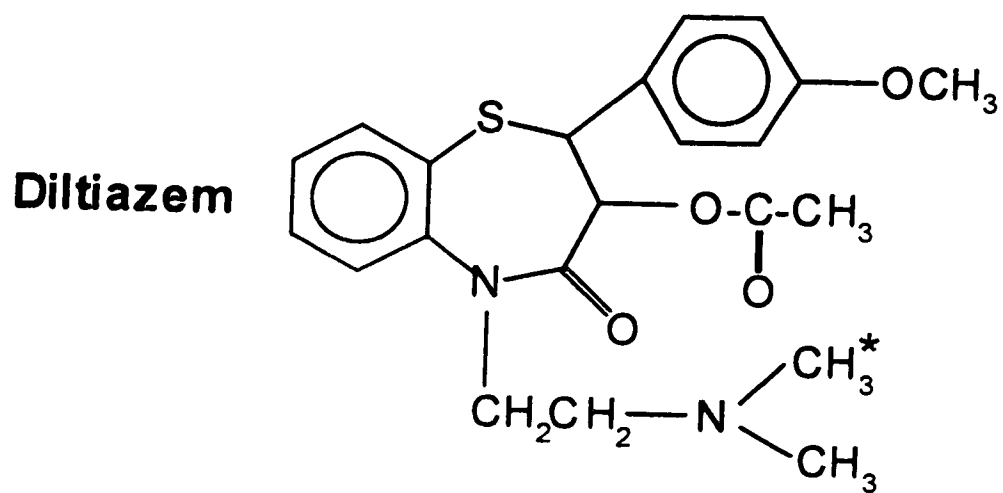


Figure 3.3 Radiolabelled diltiazem, cis-(+)-[N-methyl- ^3H]-. (* = tritium label)

CHAPTER 4 - RESULTS AND DISCUSSION

4.1 Qualitative Features of Diltiazem Modeling

Figure 4.1 shows the typical experimental outlet concentrations of diltiazem and five of its metabolites obtained by infusing 37.71 μM diltiazem in an isolated rat liver for 60 minutes followed by a 60 minute washout period. Figure 4.2 shows the observed outlet concentrations of diltiazem, total measured metabolites, and total radioactive species for the same experiment. The radiolabelled and unlabelled outlet concentration profiles and raw data for the remaining experiments can be found in Appendix C. Experiments with rats #3 and 4 yielded outlet concentration profiles which were too low to be detected by HPLC methods, however the radiolabelled profiles were still measured. Variability in the experimental data arose from a wide variety of sources. The HPLC techniques provided the largest source of noise in the data while the variable levels of binding sites and the rate of metabolism provided a large interindividual variability.

Conventional pharmacokinetic parameters of diltiazem are listed in Table 4.1. The time to steady state, t_{ss} , is an important measure of the dynamics of the hepatic system. The extraction ratio at steady state, E_{ss} , is a measure of how much diltiazem is extracted or metabolized from the inlet flow and is calculated as:

$$E_{ss} = \frac{C_{in} - C_{out,ss}}{C_{in}} \quad 4.1$$

where C_{in} is the inlet concentration of diltiazem and $C_{out,ss}$ is the steady state outlet concentration of diltiazem. Hepatic clearance, Cl_h , is defined as a rate at

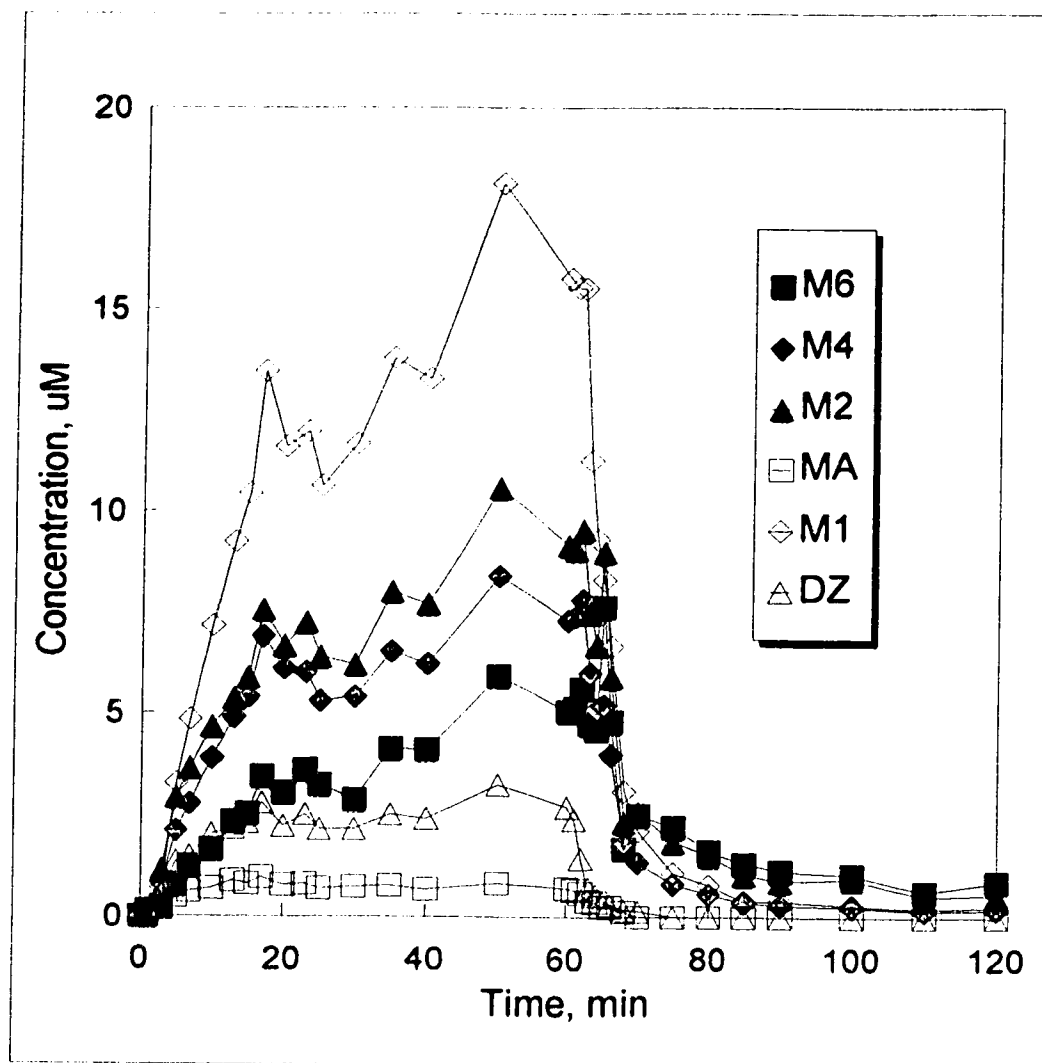


Figure 4.1 Outlet concentration of diltiazem and five of its metabolites for Rat #7 obtained by infusing $37.71 \mu\text{M}$ diltiazem for 60 minutes followed by a 60 minute washout period.

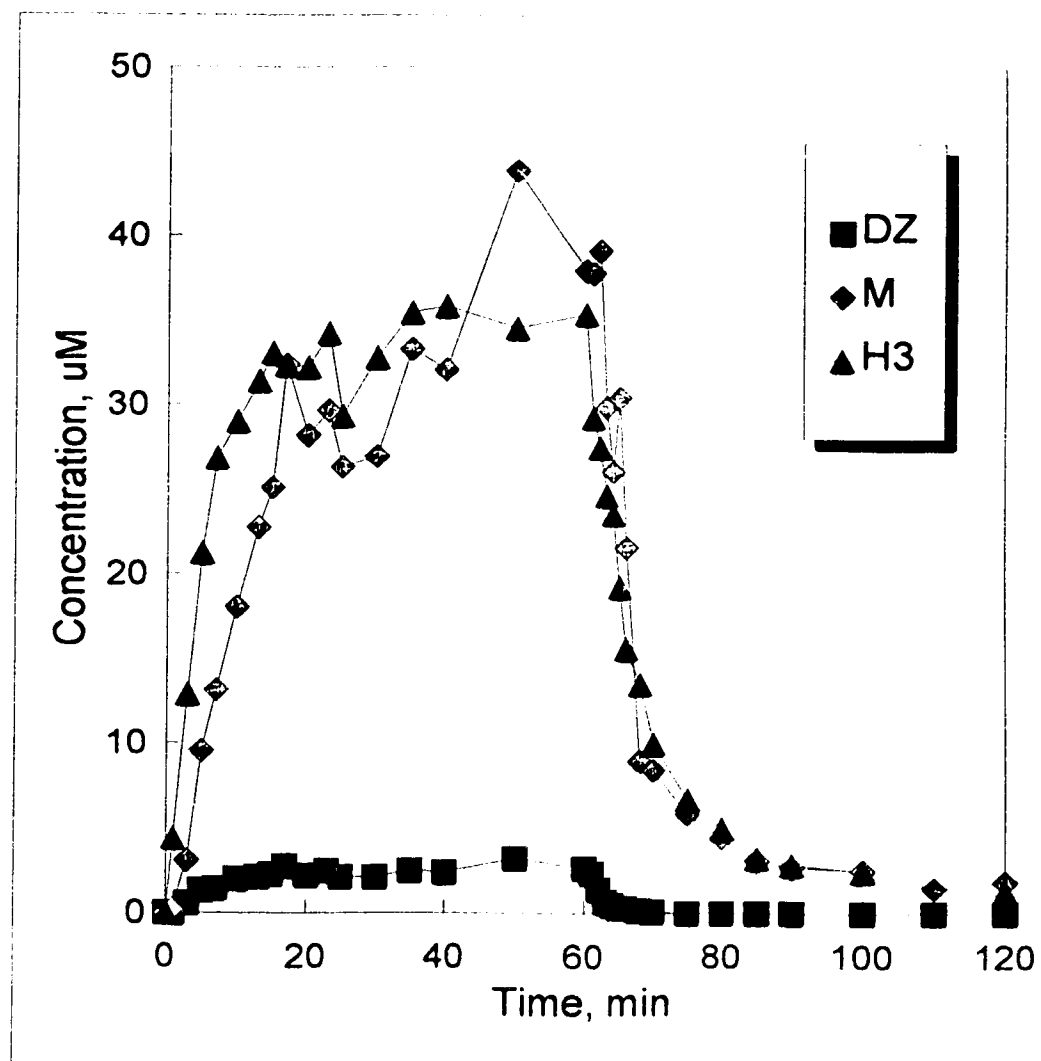


Figure 4.2 Outlet concentration of diltiazem, total measured metabolites, and radioactive species for Rat #7 obtained by infusing $37.71 \mu\text{M}$ diltiazem with a radiolabelled tracer for 60 minutes followed by a 60 minute washout period.

which drug is cleared from the blood by the liver and is calculated as follows:

$$Cl_h = QE_{ss} \quad 4.2$$

where Q is the volumetric flow rate through the liver. The parameters in Table 4.1 were calculated using steady state data from computer simulations. This steady state value reduces the error associated with scatter of the data.

Table 4.1 Conventional pharmacokinetic parameters.

Rat #	C_{in} μM	$C_{out,ss}$ μM	E_{ss}	Cl_h ml/min	t_{ss} min
5	11.59	0.128	0.989	30.1	0.279
6	12.05	0.0535	0.996	29.9	1.09
7	37.71	2.24	0.941	25.9	5.42
8	51.15	2.68	0.948	26.9	0.903
63*	41.18	3.79	0.908	27.2	15.6
64*	34.73	4.24	0.878	26.3	20.5
65*	39.79	3.90	0.902	26.2	13.5
66*	30.89	2.65	0.914	26.5	18.4
67*	42.87	7.26	0.831	24.9	19.5

* - experimental data from Hussain et al.

The first step in developing a model to describe diltiazem metabolism is to consider the qualitative features of Figures 4.1 and 4.2 to determine the significant mechanisms involved. These mechanisms must also be consistent with known properties of diltiazem and its metabolites, specifically its high partitioning and tight binding.

The important qualitative features of Figure 4.1 which must be considered in the proposed model are:

1. Initial lag in diltiazem and metabolite concentration profiles giving a sigmoidal profile in the efflux concentrations.
2. Long time to achieve steady state for diltiazem and metabolites.
3. The metabolite profiles follow the same time profile as for diltiazem, except during the prolonged washout.

4. During washout there is an initial rapid drop in both diltiazem and metabolite concentrations.
5. Prolonged washout of low concentration metabolites with negligible amounts of diltiazem.

A qualitative description of these data may be given with the use of Figure 4.3. Phase 1 of this figure shows an initial lag which is consistent with very strong binding which removes all drug and metabolites from the sinusoids and holds them very tightly in the liver tissues. Once the binding sites are saturated, the drug and metabolites begin to partition, as in Phase 2, into other tissues in the liver and the concentration in the sinusoids begins to rise. As an equilibrium between the sinusoids and tissue is reached, Phase 3 or steady state is achieved. During washout, the drug partitioned into the tissues is removed very quickly giving a rapid drop in sinusoid concentration as shown in Phase 4. Subsequently, in Phase 5 the bound drug and metabolites elute very slowly due to the tightness of the binding.

It is difficult to distinguish from the data of Figure 4.1 whether or not the metabolites bind. Figure 4.2 provided insight to this problem. The radioactive species did not show any lag initially or a sigmoidal efflux profile. This observation can be explained by considering the pathway for diltiazem found in Figure 2.4 and the location of the radioactive label shown in Figure 3.3. There are several pathways in Figure 2.4 whereby the tritium label could be cleaved from the drug or metabolite and be released as radiolabelled methanol. Since radioactivity was detected in the effluent before diltiazem or metabolites had appeared, methanol must be released during this time indicating that the metabolites are retained in the liver after they are formed. Metabolism was occurring during the initial lag phase, therefore the metabolites were bound to the liver tissue. Since the profiles for the

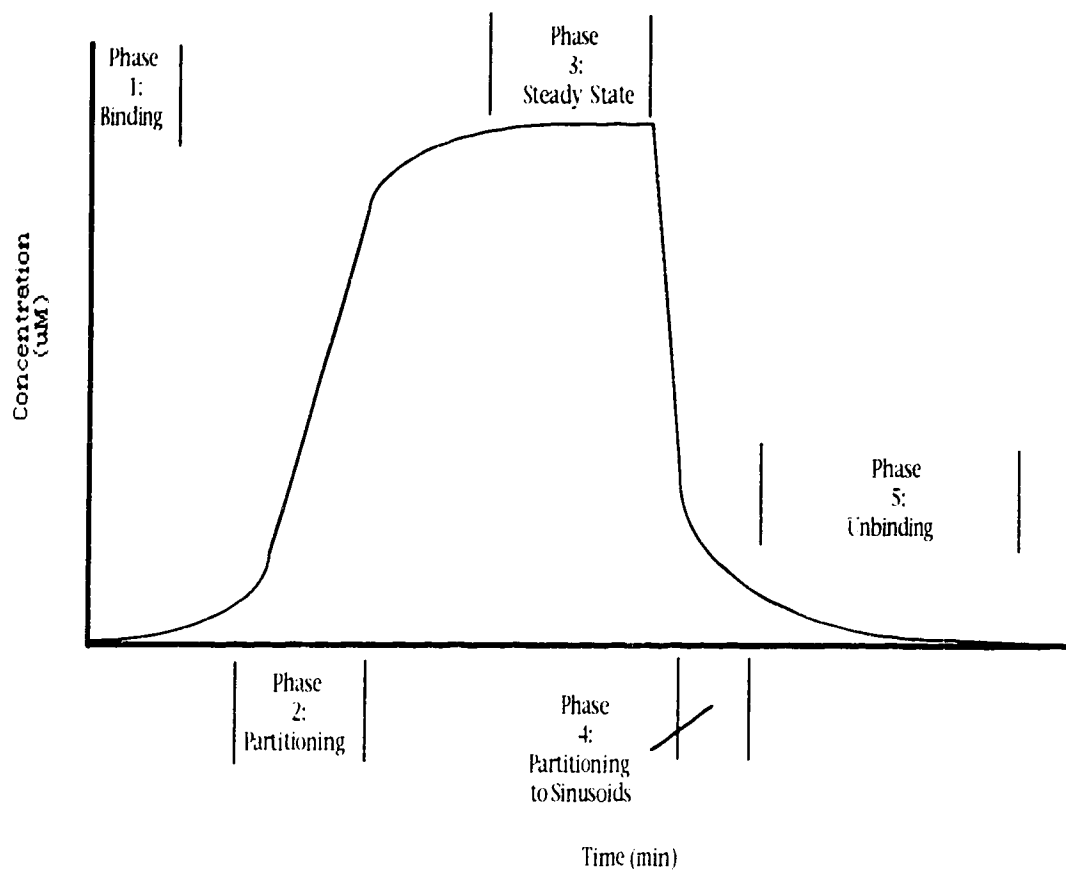


Figure 4.3 Typical diltiazem concentration profile from a perfused rat liver describing the phases of diltiazem metabolism.

metabolites follow the profile for diltiazem, it is reasonable to assume binding is approximately equivalent for all compounds. Otherwise the metabolites would emerge before or after diltiazem depending on their affinity. The possibility of unknown metabolites produced, when diltiazem concentration is low, would also increase the unaccounted amount of radioactivity.

Figure 4.4 shows the relationship between the time to steady state and the concentration of diltiazem in the outlet of the liver observed by Hussain et al. (1994). The outlet concentration was used as the independent variable in this figure since, in the well stirred model, this is the concentration that is in equilibrium with the liver tissue. The scatter of the data in this figure was very large which was consistent with the large interindividual variation observed by other researchers (Chaffman et al., 1985, Hermann et al., 1985). Thus the data are most useful for their qualitative features. As the outlet concentration of diltiazem decreased below approximately 5 μM , the time to steady state increased dramatically. In this region the dynamics of diltiazem effluent concentration was dominated by tissue binding and a longer time was required to fill the binding sites in the liver at low concentration of drug. At higher concentrations, the binding sites were saturated very quickly and the dynamics were dominated by the partitioning of the drug into tissue. This partitioning was a linear phenomenon, therefore, the time to steady state was constant even at higher outlet concentrations. The data in this figure were, therefore, also consistent with the two phenomenon important in diltiazem kinetics: saturable or nonlinear binding and linear partitioning.

The washout data from the efflux profiles obtained in this study are shown on a normalized concentration scale in Figure 4.5. On a log-linear scale no linear behavior was observed thus it can be concluded that the processes involved in washout are not first-order processes. This conclusion provides

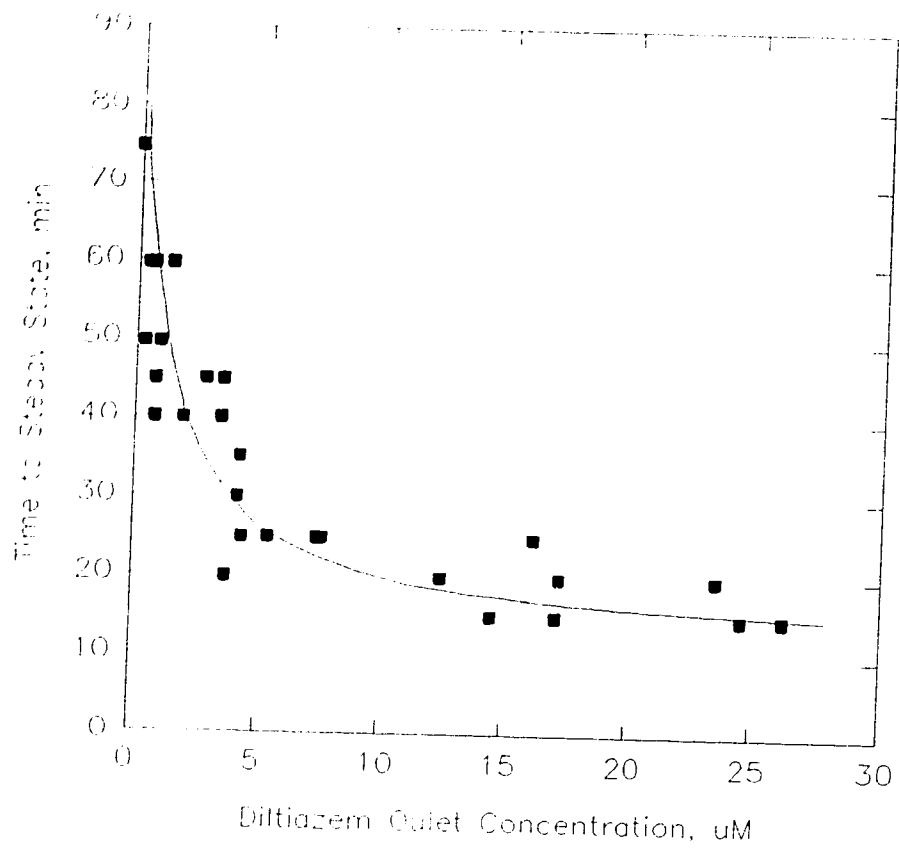


Figure 4.4 Time to reach steady state vs. diltiazem outlet concentration. Experimental data taken from Hussain et al. (1994).

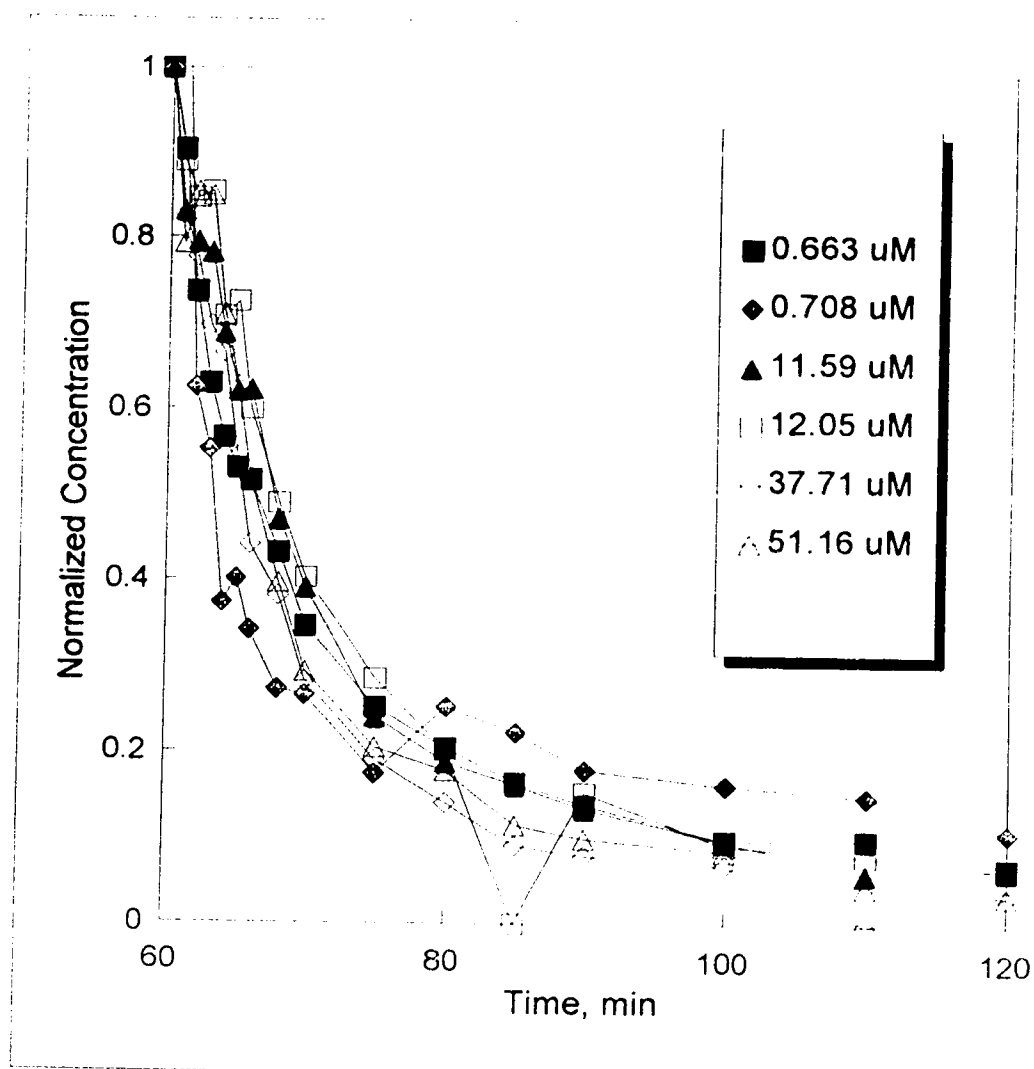


Figure 4.5 Normalized washout profiles of six different radioactive experiments.

evidence that nonlinear binding must be important to the dynamics of diltiazem metabolism. Figure 4.5 also shows that the normalized washout concentration profile is relatively insensitive to the steady state concentration in the liver. This may suggest that more binding is available at higher concentrations.

A good liver model must be physiologically consistent. A simplified diagram of a hepatocyte is shown in Figure 4.6. A qualitative description of the steps involved in diltiazem metabolism in terms of this simplified physiology are as follows:

Step 1: Transport into membrane and/or binding to a membrane protein binding.

Step 2: Diffusion through the cytosol.

Step 3: Binding or metabolism by cytosolic, mitochondrial, and microsomal proteins.

It is assumed in this description that active proteins are either binding sites or metabolic sites. Binding of substrate to metabolic enzymes would be insignificant to non-reactive binding to a variety of tissue proteins. Cellular proteins, which may be considered potential binding sites, are located within the cytoplasm and the cell wall. It is very difficult to distinguish which of these sites is most dominant in the binding of diltiazem and its metabolites. The conclusions of Kwong et al. (1985) that show strong binding of diltiazem to lipoproteins provide some evidence for a strong binding site in the cell membrane lipoproteins, however, this result does not rule out binding to cytosolic proteins.

The schematic physiology of Figure 4.6 may be described mathematically by a three compartment model as shown in Figure 4.7. This

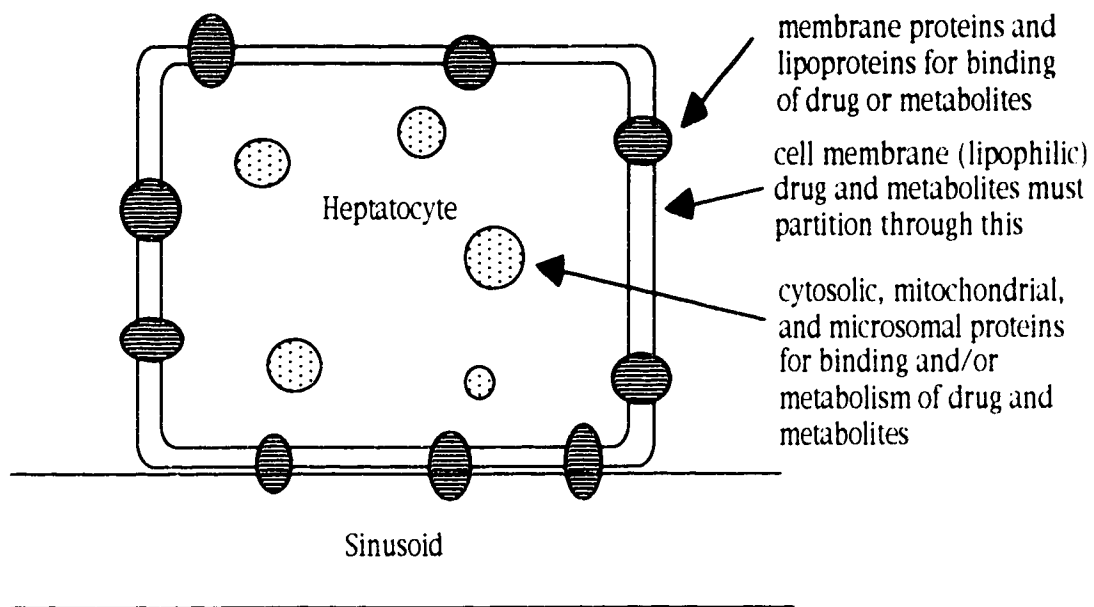


Figure 4.6 Schematic diagram depicting a simplified hepatocyte.

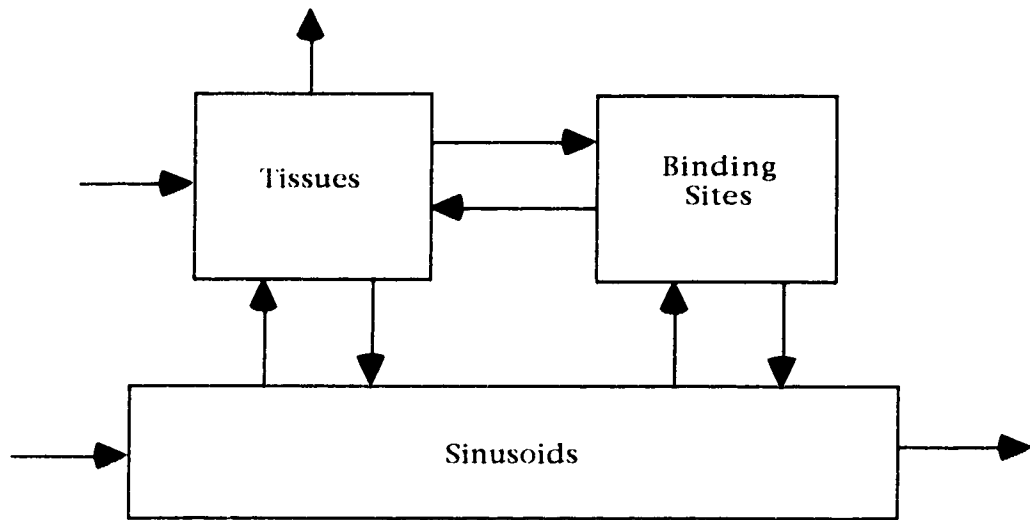


Figure 4.7 Schematic diagram of a three compartment model for diltiazem metabolism.

model accounts for flow through the sinusoids, partitioning of drug into the tissue in parallel with binding to membrane proteins, metabolism and formation of metabolites within the cytosol and microsomes, and binding to cytosolic proteins. Although this model appears complete, the equations required would over specify the problem and the parameters would be meaningless. Mathematically it is very difficult to distinguish whether the drug and metabolites enter the binding compartment from the sinusoids or from the tissue. Since Kwong et al. (1985) demonstrated binding to a class of proteins that would be abundant in the cell membrane, we selected the model wherein binding occurs in parallel to tissue uptake from the sinusoids.

4.2 Development of Model Equations

The Langmuir adsorption model is frequently used in pharmacokinetics to model saturable binding of drugs to proteins (Gibaldi et al., 1982). This model is shown in a compartmental form in Figure 4.8. The rate of binding of drug and metabolites in the protein compartment is given by the following equation:

$$\frac{dn}{dt} = V_1 k_b (n_{\text{sat}} - n) C_1 - k_{\text{dis}} n \quad 4.3$$

where n is the number of sites with drug bound, n_{sat} is the total moles of sites available for binding, k_b is a second order rate constant for binding, and k_{dis} is a first order rate constant for dissociation of the binding complex. In this model the rate of adsorption is transport and capacity limited, and depends on the concentration of adsorbate, C_1 , the rate constants for binding, k_b and k_{dis} , as well as the moles of adsorption sites available, $(n_{\text{sat}} - n)$.

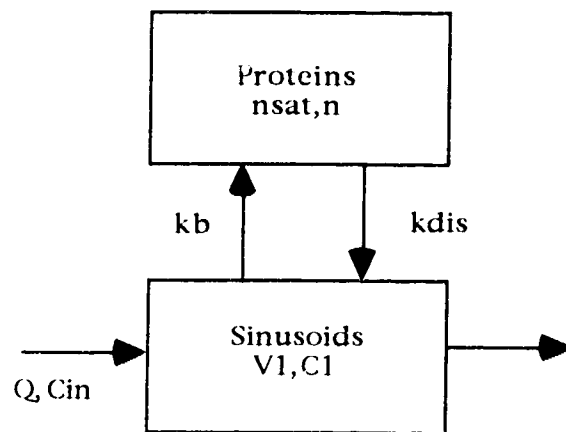


Figure 4.8 Compartmental model of Langmuir adsorption model.

The assumptions inherent in the Langmuir adsorption model are as follows (Gates, 1992):

1. All binding sites are equivalent.
2. Interactions between bound molecules are negligible.
3. Only one molecule of adsorbate can be bound to each binding site.

When using this model for binding to liver tissue these assumptions are not necessarily valid. It is possible that many different binding proteins may be available to the drug or metabolites. These proteins may have multiple binding sites and the interaction between bound molecules is unknown. Thus the model is used to give an approximate overall binding isotherm. The parameters of n_{sat} , k_b , and k_{dis} must be regarded as apparent parameters to describe this average binding isotherm.

In order to describe the dynamics of diltiazem and its metabolites, a three compartment model has been proposed which combines the two compartment model of Saville et al. (1992a) and the Langmuir model described above. This model is illustrated schematically in Figure 4.9. The first compartment represents the sinusoids where material can flow through the liver. The second compartment represents partitioning of the drug into the liver tissue. The third compartment represents saturable binding to liver proteins. The amount of drug and metabolites in each compartment can be described by the following equations:

Diltiazem in compartment 1:

$$V_1 \frac{dC_{1,DZ}}{dt} = Q(C_{\text{in}} - C_{1,DZ}) - V_1 k_{12,DZ} C_{1,DZ} + V_2 k_{21,DZ} C_{2,DZ} - V_1 k_{13}(n_3^{\text{sat}} - n_3) C_{1,DZ} + k_3 n_{3,DZ} \quad 4.4$$

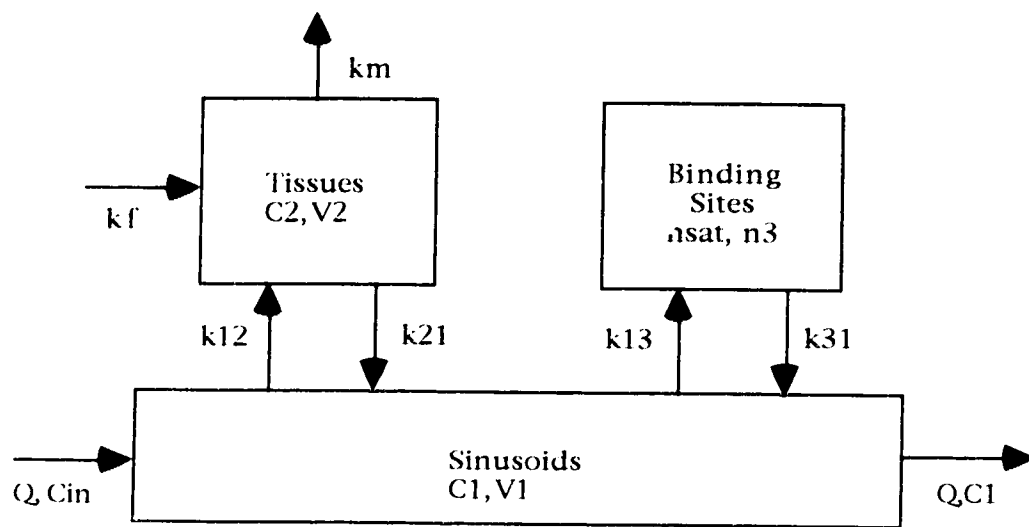


Figure 4.9 Three compartment model proposed for diltiazem metabolism.

Diltiazem in compartment 2:

$$V_2 \frac{dC_{2,DZ}}{dt} = V_1 k_{12,DZ} C_{1,DZ} - V_2 k_{21,DZ} C_{2,DZ} - V_2 k_{m,DZ} C_{2,DZ} \quad 4.5$$

Diltiazem in compartment 3:

$$\frac{dn_{3,DZ}}{dt} = V_1 k_{13}(n_3^{\text{sat}} - n_3) C_{1,DZ} - k_{31} n_{3,DZ} \quad 4.6$$

Metabolites in compartment 1:

$$\begin{aligned} V_1 \frac{dC_{1,M}}{dt} = & -QC_{1,M} - V_1 k_{12,M} C_{1,M} + V_2 k_{21,M} C_{2,M} \\ & - V_1 k_{13}(n_3^{\text{sat}} - n_3) C_{1,M} + k_{31} n_{3,M} \end{aligned} \quad 4.7$$

Metabolites in compartment 2:

$$V_2 \frac{dC_{2,M}}{dt} = V_1 k_{12,M} C_{1,M} - V_2 k_{21,M} C_{2,M} + V_2 k_{f,M} C_{2,DZ} \quad 4.8$$

Metabolites in compartment 3:

$$\frac{dn_{3,M}}{dt} = V_1 k_{13}(n_3^{\text{sat}} - n_3) C_{1,M} - k_{31} n_{3,M} \quad 4.9$$

where,

$$n_3 = n_{3,DZ} + n_{3,M} \quad 4.10$$

The rate constants for cellular release and uptake are given by k_{12} and k_{21} respectively for both diltiazem, DZ, and total metabolites, M. The rate constants for binding and dissociation of both diltiazem and metabolites are k_{13} and k_{31} respectively. The rate constants for metabolism of diltiazem and formation of metabolites is given by $k_{m,DZ}$ and $k_{f,M}$ respectively. If all diltiazem was reacted to form the measured metabolites these two values would be equal. However,

there are metabolites that are formed, particularly at low concentrations of diltiazem (Sugawara et al., 1988), that were not measured in these experiments.

The following assumptions are inherent in this model:

1. Diltiazem partitions differently than its metabolites, since metabolites are usually more polar than the parent compound.
2. The binding parameters k_{13} , k_{31} , and n_3^{sat} are the same for both diltiazem and its metabolites since there is no qualitative evidence to support a difference. This model will yield apparent binding parameters that will describe an average binding isotherm.
3. The rate constant for metabolism of diltiazem is constant during the experiment. Due to the saturable kinetics of some of the minor pathways (Hussain et al., 1994), the apparent first order rate constants will be larger at low concentrations of diltiazem. The error due to this approximation will be most significant at early times when binding is decreasing the diltiazem concentration significantly, and during the prolonged washout when diltiazem concentration is low.

This model accounts for both partitioning of the drug into the liver tissue and nonlinear binding to liver proteins and thus qualitatively agrees with the experimental observations of Hussain et al. (1994).

4.3 Numerical Methods

In order to determine the quantitative ability of the proposed diltiazem model to describe the experimental results of Hussain et al. (1994) as well as the experiments completed in this study, computer simulations of the experimental data were performed. The model equations were expected to be stiff equations and thus were numerically integrated using Gear's method (Burden et al.,

1989). This method of numerical integration is recommended due to its ability to use special predictor-corrector pairs suitable for stiff equations (Lambert, 1973). Gear's method can also control the step size and order of the approximation and thereby minimize the computational effort required to meet the specified local error (Lambert, 1973).

In order to estimate the model parameters that best described the experimental data, the simplex search technique of Nelder and Mead (1965) was used. This technique minimized the error between the simulation and the experimental data by manipulating the six model parameters k_{12} , k_{21} , k_{13} , k_{31} , k_{m0} and n_{sat} (Aaby et al., 1974). The error was calculated as the sum of squared residuals (SSR_{TOT}) for both the simulated diltiazem (SSR_{DZ}) and metabolite (SSR_M) curves as given by the following equations:

$$SSR_{TOT} = SSR_{DZ} + SSR_M \quad 4.11$$

$$SSR_{DZ} = \sum_{i=1}^N (C_{DZ,exp} - C_{1,DZ,sim})^2 \quad 4.12$$

$$SSR_M = \sum_{i=1}^N (C_{M,exp} - C_{1,M,sim})^2 \quad 4.13$$

Parameter estimation along with numerical integration were accomplished using Matlab (1993). A sample of these Matlab m-files can be found in Appendix D.

4.4 Simulation Results

The three compartment model was very successful at describing the dynamic metabolism of diltiazem. Figure 4.10 demonstrates the ability of the simulation to describe the stop-flow experiments completed in this study. The

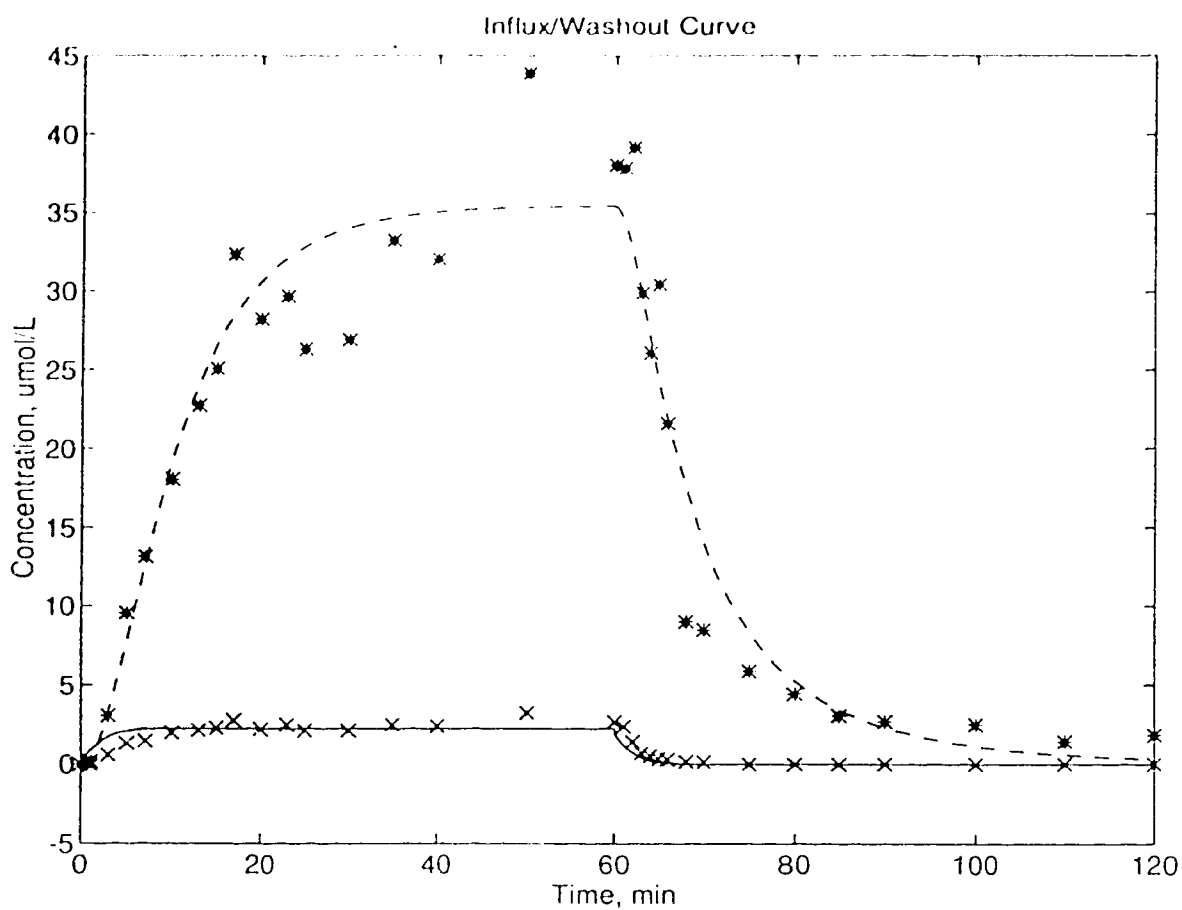


Figure 4.10 Experimental (x) and simulated (—) concentration profiles for diltiazem and experimental (*) and simulated (- -) concentration profiles for total metabolites in the effluent of an isolated liver from Rat #7 with inlet diltiazem concentration of 37.71 μ M.

simulations of the three other experiments completed in this study as well the five experiments of Hussain et al. (1994) can be found in Appendix E. The error is given in Table 4.2 measured as the sum of squared residuals. The parameter estimates for each simulation are listed in Tables 4.3, 4.4, and 4.5. The parameters obtained by the simulations appear consistent within the interindividual variability observed previously (Chaffman et al., 1985, Hermann et al., 1985) with the exception of Rat #8. The high interindividual variability of these experiments is translated to a wide range in the magnitudes of the data, however the trends of the variables for each rat is generally maintained in all simulations. The experimental data for Rat #8 shows a large scatter in the data and the parameters appear to be very different from the other experiments and thus is considered to be an outlier.

Table 4.2 Sum of squared residuals.

Rat #	SSR _{DZ}	SSR _M	SSR _{TOT}
5	0.06860	41.83	41.90
6	0.0646	28.47	28.54
7	7.201	441.1	448.3
8	29.20	311.0	340.2
63*	6.853	27.92	34.78
64*	6.074	2.840	8.914
65*	11.91	12.60	24.51
66*	1.995	7.377	9.372
67*	16.73	9.299	26.03

*-experimental data from Hussain et al. (1994).

Table 4.3 Three compartment optimization parameters.

Rat #	k _{12,DZ} min ⁻¹	k _{21,DZ} min ⁻¹	k _{m,DZ} min ⁻¹	K _{p,DZ}
5	1586	1.010	11.23	277.3
6	3908	1.488	52.38	463.5
7	2537	4.699	0.5051	95.27
8	3651	51.43	4.008	12.53
63*	1994	1.527	0.1630	230.5
64*	1088	0.7810	0.1198	245.9
65*	1731	1.533	0.1839	199.2
66*	2026	1.173	0.1417	304.9
67*	1086	1.165	0.1221	164.4

*-experimental data from Hussain et al. (1994).

Table 4.4 Three compartment optimization parameters for total measured metabolites.

Rat #	$k_{12,M}$ min^{-1}	$k_{21,M}$ min^{-1}	$k_{f,M}$ min^{-1}	$K_{p,M}$
5	377.6	2.313	10.20	28.81
6	735.7	5.687	44.57	22.83
7	2440	20.68	0.5045	20.82
8	15450	83.60	3.528	32.61
63*	483.3	8.432	0.1036	10.12
64*	26.03	2.458	0.08790	1.869
65*	579.0	11.00	0.1666	9.289
66*	159.3	6.579	0.1021	4.272
67*	23.39	2.816	0.08120	1.466

*-experimental data from Hussain et al. (1994).

Table 4.5 Three compartment optimization parameters for binding.

Rat #	k_{13} $\mu\text{mol}/\text{min}$	k_{31} min^{-1}	n_3^{sat} $\mu\text{mol}/\text{g liver}$
5	2.365	33.75	104.0
6	11.92	28.53	309.7
7	10.20	163.1	187.3
8	181.8	1895	46.40
63*	15.52	7.162	83.39
64*	7.322	13.98	85.30
65*	10.45	34.70	161.5
66*	3.569	10.66	57.62
67*	3.286	9.188	102.4

*-experimental data from Hussain et al. (1994).

The rate constants for mass transport of diltiazem into the liver tissue were significantly higher than for metabolism, therefore, cellular metabolism was considered to be the rate limiting step in the dynamic process. The rate constants for cellular uptake of both diltiazem and metabolites were consistently higher than for release from the cells, in accordance with a high affinity for the liver tissue. A partition coefficient, K_p , was defined to describe the magnitude of partitioning in the liver for both diltiazem and the metabolites:

$$K_p = \frac{k_{12}V_1}{k_{21}V_2} \quad 4.14$$

These values for diltiazem and its metabolites are also listed in Tables 4.3 and 4.4. These values generally show a high partitioning of diltiazem into the tissue. The metabolites show a lower extent of partitioning but retain the lipophilic properties of diltiazem. This result was in agreement with the polarity of the metabolites relative to the parent drug. Thus, in summary, the parameters obtained with the proposed three compartment model appear to be consistent with the qualitative properties of diltiazem metabolism.

At early times the predicted concentration of diltiazem was higher than the experimentally observed concentration. This mismatch was likely due to the assumption that the metabolism of diltiazem was constant. At early times the rate constant for metabolism would be much higher due to minor pathways which saturate as the concentration of diltiazem increases. This conclusion is supported by the simulation results for Rats #5 and 6. The inlet concentration for these two experiments was 11.59 and 12.05 μM respectively. The rate constants for metabolism and formation of metabolites were much larger than in experiments whose inlet concentrations were between 30.89 and 51.16 μM . From these data it can be inferred that the rate constant for metabolism of diltiazem increases as the concentration decreases. However, the metabolism was analyzed using an apparent first order rate constant for simplicity which yields the conclusion that the reaction was not a first order reaction.

In summary, the three compartment model was successful in including the main features involved in the metabolism of diltiazem and in representing the experimental data. Protein binding and partitioning are the two most important processes in this dynamic process. The Langmuir model for protein binding of drug and metabolites, in combination with linear partitioning was appropriate to describe the liver functions involved in diltiazem metabolism.

CHAPTER 5 - CONCLUSIONS AND FURTHER WORK

The three compartment model proposed for the metabolism of diltiazem in Figure 4.7, which incorporates a Langmuir adsorption model for protein binding and linear partitioning occurring in parallel, provides a good description of experimental data from the isolated perfused rat liver. The only exception was for Rat #8, which was considered to be an outlier. The estimated partition coefficients for diltiazem, $K_{p,DZ}$, and metabolites, $K_{p,M}$, ranged from 95.27 to 463.5 and 1.466 to 28.81 respectively. These values agree with the lipophilic properties of diltiazem and metabolites as well as the increased polarity of the metabolites produced. The metabolic rate constant for diltiazem, $k_{m,DZ}$, ranged from 0.1198 to 52.38 min^{-1} and appears to be dependent on the inlet concentration of diltiazem. In the range of 30 to 50 μM inlet diltiazem concentration, the metabolic rate constant for diltiazem was between 0.1198 and 0.5051 min^{-1} which is much lower than the partition rate constants for diltiazem. Therefore, in this concentration range, the metabolism of diltiazem was considered to be the rate limiting step in this dynamic system. The estimated number of available binding sites in the liver ranged from 57.62 to 309.7 $\mu\text{mol/g}$ liver, indicating that the number of sites was very large.

The concentration profiles for diltiazem and total metabolites were adequately described with the three compartment model except at early efflux times. Since the metabolism of diltiazem was described by a constant rate of metabolism, the model over-predicts the concentration profile when minor pathways have not yet been saturated and increase the metabolic rate constant dramatically. It may be useful to have a greater understanding of the changes in the rate of metabolism with diltiazem concentration in the liver.

Extending the diltiazem model to predict the concentration profiles for the M1 and MA metabolites may be useful since it has been found that these metabolites also have pharmacological activity in the body (Chaffman et al., 1985). In order to achieve this an estimate for the metabolic rate constants must be obtained by infusing the metabolites into the isolated rat liver and measuring the effluent metabolite concentration profiles. This would also yield a more accurate estimate for the binding and partitioning characteristics of these metabolites.

This model may be extended to a variety of applications. Since diltiazem is predominantly metabolized by the liver (Chaffman et al., 1985), a whole body model may be constructed by simply connecting the inlet and outlet of the liver compartment with another compartment representing the peripheral tissues. The model may also be used to predict the outlet concentration profile for a transient inlet concentration such as the case with orally administered drugs which absorb into the blood from the gastrointestinal system. However, this would require an adequate mathematical expression to describe the inlet concentration profile.

CHAPTER 6 - REFERENCES

- Adby, P.R., and Dempster, M.A.H.: "The Simplex Search Technique", in Introduction to Optimization Methods, 45-48, Chapman and Hall, London, (1974).
- AHFS Drug Information: "Cardiac Drugs", in *American Hospital Formulary Service Drug Information 91*, Bethesda: American Society of Hospital Pharmacists, 871-874, (1991).
- Burden, R.L., and Faires, J.D.: "Stiff Differential Equations", in Numerical Analysis, 4th edition, 303-308, PWS-Kent Publishing Company, Boston, (1989).
- Chaffman, M., and Brogden, R.N.: "Diltiazem: A Review of its Pharmacological Properties and Therapeutic Efficacy", *Drugs*, 29, 387-454, (1985).
- DeCoursey, R.M.: "Liver" in The Human Organism, 4th edition, 438-445, McGraw-Hill Book Company, New York, (1974).
- Dorland's Pocket Medical Dictionary, 24th edition, D.M. Anderson ed., W.B. Saunders Company, Philadelphia, (1982).
- Fogler, H.S.: Elements of Chemical Reaction Engineering, 2nd edition, H.S. Fogler and C. Vennema eds., 708-803, Prentice Hall, New Jersey, (1992).
- Gates, B.C.: "Adsorption and the Kinetics of Polymer Catalyzed Reactions" in Catalytic Chemistry, 188-205, John Wiley and Sons, Inc., New York, (1992).
- Gibaldi, M., and Perrier, D.: "Nonlinear Binding", in Pharmacokinetics, 2nd edition, 307-313, Marcel Dekker Inc., New York, (1982).
- Hermann, P., and Morselli, P.L.: "Pharmacokinetics of Diltiazem and Other Calcium Entry Blockers", *Acta . Pharmacol. Toxicol.*, 57 (suppl II), 10-20, (1985).
- Hussain, M.D.: Kinetics of Diltiazem in Rats and Humans, Ph.D. Thesis, University of Alberta, Edmonton, (1993).
- Hussain, M.D., Tam, Y.K., Finegan, B.A., and Coutts, R.T.: "A Simple and Sensitive High-Performance Liquid Chromatographic Method for the Determination of Diltiazem and Six of Its Metabolites in Human Plasma", *J. Chromatogr.*, 582, 203-209, (1992).
- Hussain, M.D., Tam, Y.K., Gray, M.R., and Coutts, R.T.: "Mechanisms of Time-dependent Kinetics of Diltiazem in the Isolated Perfused Rat Liver", *Drug Metabo. Disp.*, 22(1), 36-42, (1994).
- Kwong, T.C., Sparks, J.D., and Sparks, C.E.: "Lipoprotein and Protein Binding of Calcium Channel Blocker Diltiazem", *Proc. Soc. Exp. Biol. Med.*, 178, 313-316, (1985).

- Lambert, J.D.: "Implementation of Predictor-Corrector Methods: Gear's Method", in Computational Methods in Ordinary Differential Equations, 108-113, John Wiley and Sons, Inc., New York, (1973).
- Levenspiel, O.: "Single Ideal Reactors", in Chemical Reaction Engineering, 2nd edition, 97-123, John Wiley and Sons, New York, (1972).
- Matlab, Version 4.1.1, The MathWorks, Inc., Natick, Mass., (1993).
- Miller, L.L.: "Techniques of Isolated Rat Liver Perfusion", in Isolated Rat Liver Perfusion and its Applications, I. Bortosek, A. Guaitani, and L.L. Miller, eds., 11-52, Raven Press, New York, (1973).
- Motta, P., Muto, M., and Fujita, T.: The Liver: An Atlas of Scanning Electron Microscopy, Igaku Shoin, New York, (1978).
- Nelder, J.A., and Mead, R.: "A Simplex Method for Function Minimization", *Comput. J.*, 7, 308-315, (1965).
- The New Merriam-Webster Dictionary, F.C. Mish et al. eds, Merriam-Webster Inc., Springfield, Mass., (1989).
- Saville, B.A., Gray, M.R., and Tam, Y.K.: "Experimental Studies of Transient Mass Transfer and Reaction in the Liver: Interpretation Using a Heterogeneous Compartment Model", *J. Pharm. Sci.*, 81(3), 265-271, (1992a).
- Saville, B.A., Gray, M.R., and Tam, Y.K.: "Models of Hepatic Drug Elimination", *Drug Metabo. Rev.*, 24(1), 49-88, (1992b).
- Shargel, L., and Yu, A.B.C.: "Hepatic Elimination of Drugs", in Applied Biopharmaceutics and Pharmacokinetics, 3rd edition, 293-334, Appleton and Lange, Norwork, (1983).
- Stryer, L.: Biochemistry, 3rd edition, 955, W.H. Freeman and Company, New York, (1988).
- Sugawara, Y., Ohashi, M., Nakamura, S., Usuki, S., Suzuki, T., Ito, Y., Kume, T., Harigaya, S., Nakao, A., Gaino, M., and Inoue, H.: "Metabolism of Diltiazem. I. Structures of New Acidic and Basic Metabolites in Rat, Dog and Man.", *J. Pharmacobio-Dyn.*, 11, 211-213, (1988).
- Tam, Y.K., Yau, M., Berzins, R., Montgomery, P.R., and Gray, M.: "Mechanisms of Lidocaine Kinetics in the Isolated Perfused Rat Liver. I. Effects of Continuous Infusion", *Drug Metabo. Disp.*, 15(1), 12-16, (1987).
- Weisiger, R.A.: "Dissociation From Albumin: A Potentially Rate-Limiting Step in the Clearance of Substances by the Liver", *Proc. Natl. Acad. Sci. USA*, 82, 1563-1567, (1985).

Appendix A - Experimental Data

	Page
Table A.1 Experimentally measured values.	61
Table A.2 Results of Liver Function Tests.	61

Table A.1 Experimentally measured values.

Rat #	Inlet Concentration (μ M)	Liver Weight (g)	Flow Rate (ml./min)	Rat Weight (g)
3	0.663	12.9	28.1	265.5
4	0.708	14.0	28.0	281.2
5	11.59	12.5	30.4	250.0
6	12.05	11.8	30.0	248.7
7	37.71	11.8	27.5	230.6
8	51.16	13.0	28.4	226.0
63*	41.18	10.3	30.0	NA
64*	34.73	9.9	30.0	NA
65*	39.79	9.6	29.0	NA
66*	30.89	9.4	29.0	NA
67*	42.87	9.5	30.0	NA

* - experimental data from Hussain et al. (1994)

NA - not available

Table A.2 Results of Liver Function Tests.

Rat #	Time of Test min	ALP IU/L	AST IU/L	ALT IU/L
3	0	2.1	15.0	1.4
3	120	1.1	5.4	5.5
4	0	1.1	10.2	1.7
4	120	1.7	10.2	0.6
5	0	0.9	0.2	1.0
5	120	1.2	9.8	0.8
6	0	1.2	14.0	3.8
6	120	1.3	13.5	2.6
7	0	1.6	9.0	1.4
7	120	0.7	8.6	19.3
8	0	0.9	11.1	2.3
8	120	0.8	15.5	3.5

IU/L = Imperial Units per Litre

ALP = Alkaline Phosphatase

AST = Aspartate Amino Transferase

ALT = Alanine Amino Transferase

Appendix B - HPLC Standard Curves

	Page
Figure B.1 Typical standard curve for M6.	63
Figure B.2 Typical standard curve for M4.	64
Figure B.3 Typical standard curve for M2.	65
Figure B.4 Typical standard curve for MA.	66
Figure B.5 Typical standard curve for M1.	67

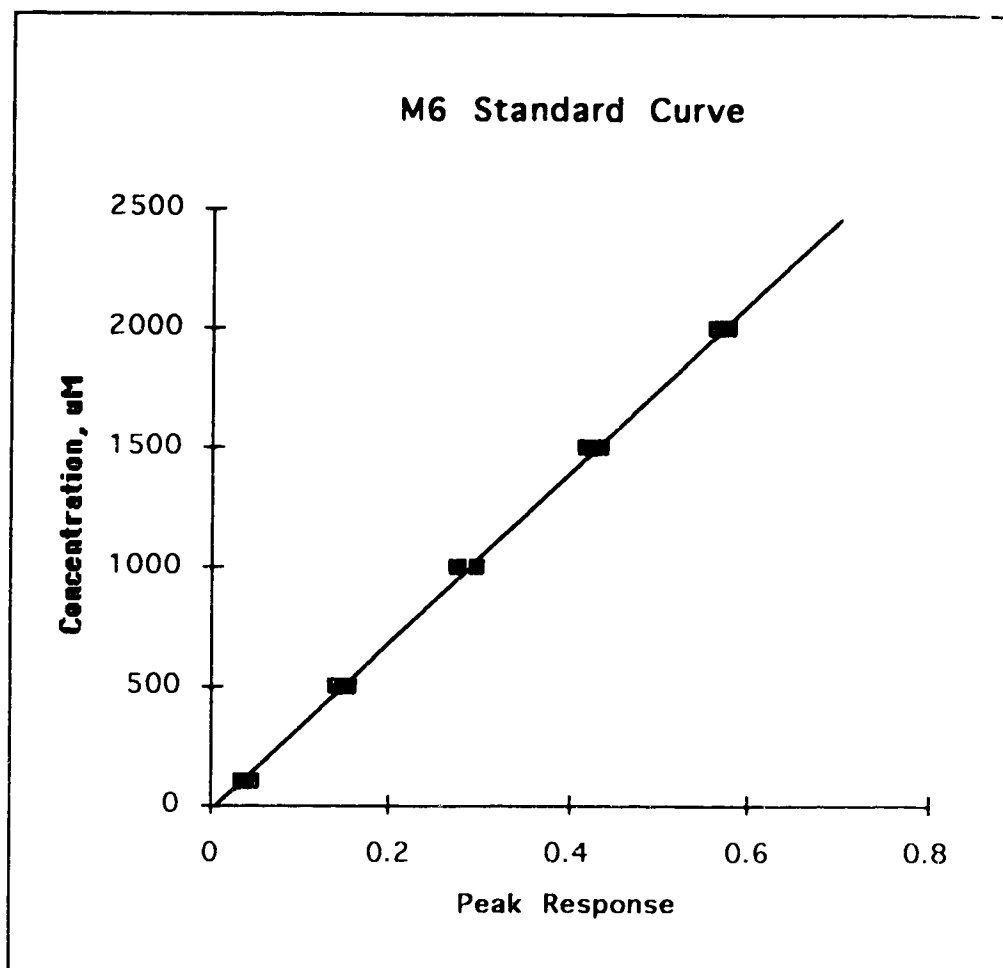


Figure B.1 Typical standard curve for M6. The coefficient of determination, $r^2=0.9984$. The calibration equation was calculated to be:
M6 concentration = $-20.91 + 3544 * \text{Peak Response} * \text{Internal Standard Area}$

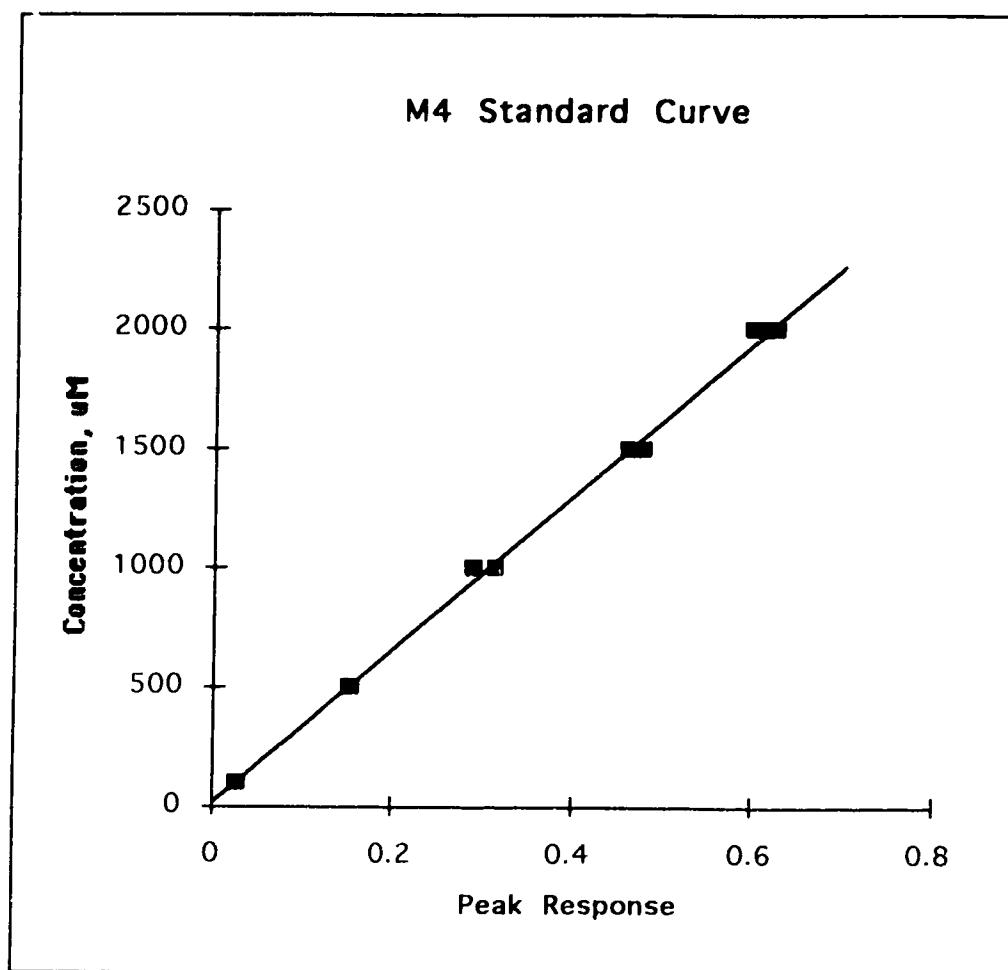


Figure B.2 Typical standard curve for M4. The coefficient of determination, $r^2=0.9987$. The calibration equation was calculated to be:

$$\text{M4 concentration} = 13.57 + 3219 * \text{Peak Response} * \text{Internal Standard Area}$$

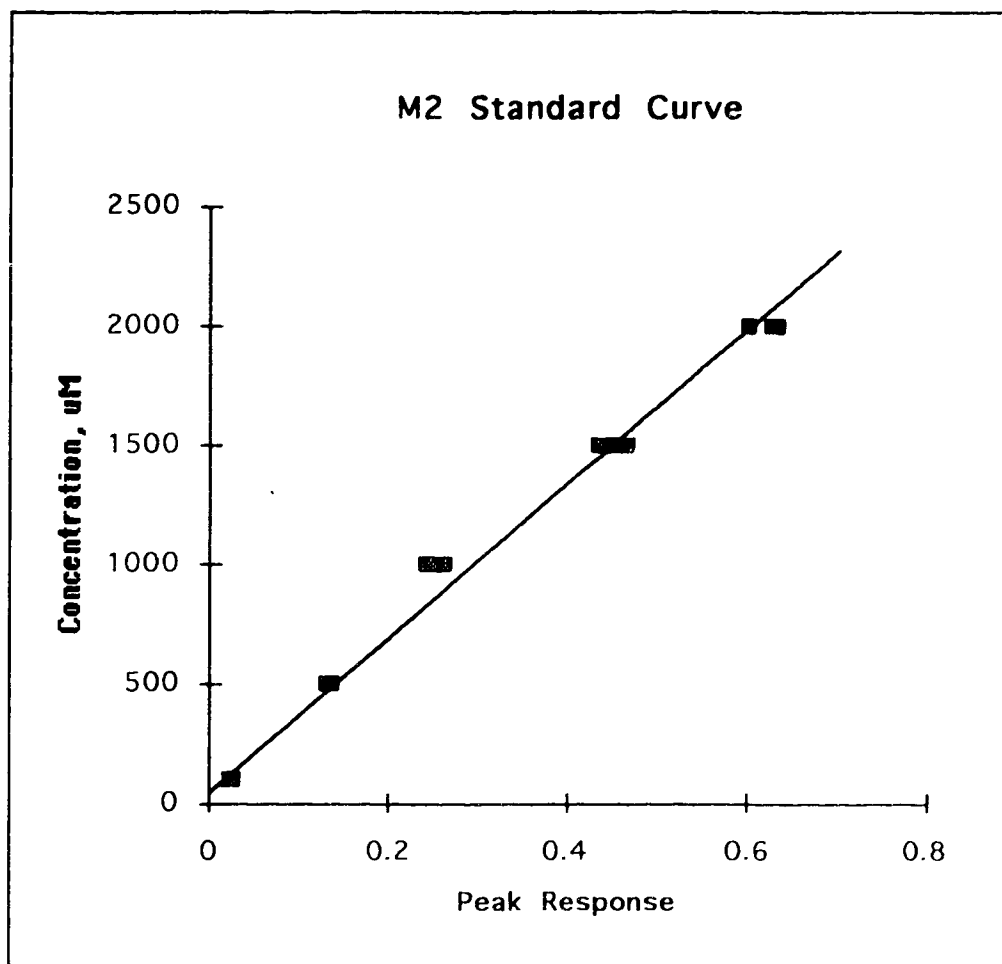


Figure B.3 Typical standard curve for M2. The coefficient of determination, $r^2=0.9961$. The calibration equation was calculated to be:

$$\text{M2 concentration} = 35.91 + 3241 * \text{Peak Response} * \text{Internal Standard Area}$$

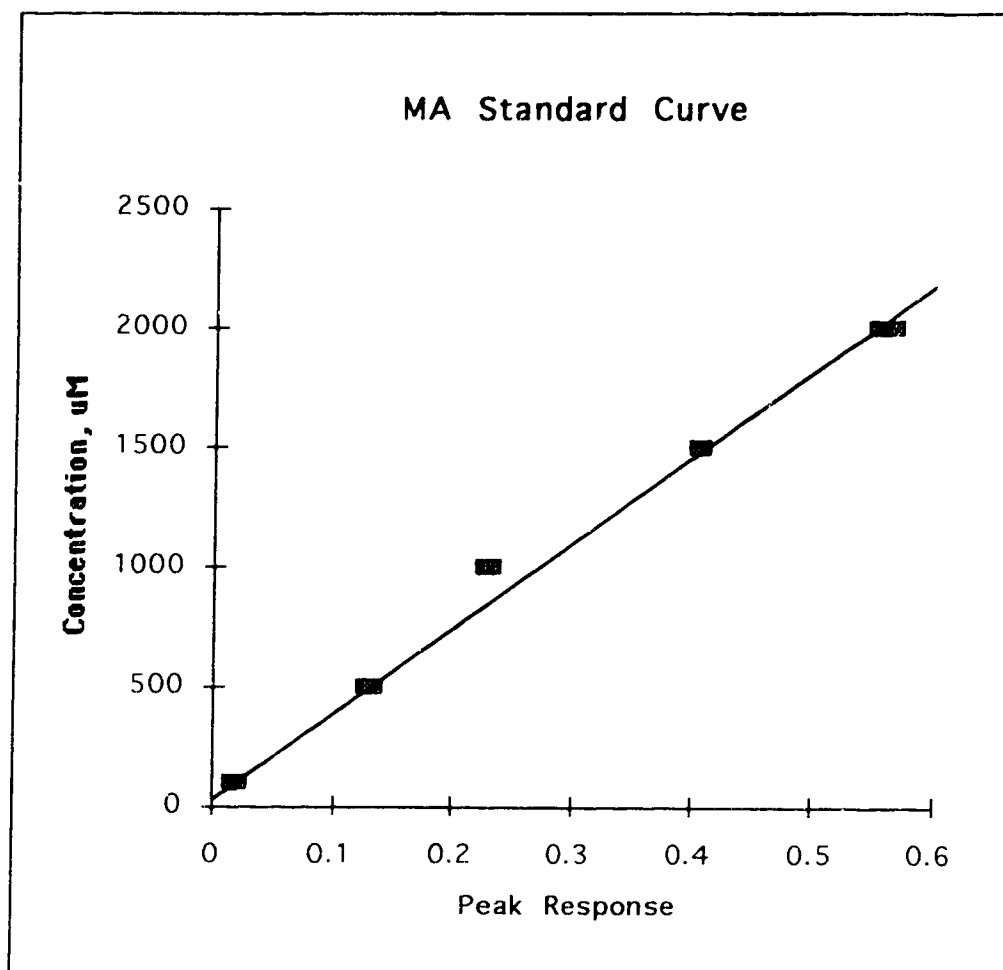


Figure B.4 Typical standard curve for MA. The coefficient of determination, $r^2=0.9973$. The calibration equation was calculated to be:

$$\text{MA concentration} = 33.84 + 3579 * \text{Peak Response} * \text{Internal Standard Area}$$

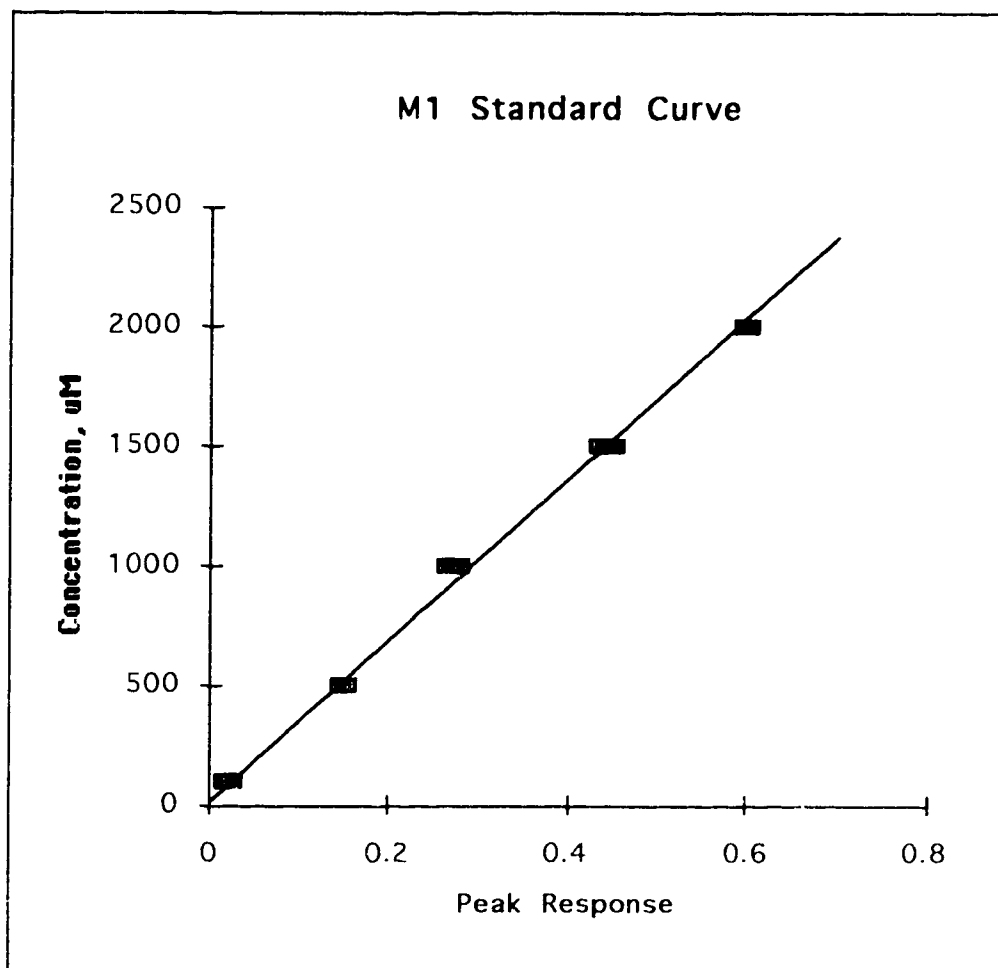


Figure B.5 Typical standard curve for M1. The coefficient of determination, $r^2=0.9965$. The calibration equation was calculated to be:

$$\text{M1 concentration} = 8.528 + 3364 * \text{Peak Response} * \text{Internal Standard Area}$$

Appendix C - Experimental Concentration Data

	Page
Figure C.1 Outlet concentration of radioactive species for Rat #3 obtained by infusing 0.663 μM diltiazem with a radiolabelled tracer for 60 minutes followed by a 60 minute washout period.	70
Table C.1 Experimental data from Rat #3.	71
Figure C.2 Outlet concentration of radioactive species for Rat #4 obtained by infusing 0.708 μM diltiazem with a radiolabelled tracer for 60 minutes followed by a 60 minute washout period.	72
Table C.2 Experimental data from Rat #4.	73
Figure C.3 Outlet concentration of diltiazem and five of its metabolites for Rat #5 obtained by infusing 11.59 μM diltiazem for 60 minutes followed by a 60 minute washout period.	74
Figure C.4 Outlet concentration of diltiazem, DZ, total measured metabolites, M, and total radioactive species, H3, for Rat #5 obtained by infusing 11.59 μM diltiazem with a radiolabelled tracer for 60 minutes followed by a 60 minute washout period. The total radioactive species concentration was obtained by a scintillation counter whereas the diltiazem and metabolite concentrations was obtained by HPLC.	75
Table C.3 Experimental data from Rat #5.	76
Figure C.5 Outlet concentration of diltiazem and five of its metabolites for Rat #6 obtained by infusing 12.05 μM diltiazem for 60 minutes followed by a 60 minute washout period.	77
Figure C.6 Outlet concentration of diltiazem, DZ, total measured metabolites, M, and total radioactive species, H3, for Rat #6 obtained by infusing 12.05 μM diltiazem with a radiolabelled tracer for 60 minutes followed by a 60 minute washout period. The total radioactive species concentration was obtained by a scintillation counter whereas the diltiazem and metabolite concentrations was obtained by HPLC.	78
Table C.4 Experimental data from Rat #6.	79
Table C.5 Experimental data from Rat #7.	80

	Page
Figure C.7 Outlet concentration of diltiazem and five of its metabolites for Rat #8 obtained by infusing 51.16 μ M diltiazem for 60 minutes followed by a 60 minute washout period.	81
Figure C.8 Outlet concentration of diltiazem, DZ, total measured metabolites, M, and total radioactive species, H3, for Rat #8 obtained by infusing 51.16 μ M diltiazem with a radiolabelled tracer for 60 minutes followed by a 60 minute washout period. The total radioactive species concentration was obtained by a scintillation counter whereas the diltiazem and metabolite concentrations was obtained by HPLC.	82
Table C.6 Experimental data from Rat #8.	83
Figure C.9 Outlet concentration of diltiazem and six of its metabolites for Rat #63 obtained by infusing 41.18 μ M diltiazem for 40 minutes followed by a 30 minute washout period.	84
Figure C.10 Outlet concentration of diltiazem and six of its metabolites for Rat #64 obtained by infusing 34.73 μ M diltiazem for 40 minutes followed by a 30 minute washout period.	85
Figure C.11 Outlet concentration of diltiazem and six of its metabolites for Rat #65 obtained by infusing 39.79 μ M diltiazem for 40 minutes followed by a 30 minute washout period.	86
Figure C.12 Outlet concentration of diltiazem and six of its metabolites for Rat #66 obtained by infusing 30.89 μ M diltiazem for 40 minutes followed by a 30 minute washout period.	87
Figure C.13 Outlet concentration of diltiazem and six of its metabolites for Rat #67 obtained by infusing 42.87 μ M diltiazem for 40 minutes followed by a 30 minute washout period.	88

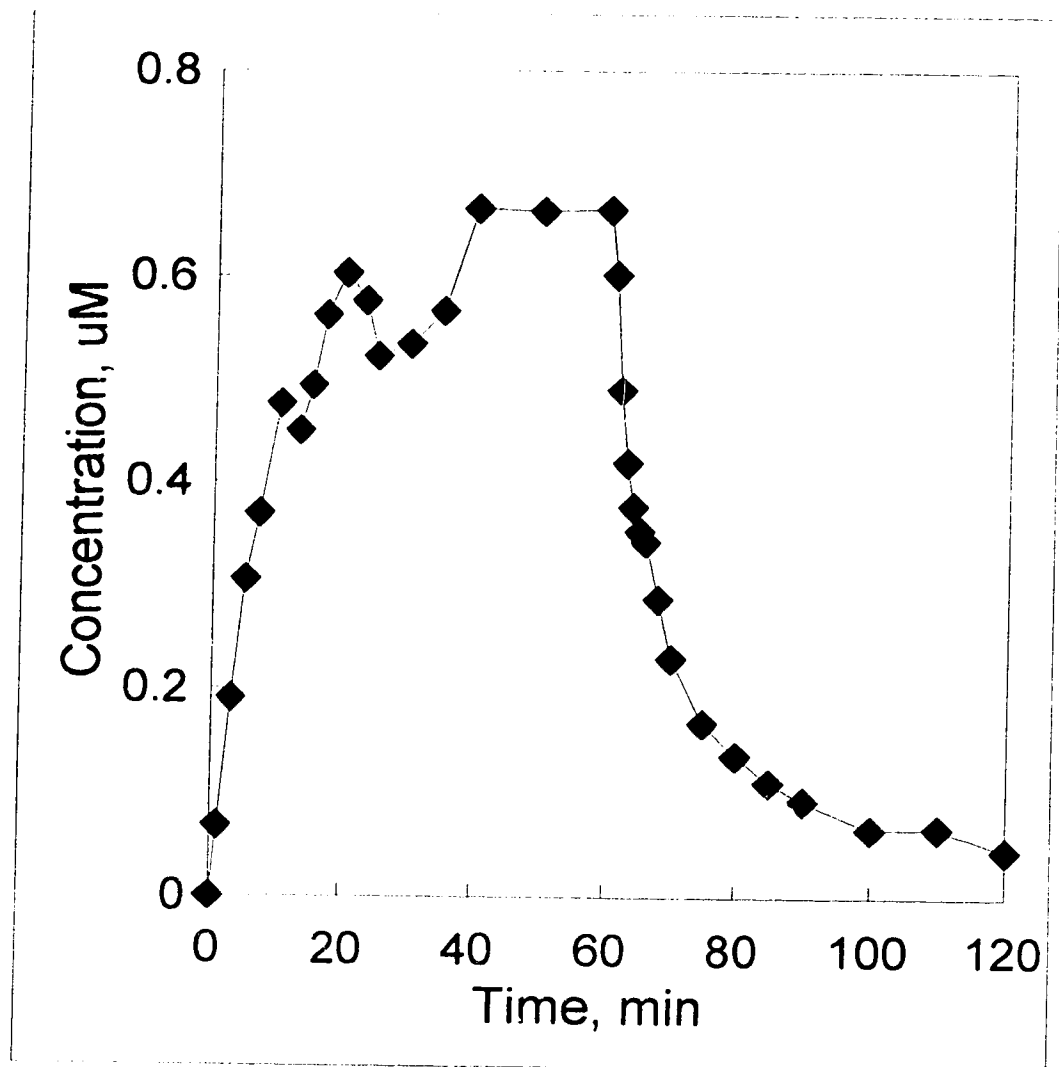


Figure C.1 Outlet concentration of radioactive species for Rat #3 obtained by infusing 0.663 μ M diltiazem with a radiolabelled tracer for 60 minutes followed by a 60 minute washout period.

Concentration Profile, uM - Rat #3.

Time, min	H3
0	0
1	0.0675825
3	0.1918556
5	0.3066586
7	0.3705889
10	0.4769563
13	0.4500655
15	0.4945387
17	0.5629293
20	0.6035241
23	0.5762131
25	0.5230456
30	0.5349396
35	0.5668078
40	0.6664524
50	0.6641577
60	0.6659676
61	0.6020373
62	0.4905633
63	0.4196194
64	0.3772793
65	0.3536852
66	0.343892
68	0.2881389
70	0.2306081
75	0.1682938
80	0.1364579
85	0.1100196
90	0.0924048
100	0.0653201
110	0.066516
120	0.0455398

Table C.1 Experimental data for Rat #3.

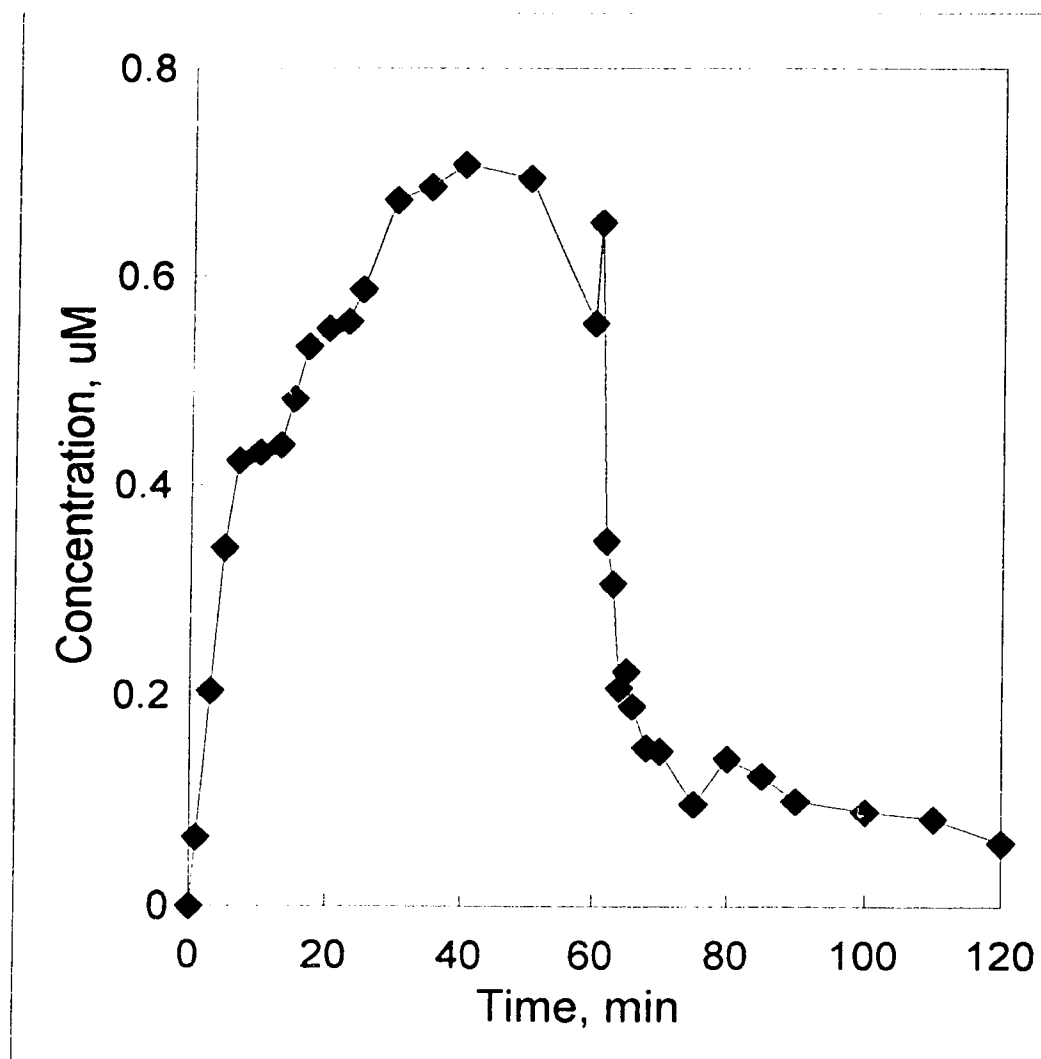


Figure C.2 Outlet concentration of radioactive species for Rat #4 obtained by infusing 0.708 μ M diltiazem with a radiolabelled tracer for 60 minutes followed by a 60 minute washout period.

Concentration Profile, uM - Rat #4

Time, min	H3
0	0
1	0.0648029
3	0.2042816
5	0.3404821
7	0.4238491
10	0.4317017
13	0.4389443
15	0.4830865
17	0.5331373
20	0.5500241
23	0.5570381
25	0.5875717
30	0.6733784
35	0.6856147
40	0.7070377
50	0.6941915
60	0.5551321
61	0.6517647
62	0.3471911
63	0.3065177
64	0.2072549
65	0.222922
66	0.1897581
68	0.1514101
70	0.1475981
75	0.0968613
80	0.1404698
85	0.1240023
90	0.0996059
100	0.0899236
110	0.0831002
120	0.0599999

Table C.2 Experimental data for Rat #4.

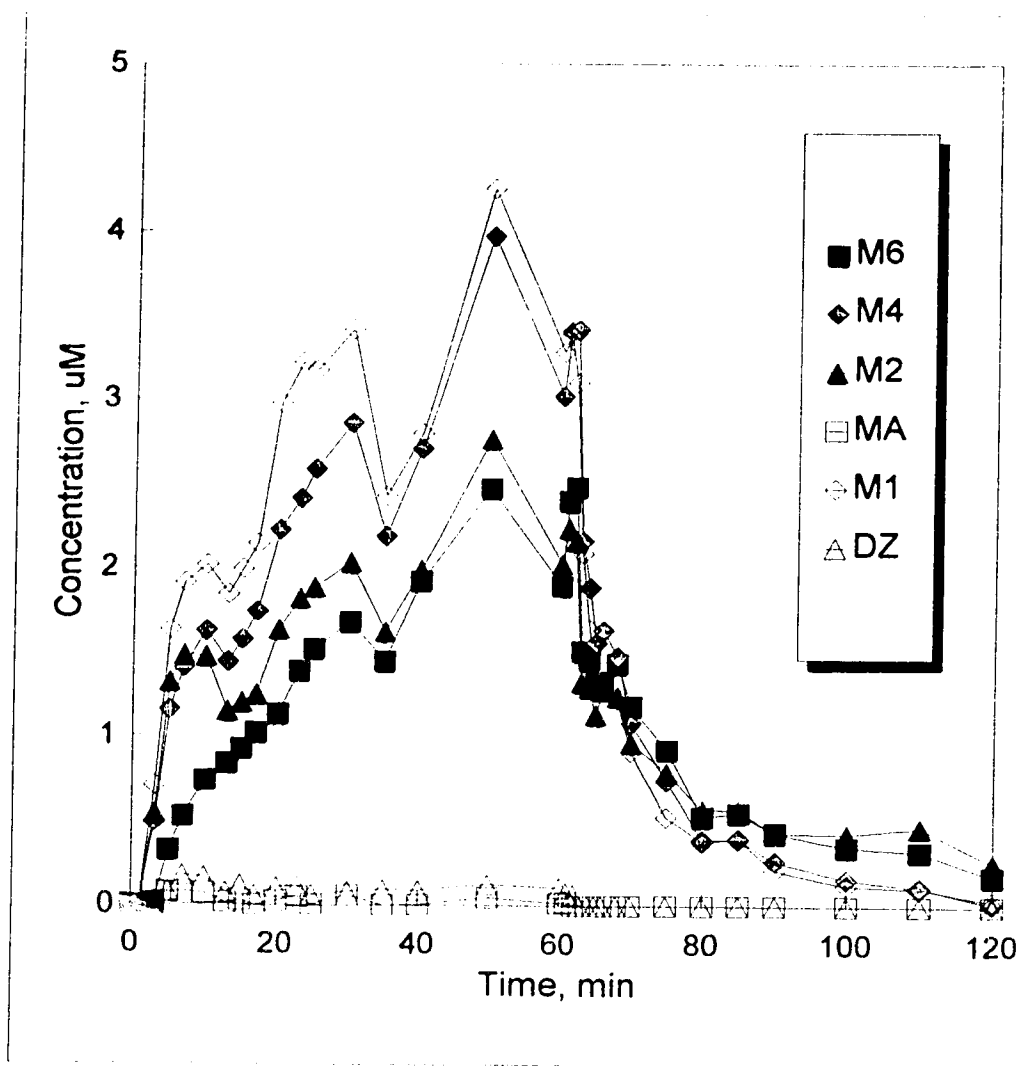


Figure C.3 Outlet concentration of diltiazem and five of its metabolites for Rat #5 obtained by infusing 11.59 μM diltiazem for 60 minutes followed by a 60 minute washout period.

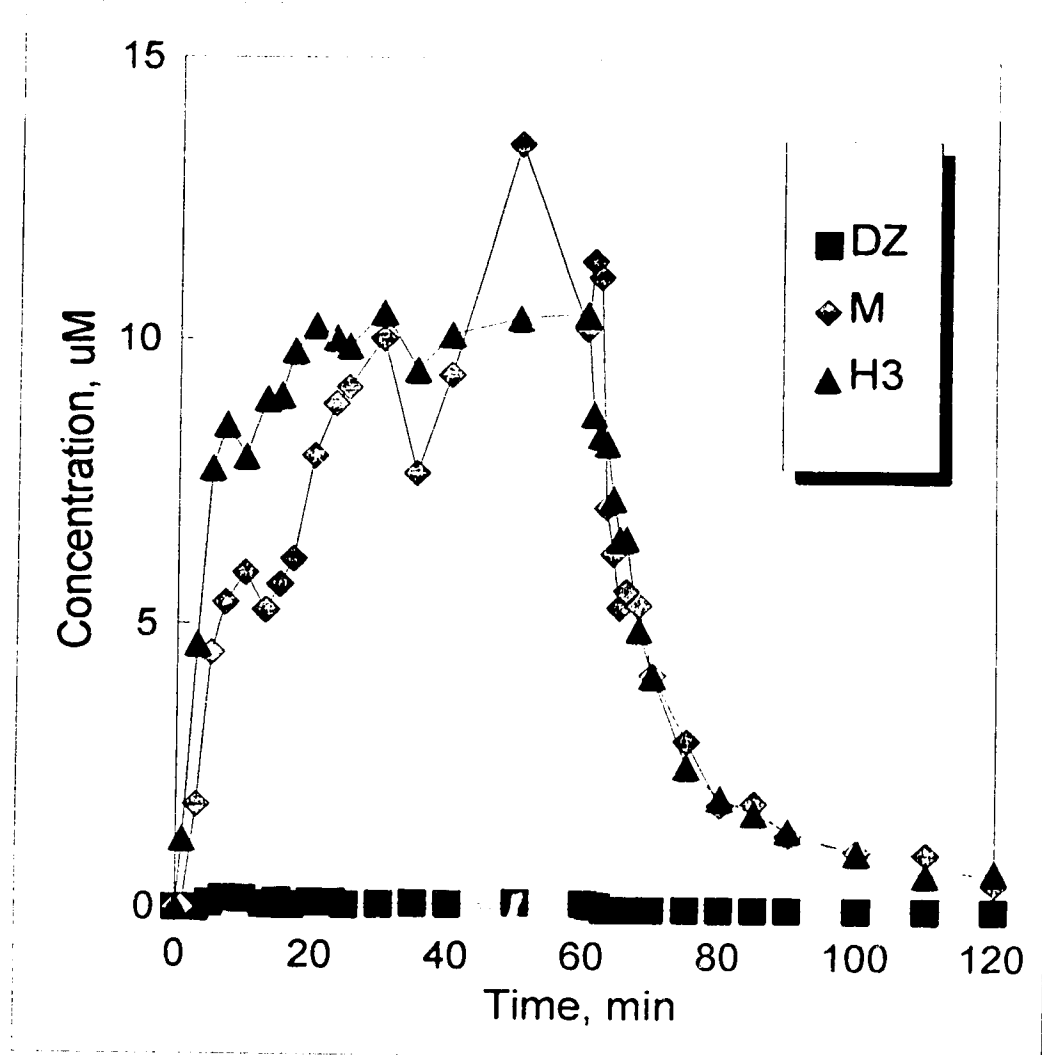


Figure C.4 Outlet concentration of diltiazem, total measured metabolites and radioactive species for Rat #5 obtained by infusing 11.59 μ M diltiazem with a radiolabelled tracer for 60 minutes followed by a 60 minute washout period.

Concentration Profiles, uM - Rat #5

Time, min	M6	M4	M2	MA	M1	DZ	H3
0	0	0	0	0	0	0	0
1	0	0	0	0	0	0	1.2109952
3	0.0132078	0.4871805	0.534403	0.0782548	0.7039414	0	4.6378778
5	0.3189765	1.151923	1.3154873	0.0725355	1.625757	0.0815845	7.7377806
7	0.5167118	1.3976216	1.4738317	0.0762309	1.9070839	0.1672082	8.5076037
10	0.731164	1.6159571	1.4635203	0.0639268	2.0102115	0.1567342	7.9444407
13	0.830758	1.4304528	1.1404561	0.0075221	1.8348619	0.0666256	8.9638158
15	0.918554	1.5669137	1.1932944	0.0250743	1.9893088	0.1137118	9.0250897
17	1.0165641	1.7364558	1.2426557	0	2.1386773	0.0555287	9.8066105
20	1.1265918	2.2208625	1.6296606	0.0218236	2.9739805	0.10185	10.263937
23	1.3832557	2.4114958	1.8160295	0.0523082	3.2186967	0.1086213	10.053377
25	1.5142338	2.5861155	1.8841201	0.0055764	3.1746027	0.0615033	9.9091051
30	1.6758161	2.8575413	2.0322317	0.0584235	3.4095104	0.0790396	10.498449
35	1.4386377	2.1852496	1.6168576	0	2.4206385	0.089146	9.485758
40	1.9179825	2.7016433	1.9848687	0.0016632	2.793693	0.0852311	10.124121
50	2.4661027	3.9708836	2.762547	0.0422725	4.255429	0.1190205	10.423249
60	1.8962375	3.0226913	2.0233864	0.0120694	3.281212	0.1031851	10.507361
61	2.3974201	3.4048859	2.2377713	0.0181144	3.3821575	0.0747104	8.7315319
62	2.4746937	3.4155367	2.1656362	0	3.101903	0.0640964	8.3599892
63	1.5043001	2.1598592	1.3195172	0	2.0849267	0	8.2162741
64	1.45122	1.8855859	1.2893729	0	1.6323424	0	7.2381197
65	1.3233254	1.5527	1.1281806	0	1.3099131	0	6.5290135
66	1.3127633	1.6260616	1.2788294	0	1.3888908	0	6.5407112
7	1.4282499	1.4680264	1.2347084	0	1.2297506	0	4.9470325
70	1.1760094	1.078229	0.962742	0	0.9064076	0	4.1109222
75	0.9190648	0.7369527	0.7864647	0	0.5188255	0	2.5289413
80	0.5213451	0.3860373	0.562683	0	0.3757656	0	1.9774761
85	0.5434184	0.3891388	0.5614206	0	0.3930977	0	1.7056428
90	0.4267351	0.2600508	0.4259973	0	0.2051626	0	1.4131991
100	0.3443064	0.1559757	0.4198091	0	0.118832	0	1.018818
110	0.3187443	0.1108974	0.4586826	0	0.1017661	0	0.6355775
120	0.1742255	0.0101752	0.251818	0	0.0302852	0	0.6974085

Table C.3 Experimental data for Rat #5.

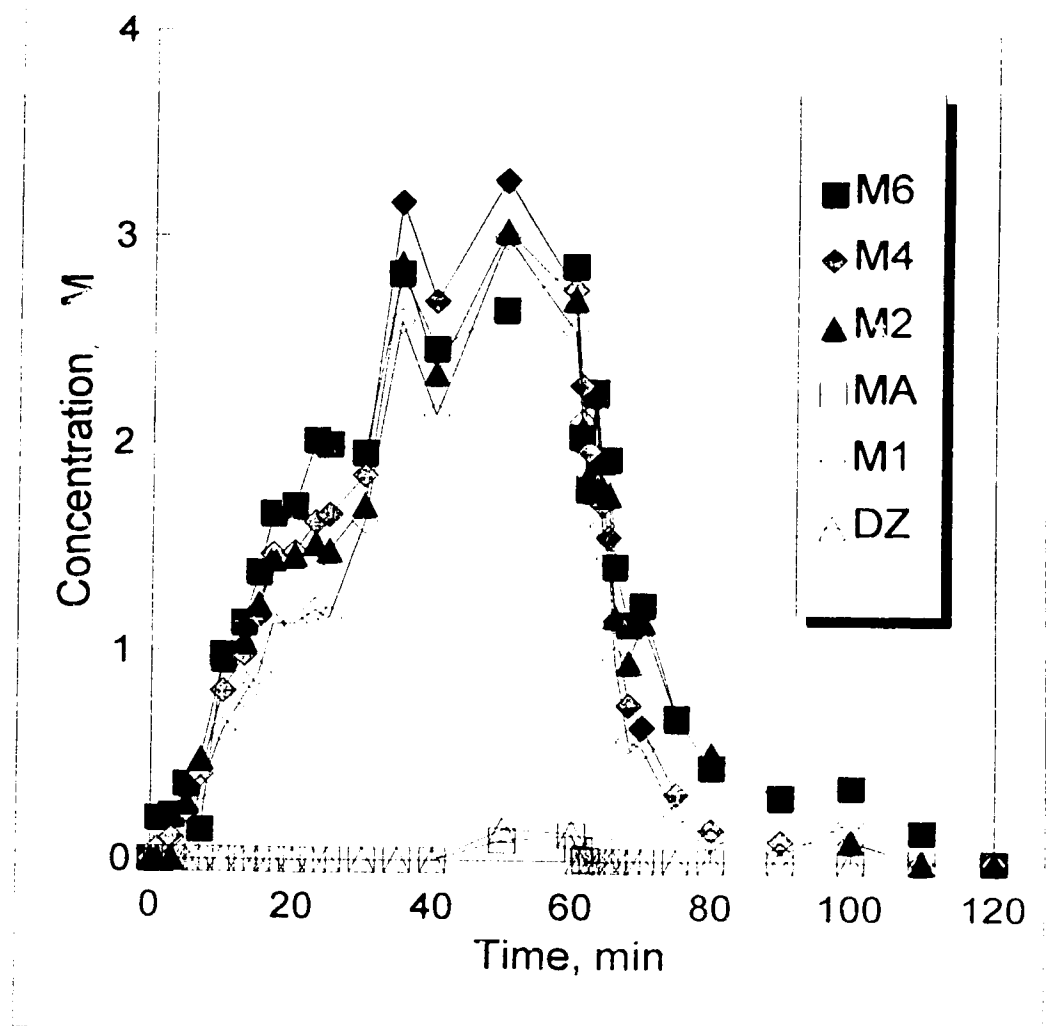


Figure C.5 Outlet concentration of diltiazem and five of its metabolites for Rat #6 obtained by infusing 12.65 μ M diltiazem for 60 minutes followed by a 60 minute washout period.

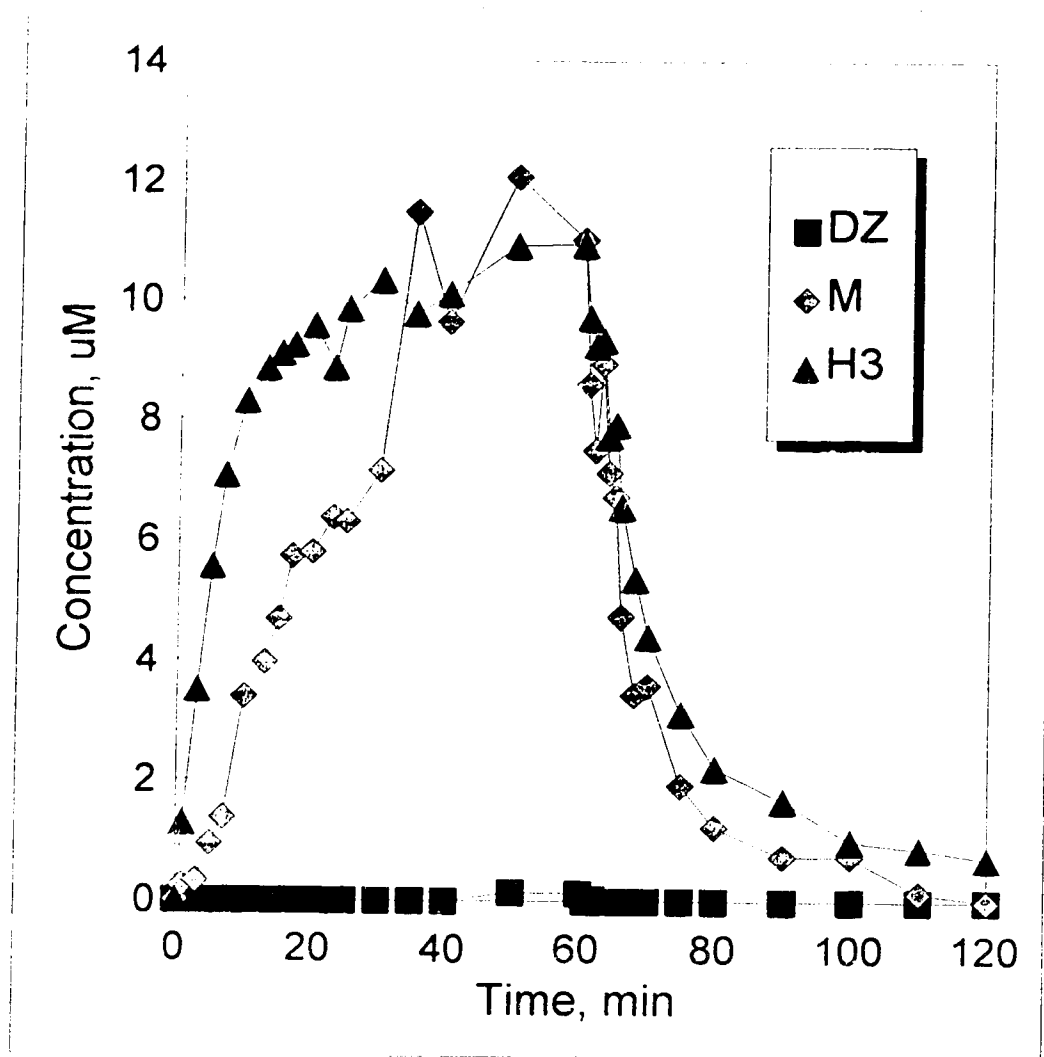


Figure C.6 Outlet concentration of diltiazem, total measured metabolites and radioactive species for Rat #6 obtained by infusing $12.05 \mu\text{M}$ diltiazem with a radiolabelled tracer for 60 minutes followed by a 60 minute washout period.

Concentration Profiles, uM - Rat #6

Time, min	M6	M4	M2	MA	M1	DZ	H3
0	0	0	0	0	0	0	0
1	0.1947762	0.0510906	0	0	0	0	1.2762499
3	0.2037393	0.1004212	0.00844	0	0	0	3.4969582
5	0.3610348	0.2319037	0.2726197	0	0.0692757	0	5.5380628
7	0.1420984	0.4056858	0.4834096	0	0.3355591	0	7.0716888
10	0.984451	0.8110773	0.9621534	0	0.6171134	0	8.2919873
13	1.138464	0.9835939	1.0517066	0	0.7889582	0	8.8492626
15	1.3792867	1.1699434	1.2253106	0	0.8955876	0	9.1044007
17	1.6670685	1.4683471	1.4470467	0	1.1286513	0	9.2526717
20	1.702267	1.478611	1.465191	0	1.1310416	0	9.5715943
23	2.0171963	1.6276838	1.5258942	0	1.1999361	0	8.3554172
25	1.9979077	1.6605967	1.4867352	0	1.1606905	0	9.8597436
30	1.9598031	1.8514126	1.7081255	0	1.6308808	0	10.337568
35	2.8267969	3.1710568	2.8733861	0	2.5957586	0	9.7836498
40	2.4625193	2.6913477	2.3456589	0	2.1395575	0	10.109287
50	2.6512411	3.2812897	3.0349356	0.0977618	3.0031588	0.1483359	10.90995
60	2.8665952	2.7524273	2.7085689	0.1209305	2.5522185	0.1348392	10.922259
61	2.0402912	2.2886539	2.078849	0.0604095	2.1154236	0	9.7137107
62	1.7877377	1.9754543	1.8604686	0.0081026	1.854012	0.0446569	9.2481956
63	2.2631178	2.2306543	2.2529705	0	2.1773217	0.000572	9.3321226
64	1.9263102	1.7160193	1.7965386	0.0554877	1.6164361	0	7.7296765
65	1.9327899	1.5580107	1.765717	0	1.4579982	0	7.9171134
66	1.4166381	1.1546025	1.1777532	0	0.9696429	0	6.5440677
68	1.1374529	0.7522582	0.9579359	0	0.5778018	0	5.3450277
70	1.2295677	0.6469774	1.1532127	0	0.5437535	0	4.3983342
75	0.6950785	0.3233638	0.6823266	0	0.2221678	0	3.1192867
80	0.4508926	0.1520693	0.5183562	0	0.1063854	0	2.2078395
90	0.3117945	0.0975254	0.3072135	0	0.0339135	0	1.6729448
100	0.3591427	0.0942613	0.1008832	0	0.1969726	0	1.0037669
110	0.1441826	0	0	0	0	0	0.882912
120	0	0	0	0	0	0	0.7156175

Table C.4 Experimental data for Rat #6.

Concentration Profiles, μM - Rat 7

Time, min	M6	M4	M2	MA	M1	DZ	H3
0	0	0	0	0	0	0	0
1	0.1365655	0.0636461	0	0	0	0	4.4035454
3	0.2312714	0.8231519	1.1434421	0.1935001	0.6837402	0.5858281	12.866523
5	0.7762533	2.095702	2.91946	0.4853004	3.270699	1.3446331	21.22093
7	1.238309	2.7610623	3.6509548	0.611722	4.8503092	1.4750572	26.844513
10	1.6398456	3.8919445	4.6719681	0.6815241	7.1647933	2.0024853	29.014083
13	2.3263965	4.8988759	5.3799828	0.8712298	9.240735	2.1508642	31.417355
15	2.5125976	5.4239658	5.8946313	0.7971095	10.432729	2.3012022	33.075355
17	3.4458452	6.9152884	7.5526782	0.9711433	13.473491	2.7863983	32.335604
20	3.0428148	6.1151082	6.6614727	0.7743427	11.592033	2.2122074	32.210472
23	3.5955936	6.0334302	7.2425973	0.8030305	11.977605	2.5054466	34.201544
25	3.2339573	5.3228741	6.4081764	0.68254	10.626187	2.1300162	29.332434
30	2.8704789	5.4189736	6.1966429	0.7372178	11.665653	2.135606	32.762525
35	4.1164956	6.5338631	8.0125332	0.7583629	13.807842	2.5022008	35.423422
40	4.1050951	6.2232735	7.7137727	0.6787806	13.292626	2.3941243	35.81906
50	5.941294	8.4088787	10.580994	0.8135735	18.116565	3.2457495	34.529096
60	5.0637492	7.3010928	9.1657603	0.6963774	15.755539	2.6831666	35.392139
61	5.157318	7.4013946	9.0687236	0.6574592	15.517238	2.3825675	29.245945
62	5.6336364	7.8244249	9.5525767	0.5901147	15.506022	1.4240033	27.488576
63	4.7515267	5.990347	7.4927742	0.3771348	11.246138	0.7034015	24.674944
64	4.5992226	5.1136157	6.6859963	0.3581595	9.2939203	0.5220651	23.532193
65	7.6329125	5.2123553	9.0032913	0.2325373	8.3062488	0.3579177	19.235378
66	4.8024038	3.9708132	5.9010951	0.2340913	6.6526635	0.2984642	15.62679
68	1.6680831	1.8046432	2.3140535	0.1270212	3.0663626	0.1638903	13.508745
70	2.4870303	1.3345221	2.5477139	0	2.0912224	0.129071	10.012407
75	2.186627	0.7993111	1.8236587	0	1.0588751	0	6.7368908
80	1.6003934	0.5489343	1.5041994	0	0.7724237	0	4.9942425
85	1.2998238	0.3545881	1.0323803	0	0.3853417	0	3.2368727
90	1.1239558	0.2933734	0.8807772	0	0.3882175	0	2.8246729
100	1.042071	0.2478709	0.931583	0	0.2956485	0	2.4504775
110	0.6061362	0.15628	0.4978369	0	0.1911457	0	0
120	0.8589155	0.1770488	0.5610776	0	0.2556148	0	1.2402798

Table C.5 Experimental data for Rat #7.

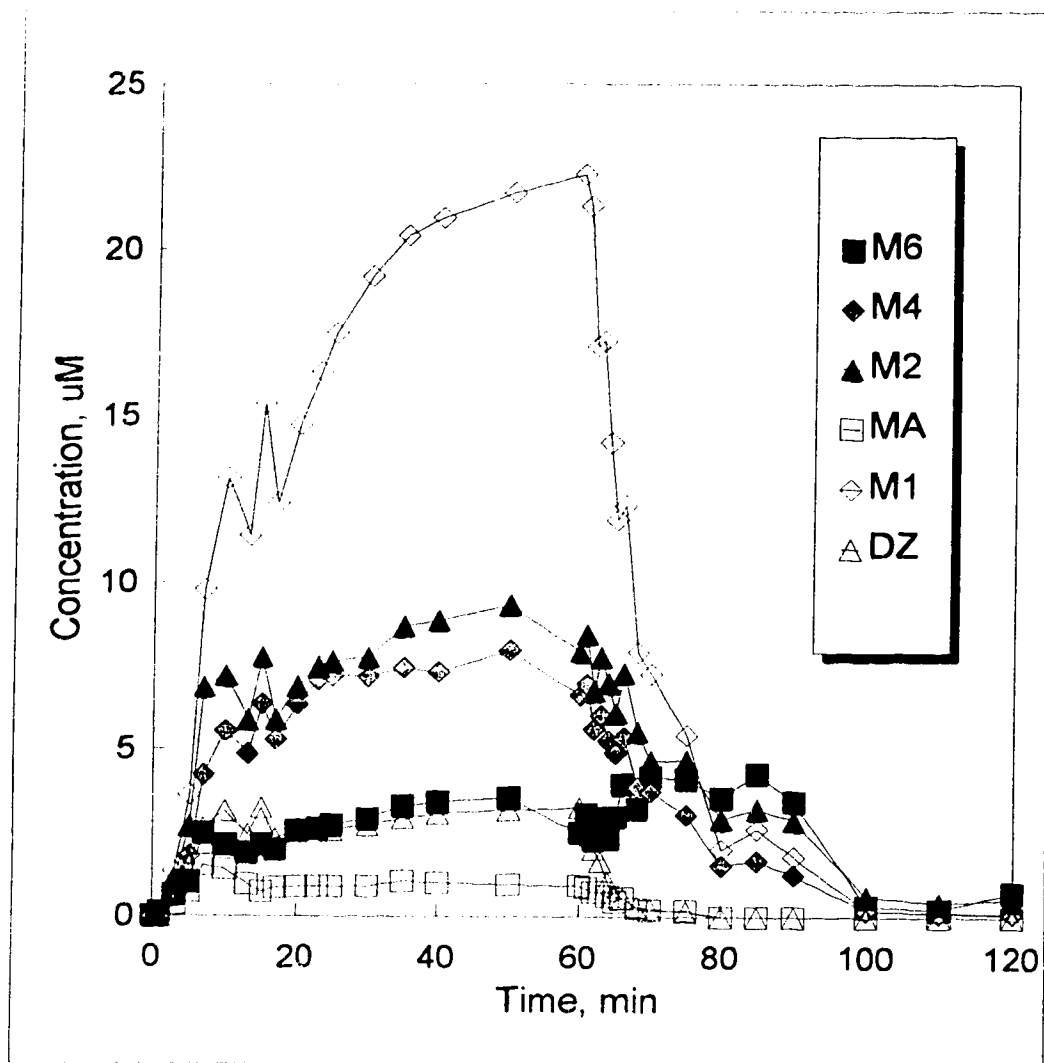


Figure C.7 Outlet concentration of diltiazem and five of its metabolites for Rat #8 obtained by infusing 51.16 μ M diltiazem for 60 minutes followed by a 60 minute washout period.

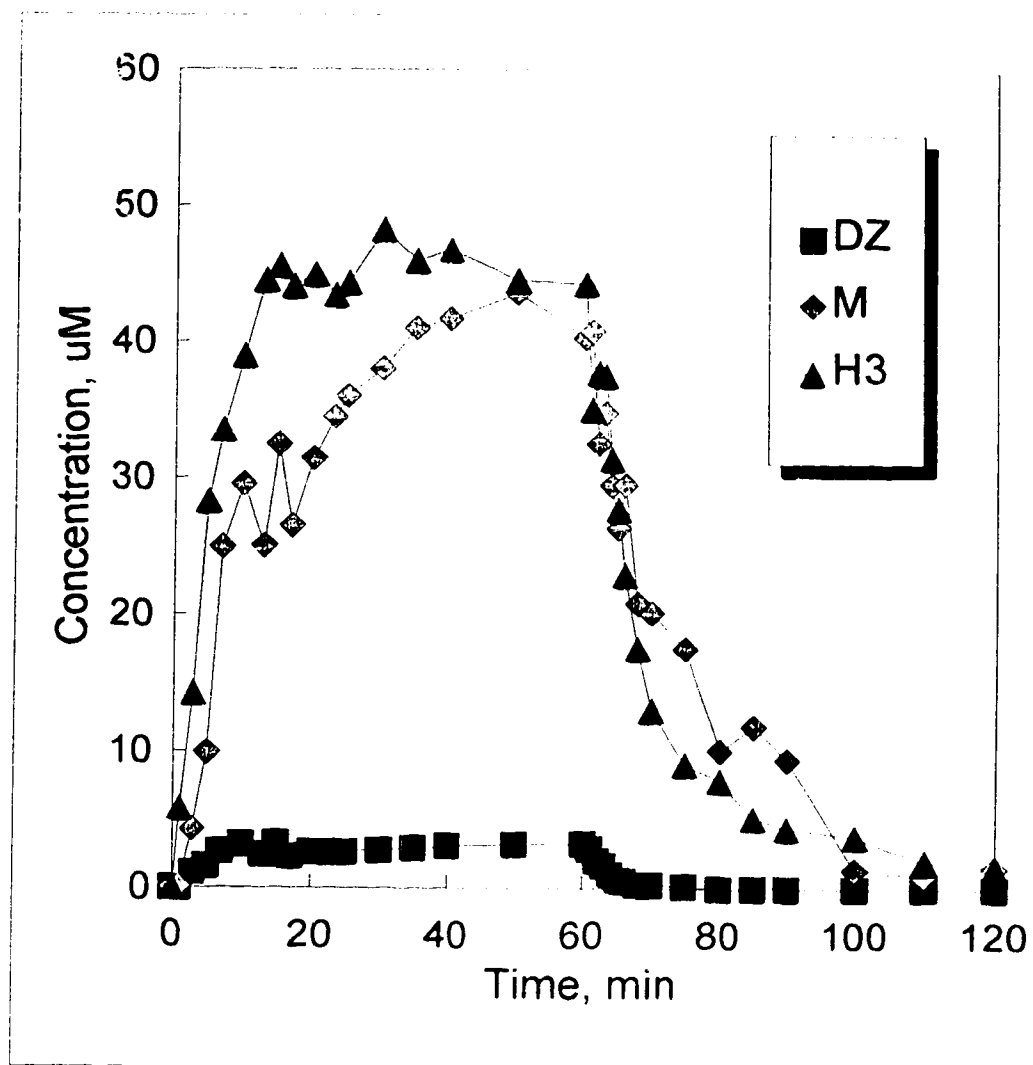


Figure C.8 Outlet concentration of diltiazem, total measured metabolites and radioactive species for Rat #8 obtained by infusing 51.16 μM diltiazem with a radiolabelled tracer for 60 minutes followed by a 60 minute washout period.

Concentration Profiles, uM - Rat 8

Time, min	M6	M4	M2	MA	M1	DZ	H3
0	0	0	0	0	0	0	0
1	0.133124	0	0	0	0	0	5.8222617
3	0.6402624	0.8636048	1.0485188	0.3841106	1.3377589	1.1213078	14.229617
5	1.0345721	1.8003459	2.7052725	0.72595	3.6308091	1.5823079	28.268949
7	2.5110507	4.2427176	6.8794528	1.5325658	9.8092317	2.6580886	33.534278
10	2.1673802	5.5553552	7.2165162	1.4261063	13.148103	3.1646201	38.948123
13	1.911992	4.8564471	5.8782578	0.962739	11.418133	2.4481695	44.466393
15	2.1822256	6.3833839	7.7966858	0.743045	15.361338	3.2683896	45.536166
17	2.021843	5.30119	5.8973491	0.8588565	12.403521	2.3350038	44.062617
20	2.5889045	6.3366245	6.8954602	0.8812131	14.724038	2.622847	44.898015
23	2.6551173	7.0842436	7.4950798	0.9021207	16.334337	2.5751126	43.391978
25	2.7595351	7.200598	7.67161	0.8995912	17.512975	2.5991105	44.303954
30	2.9320834	7.1850379	7.7674657	0.9069029	19.205831	2.7425211	48.234967
35	3.316725	7.4665151	8.7072253	1.0636416	20.433179	2.9480443	45.960827
40	3.4465528	7.3393267	8.8891816	1.0196184	20.963672	3.0982857	46.763738
50	3.5692414	7.9910755	9.3467092	0.9514721	21.721278	3.1987507	44.501201
60	2.5095895	6.6328049	7.9385909	0.9214831	22.28612	3.2712965	44.252902
61	3.0898632	6.9774333	8.4848589	0.859137	21.341153	2.9000534	35.077444
62	2.3109644	5.6267617	6.7709779	0.7382635	17.112974	2.0426399	37.806412
63	2.9930817	6.0270306	7.7927636	0.7463813	17.267937	1.6628118	37.58828
64	2.3561826	5.2660497	7.0190316	0.6126224	14.208288	1.0439959	31.429539
65	3.001866	4.9074421	6.096654	0.4598984	11.910493	0.6183501	27.77003
66	3.9840045	5.3452125	7.3021388	0.5674681	12.335862	0.5529967	22.954888
68	3.2457933	3.8768819	5.5574032	0.2406613	7.9283824	0.3005149	17.554966
70	4.1974747	3.7706549	4.6720529	0.1961706	7.2881534	0.2488244	13.004366
75	4.1255927	3.0583853	4.6819357	0.1962867	5.4351707	0.1632888	9.0803149
80	3.5727223	1.552193	2.9337535	0	2.0217173	0	7.8736285
85	4.3007065	1.6891997	3.2372289	0	2.6264144	0	5.1144938
90	3.4717009	1.2632091	2.8895401	0	1.8100107	0	4.4090463
100	0.3330367	0.2001647	0.6181325	0	0.2194638	0	3.7662538
110	0.2373395	0.1402936	0.434559	0	0.117597	0	1.967827
120	0.7469954	0.1343038	0.5473493	0	0.1149679	0	1.5779745

Table C.6 Experimental data for Rat #8.

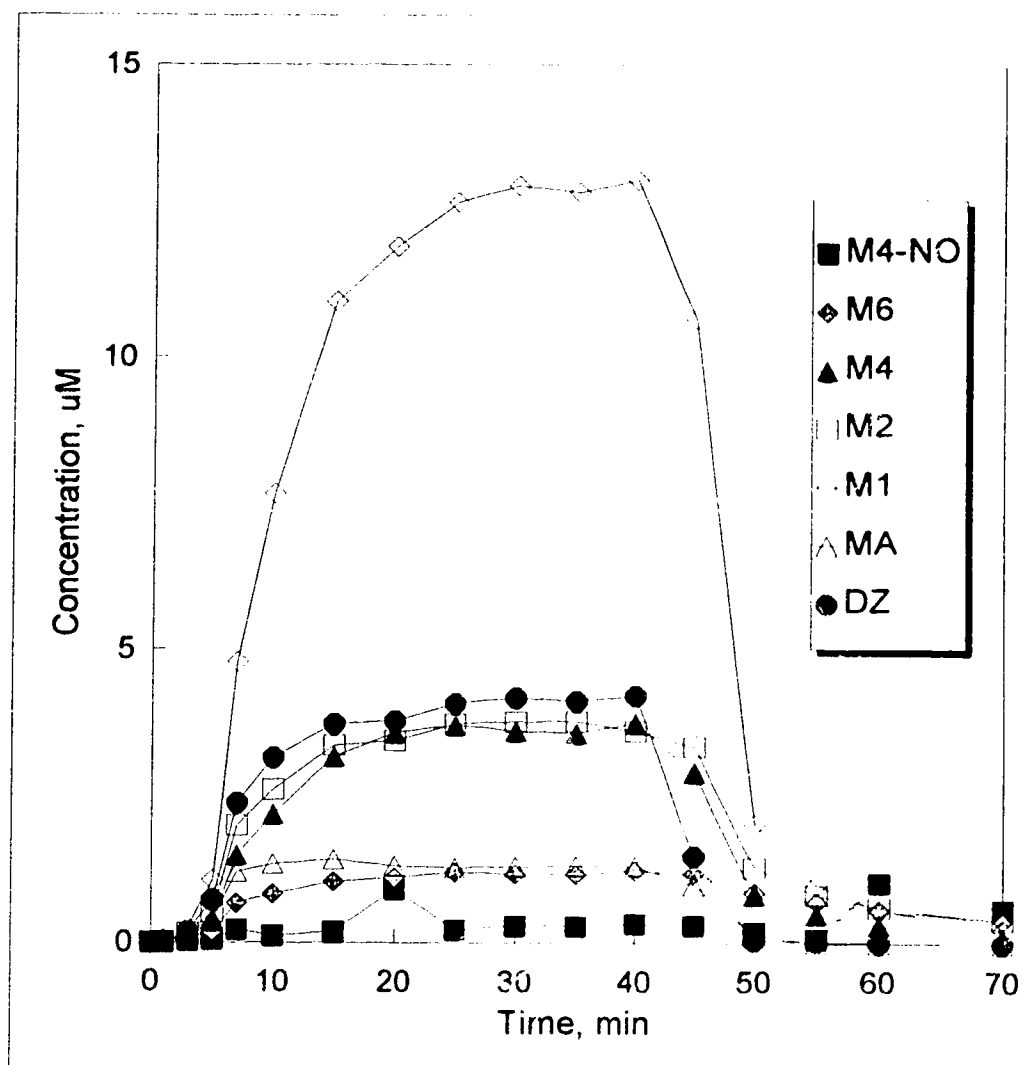


Figure C.9 Outlet concentration of diltiazem and six of its metabolites for Rat #63 obtained by infusing 41.18 μM diltiazem for 40 minutes followed by a 30 minute washout period.

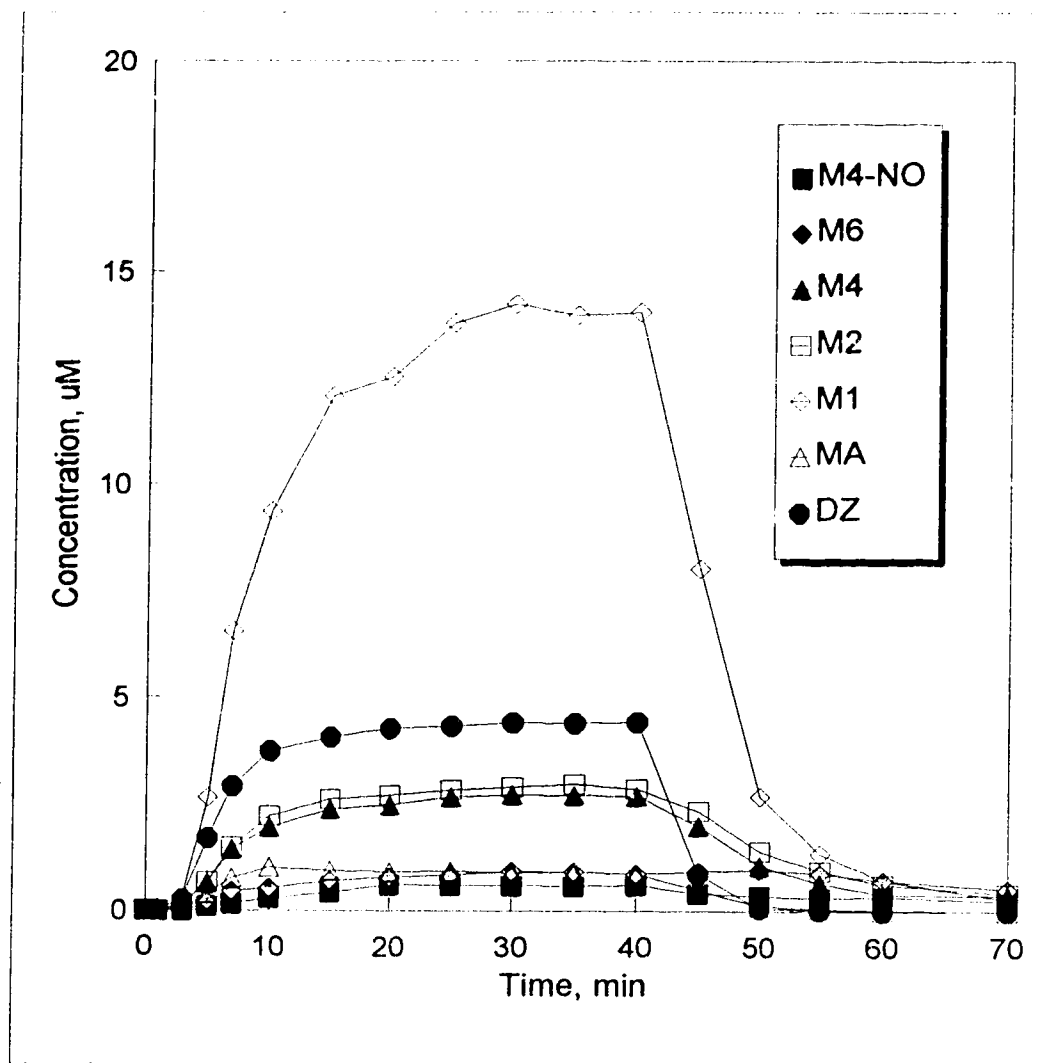


Figure C.10 Outlet concentration of diltiazem and six of its metabolites for Rat #64 obtained by infusing 34.73 μ M diltiazem for 40 minutes followed by a 30 minute washout period.

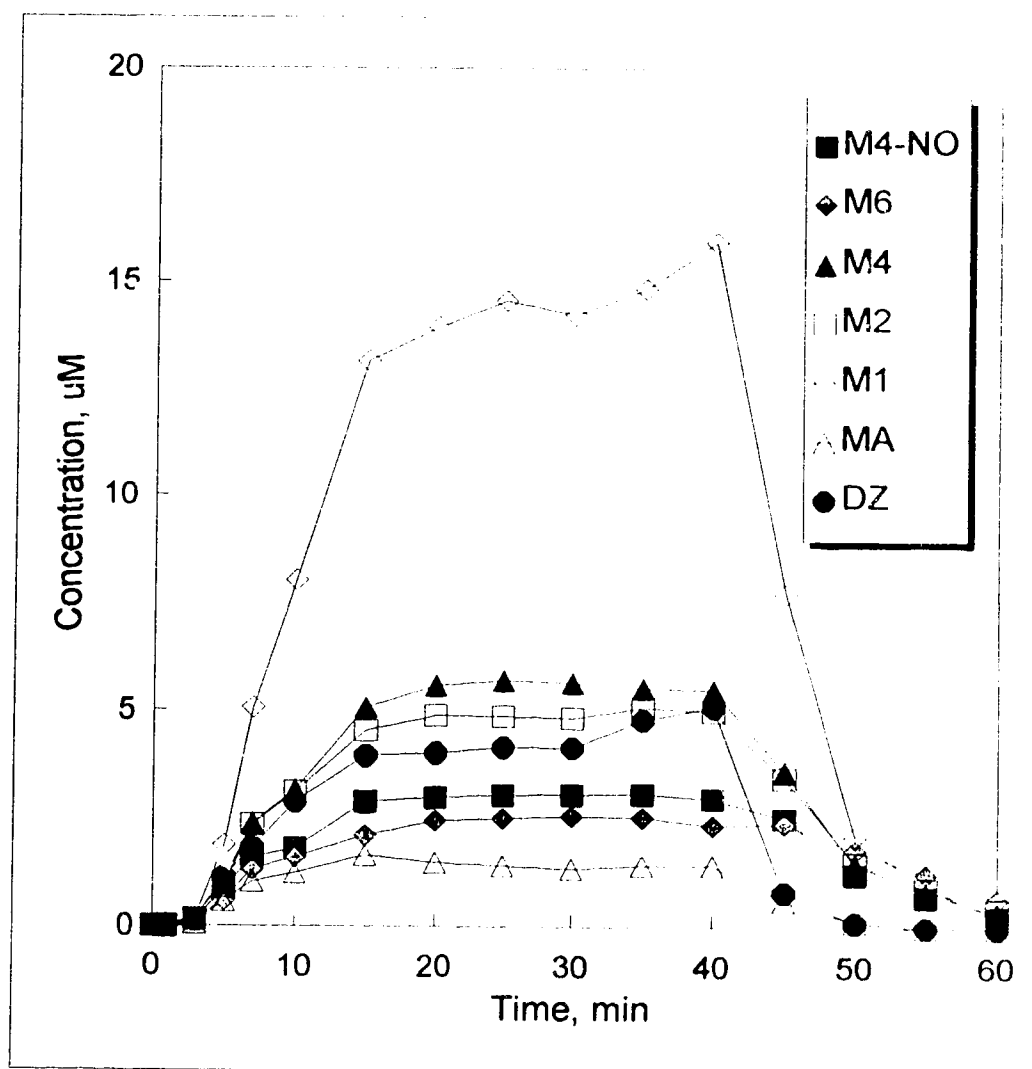


Figure C.11 Outlet concentration of diltiazem and six of its metabolites for Rat #65 obtained by infusing 39.79 μM diltiazem for 40 minutes followed by a 30 minute washout period.

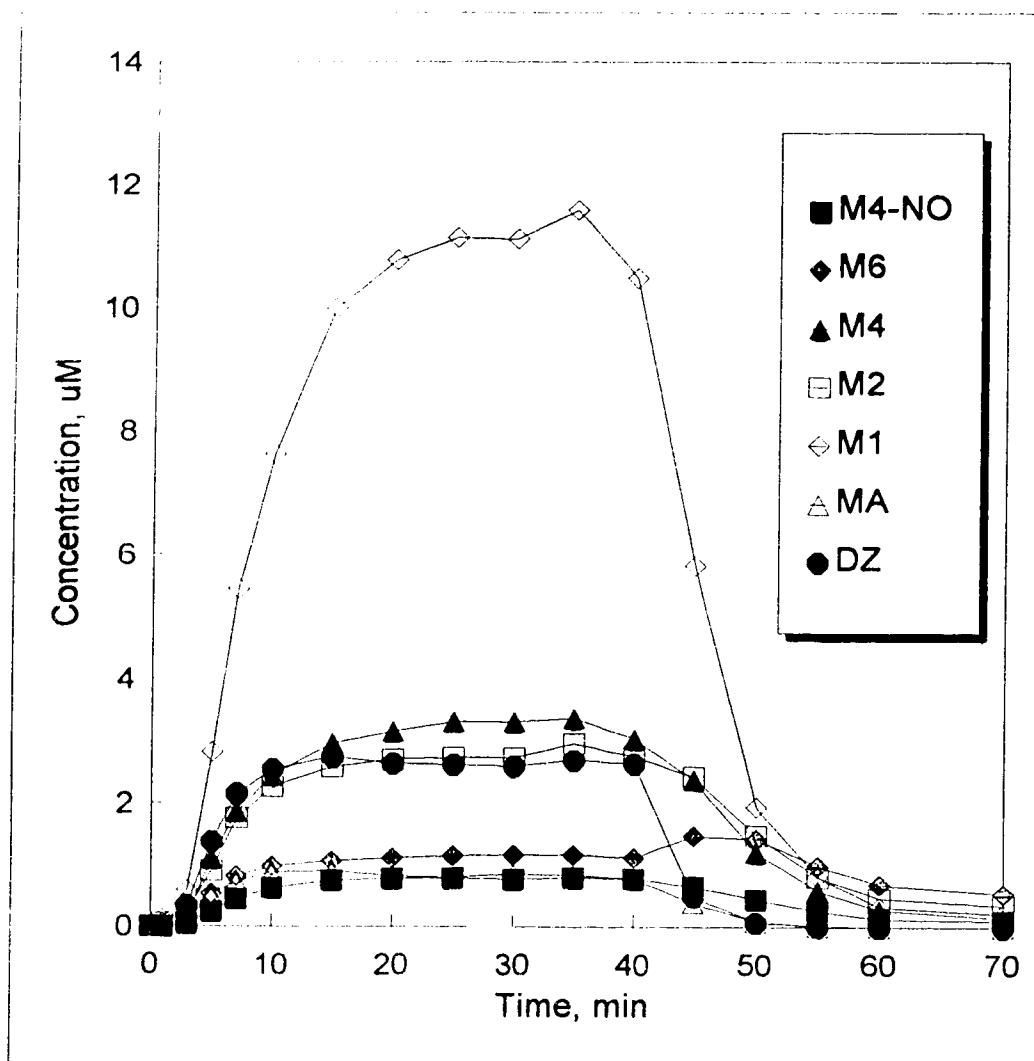


Figure C.12 Outlet concentration of diltiazem and six of its metabolites for Rat #66 obtained by infusing 30.89 μ M diltiazem for 40 minutes followed by a 30 minute washout period.

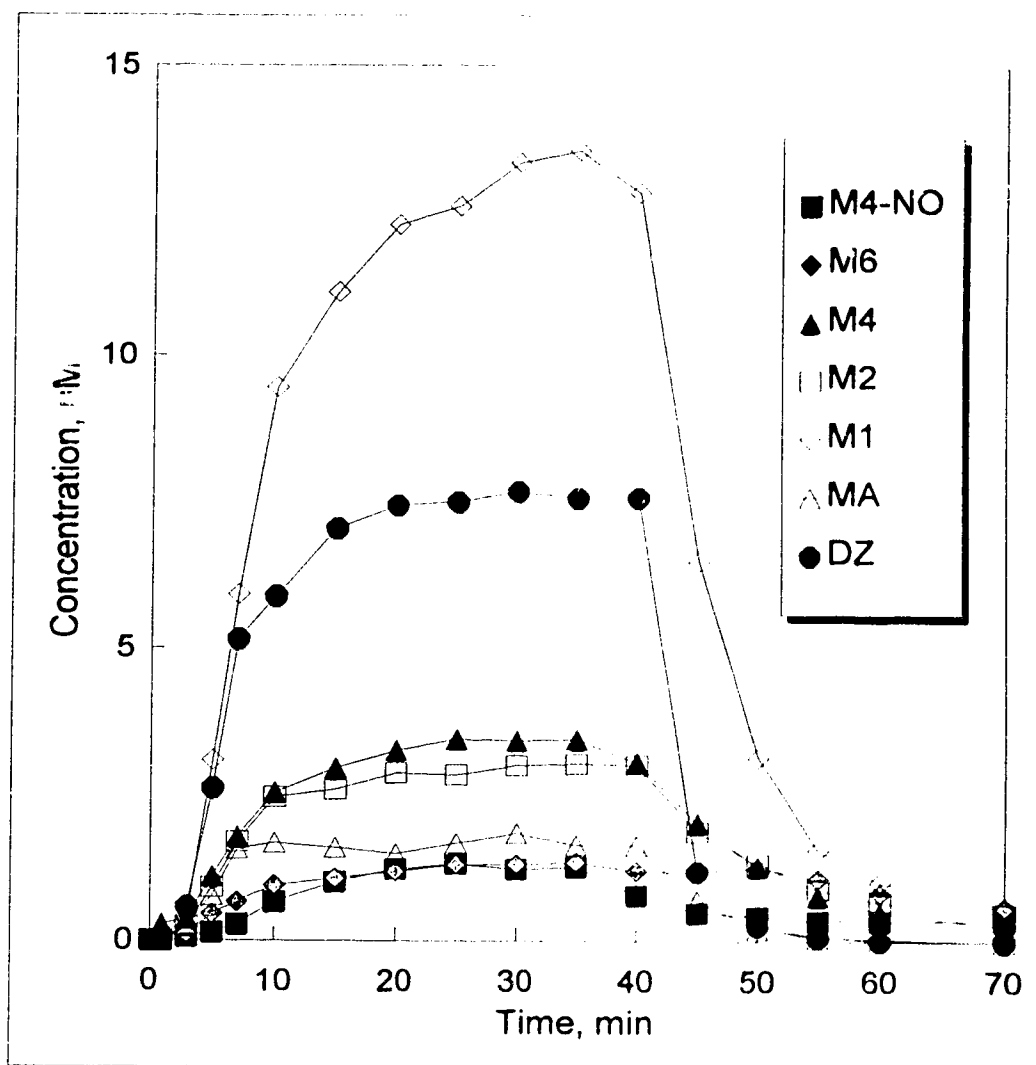


Figure C.13 Outlet concentration of diltiazem and six of its metabolites for Rat #67 obtained by infusing 42.87 µM diltiazem for 40 minutes followed by a 30 minute washout period.

Appendix D - Matlab m-files

The following appendix includes copies of Matlab m-files used to complete the computer model simulations. Below is listed the file names and a brief description of the use of each file.

File	Use	Page
simp.m	File to define parameters to manipulate by Simplex algorithm.	90
fun.m	File to define the sum of squared residuals as the function to minimize by the Simplex algorithm. This calculation requires the numerical integration of the model equations using the GEAR method.	91
fsimp3in.m	File to define the equations describing the drug influx portion of the experimental data.	92
fsimp3out.m	File to define the equations describing the drug washout portion of the experimental data.	93

```

% Tina Larson
% Estimation of parameters from Influx and washout data (Rat #7)
% July 14, 1994
% Matlab GEAR main file and SSR Minimization

function f=fun(x);
global Cin; global tin; global Cout; global tout;
global Dzin; global Dzout; global Min; global Mout; global stin; global stout;
global k1Dz; global k1Dz2; global V1; global V2; global Q; global k12M;
global k13; global k31; global nsat; global n; global Cfeed;
global k5M; global k21M; global kMDz; global Cin;
global n; global l; global SSRDZin; global SSRDZout; global SSRDZ;
global SSRMin; global SSRMout; global SSRM; global SSRtot;
global V1; global V2; global Q; global Cfeed;
k1Dz=x(1);
k1Dz2=x(2);
k12M=x(3);
k21M=x(4);
k13=x(5);
k31=x(6);
nsat=x(7);
kMDZ=x(8);
k5M=x(9);
t0=0.0;
tf=60.0;
CO=[0 0 0 0 0];
[cin,Cin]=gear('fsimp3in',[t0 tf],CO);
n=0; i=0;
n=length(cin)
t0=60.0;
tf=120.0;
CO=[Cin(n,1),Cin(n,2),Cin(n,3),Cin(n,4),Cin(n,5),Cin(n,6)];
[cout,Cout]=gear('fsimp3out',[t0 tf],CO);
l=length(cout)
stin=[0 1 3 5 7 10 13 15 17 20 23 25 30 35 40 50 60];
stout=[60 61 62 63 64 65 66 68 70 75 80 85 90 100 110 120];
Dzin=[0 0 0.5858 1.345 1.475 2.002 2.151 2.301 2.786 2.212 2.505 2.130 2.136 2.502 2.354 3.246 2.683];
Dzout=[12.683 2.383 1.424 0.7034 0.5221 0.3579 0.2985 0.1639 0.1291 0 0 0 0 0];
Cout=[0 0.2002 3.075 9.1547 13.11 18.05 22.72 25.06 32.36 28.19 29.65 26.27 26.69 33.23 32.01 43.86 37.98];
Mout=[37.98 37.80 39.11 39.86 26.05 30.39 21.56 8.980 8.460 5.868 4.425 3.172 2.686 2.517 1.451 1.853];
Cout=interp(cin,Cin(lin,1),stin);
Cout=interp(cout,Cout(lin,1),stout);
resDzin=Cout-Dzin;
resDzout=Cout-Dzout;
SSRDZin=resDzin*resDzin;
SSRDZout=resDzout*resDzout;
SSRDZ=SSRDZin+SSRDZout;
Cline=interp(cin,Cin(lin,4),stin);
Cline=interp(cout,Cout(lin,4),stout);
resM=Cline-Min;
resMout=Cline-Mout;
SSRM=resM*resM;
SSRMout=resMout*resMout;
SSRM=SSRM+SSRMout;
SSRC=SSRDZ+SSRM;
f=SSRC;
end

```

```

%
% Tina Larson
%
% Simplex minimization of SSR for parameters using influx
% and washout data (Rat #7T).
% July 14, 1994
% Simplex main file.
%
Global Cin; Global tin; Global Cout; Global tout;
Global Dzin; Global stin; Global DZout; Global scout; Global Min; Global Mout;
Global n; Global l; Global Q; Global Creed; Global V1; Global V2;
Global k3; Global nsat; Global k12Dz; Global k21Dz; Global k13; Global kmDz;
Global k1M; Global k12M; Global k21M;
Global SSRin; Global SSRout; Global SSR;
V1=0.15*11.8;
V2=0.85*11.8;
Creed=37.71;
Q=27.5;
x(1)=1650;
x(2)=1.5;
x(3)=800;
x(4)=12;
x(5)=9.2;
x(6)=50;
x(7)=1600;
x(8)=0.24;
x(9)=0.24;
x=fmins('fun',x);
k12Dz=x(1)
k21Dz=x(2)
k12M=x(3)
k21M=x(4)
k13=x(5)
k31=x(6)
nsat=x(7)
kmDz=x(8)
k1M=x(9)
KpDz=(k12Dz*V1)/(k21Dz*V2)
KpM=(k12M*V1)/(k21M*V2)
plot (tin,Cin(1:n,1),'-',tin,Cin(1:n,4),'--',tout,Cout(1:1,1),'-',tout,Cout(1:1,4),'--',stin,Dzin,'x',stin
'Min','*',stout,DZout,'x',scout,Mout,'*')
title ('Influx/Washout Curve for Minimized Function.')
xlabel ('Time, min')
ylabel ('Concentration, umol/L')
print simp3-grp
end

```


Appendix E - Simulation Results

	Page
Figure E.1 Experimental (x) and simulated (—) concentration profiles for diltiazem and experimental (*) and simulated (- -) concentration profiles for total metabolites in the effluent of an isolated liver from Rat #5 with inlet diltiazem concentration of 11.59 μ M.	96
Figure E.2 Experimental (x) and simulated (—) concentration profiles for diltiazem and experimental (*) and simulated (- -) concentration profiles for total metabolites in the effluent of an isolated liver from Rat #6 with inlet diltiazem concentration of 12.05 μ M.	97
Figure E.3 Experimental (x) and simulated (—) concentration profiles for diltiazem and experimental (*) and simulated (- -) concentration profiles for total metabolites in the effluent of an isolated liver from Rat #8 with inlet diltiazem concentration of 51.16 μ M.	98
Figure E.4 Experimental (x) and simulated (—) concentration profiles for diltiazem and experimental (*) and simulated (- -) concentration profiles for total metabolites in the effluent of an isolated liver from Rat #63 with inlet diltiazem concentration of 41.18 μ M. Experimental data taken from Hussain et al. (1994).	99
Figure E.5 Experimental (x) and simulated (—) concentration profiles for diltiazem and experimental (*) and simulated (- -) concentration profiles for total metabolites in the effluent of an isolated liver from Rat #64 with inlet diltiazem concentration of 34.73 μ M. Experimental data taken from Hussain et al. (1994).	100
Figure E.6 Experimental (x) and simulated (—) concentration profiles for diltiazem and experimental (*) and simulated (- -) concentration profiles for total metabolites in the effluent of an isolated liver from Rat #65 with inlet diltiazem concentration of 39.79 μ M. Experimental data taken from Hussain et al. (1994).	101

	Page
Figure E.7 Experimental (x) and simulated (—) concentration profiles for diltiazem and experimental (*) and simulated (- -) concentration profiles for total metabolites in the effluent of an isolated liver from Rat #66 with inlet diltiazem concentration of 30.89 μ M. Experimental data taken from Hussain et al. (1994).	102
Figure E.8 Experimental (x) and simulated (—) concentration profiles for diltiazem and experimental (*) and simulated (- -) concentration profiles for total metabolites in the effluent of an isolated liver from Rat #67 with inlet diltiazem concentration of 42.87 μ M. Experimental data taken from Hussain et al. (1994).	103

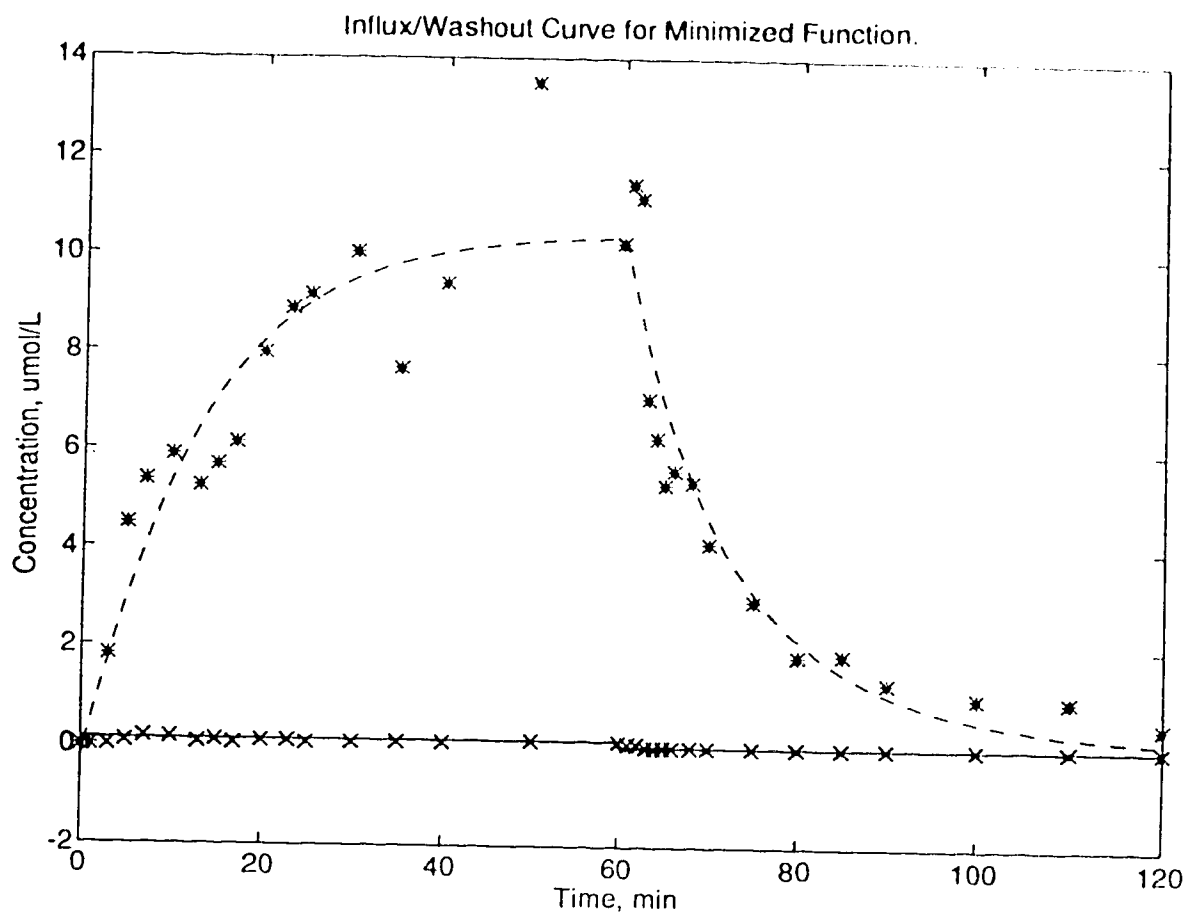


Figure E.1 Experimental (x) and simulated (—) concentration profiles for diltiazem and experimental (*) and simulated (- -) concentration profiles for total metabolites in the effluent of an isolated liver from Rat #5 with inlet diltiazem concentration of 11.59 μM .

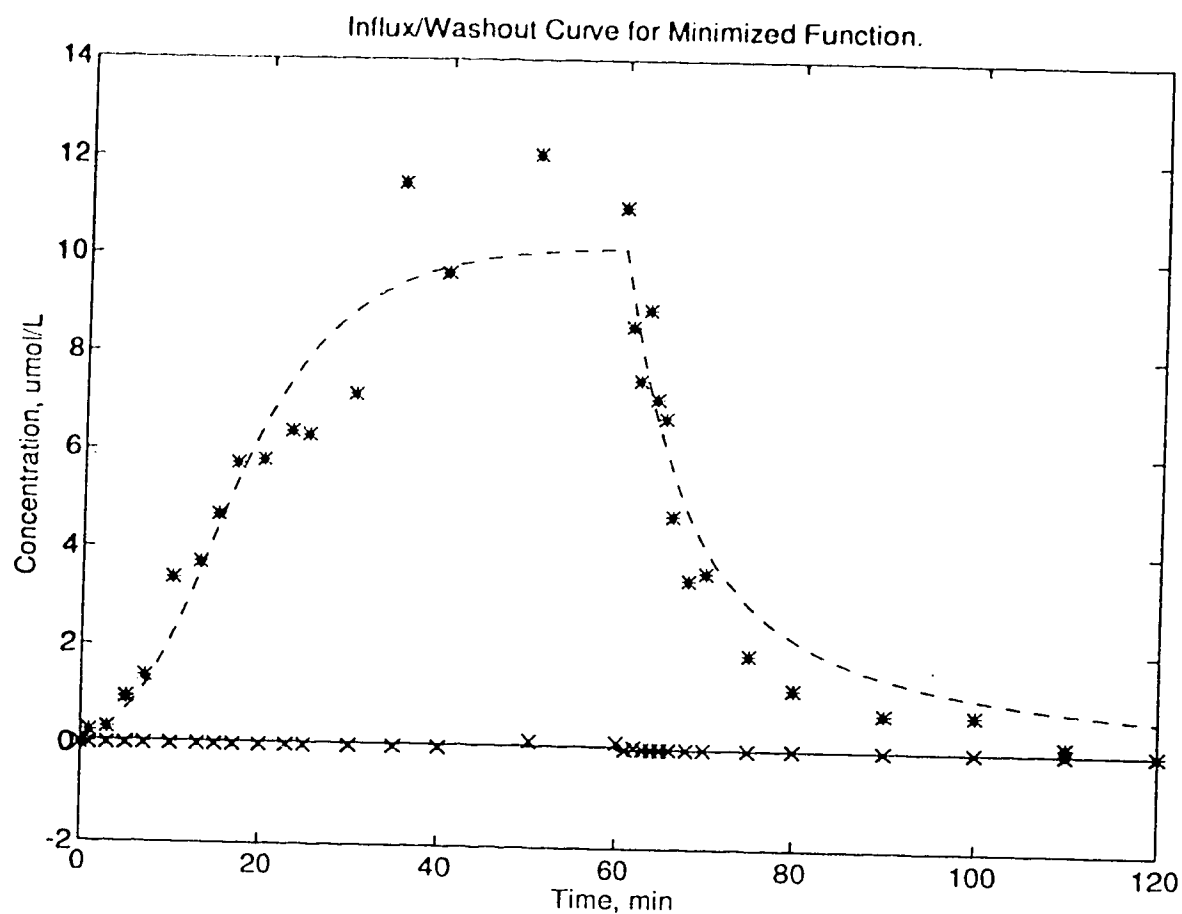


Figure E.2 Experimental (x) and simulated (—) concentration profiles for diltiazem and experimental (*) and simulated (- -) concentration profiles for total metabolites in the effluent of an isolated liver from Rat #6 with inlet diltiazem concentration of 12.05 μM .

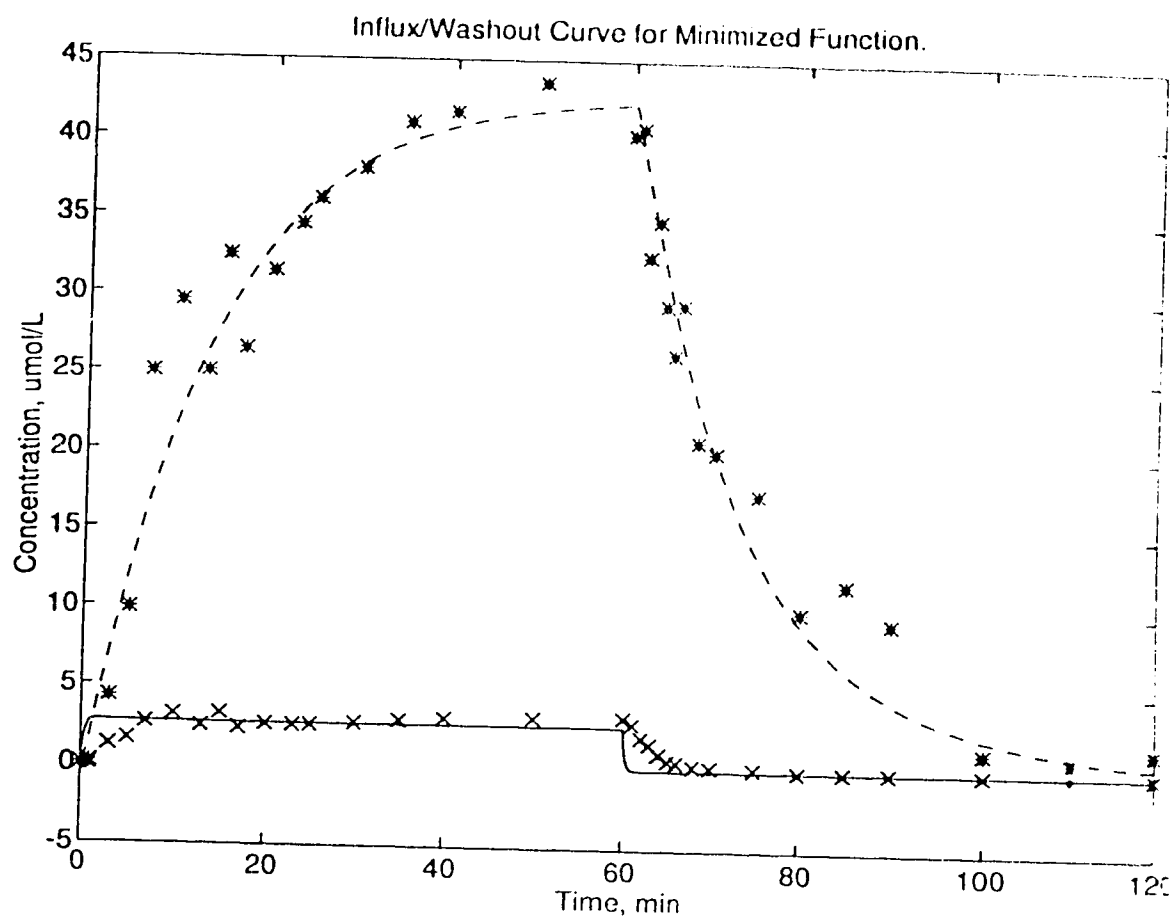


Figure E.3 Experimental (x) and simulated (—) concentration profiles for diltiazem and experimental (*) and simulated (- -) concentration profiles for total metabolites in the effluent of an isolated liver from Rat #8 with inlet diltiazem concentration of 51.16 μM .

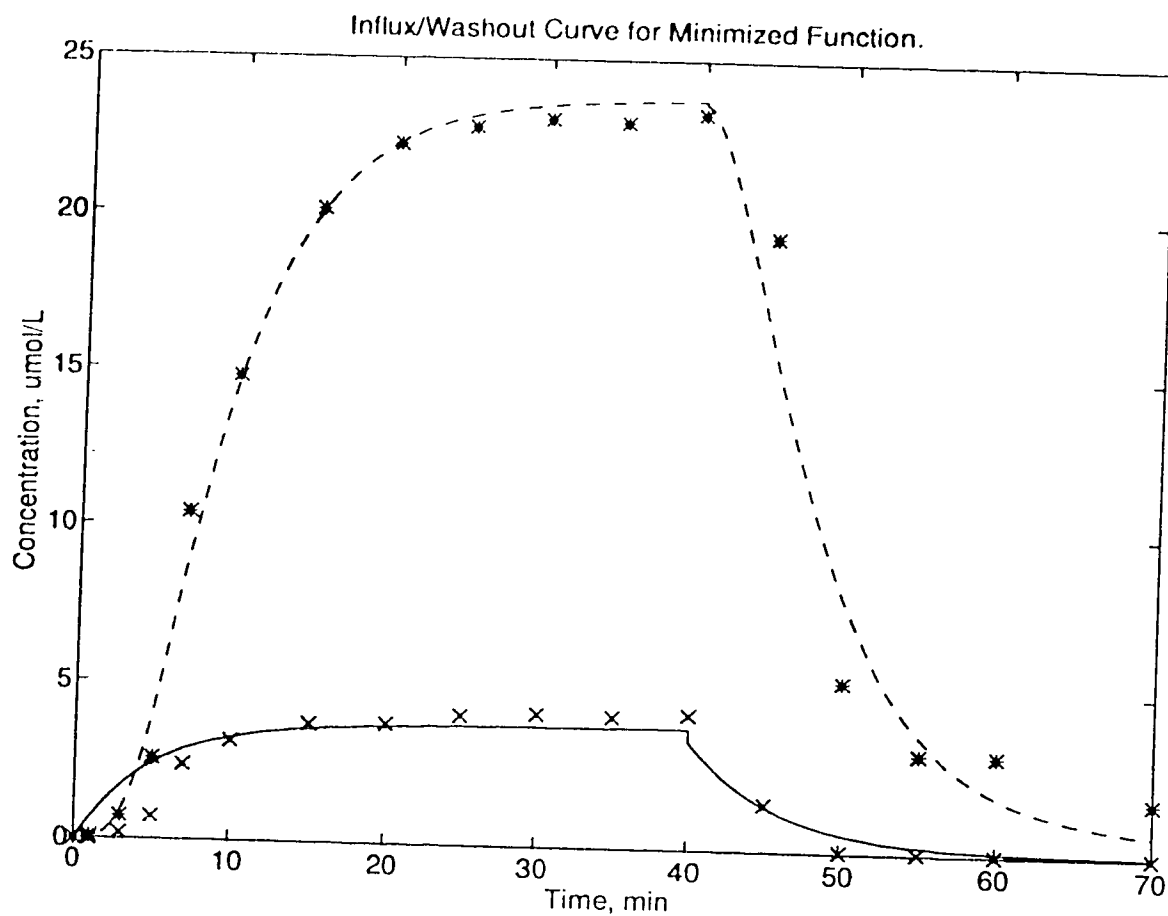


Figure E.4 Experimental (x) and simulated (—) concentration profiles for diltiazem and experimental (*) and simulated (- -) concentration profiles for total metabolites in the effluent of an isolated liver from Rat #63 with inlet diltiazem concentration of 41.18 μM . Experimental data taken from Hussain et al. (1994).

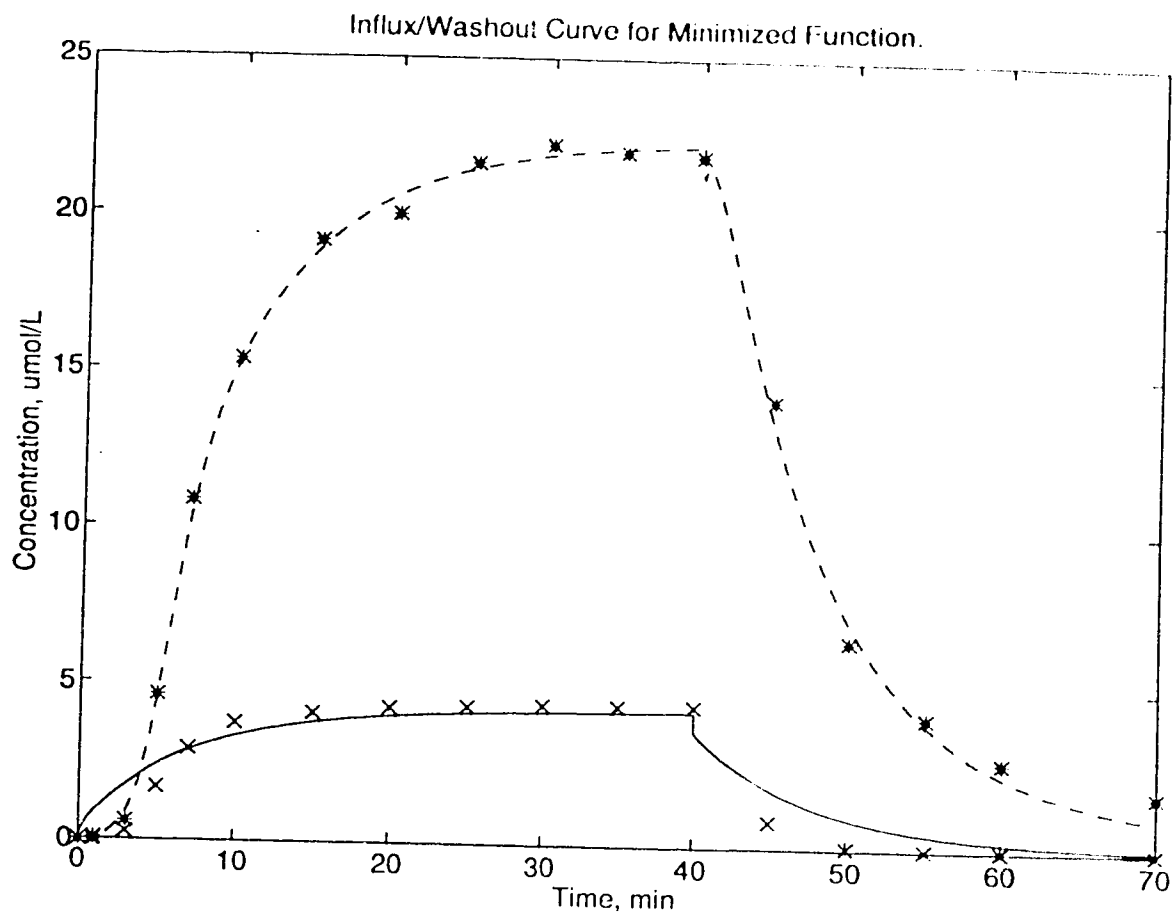


Figure E.5 Experimental (x) and simulated (—) concentration profiles for diltiazem and experimental (*) and simulated (- -) concentration profiles for total metabolites in the effluent of an isolated liver from Rat #64 with inlet diltiazem concentration of 34.73 μ M. Experimental data taken from Hussain et al. (1994).

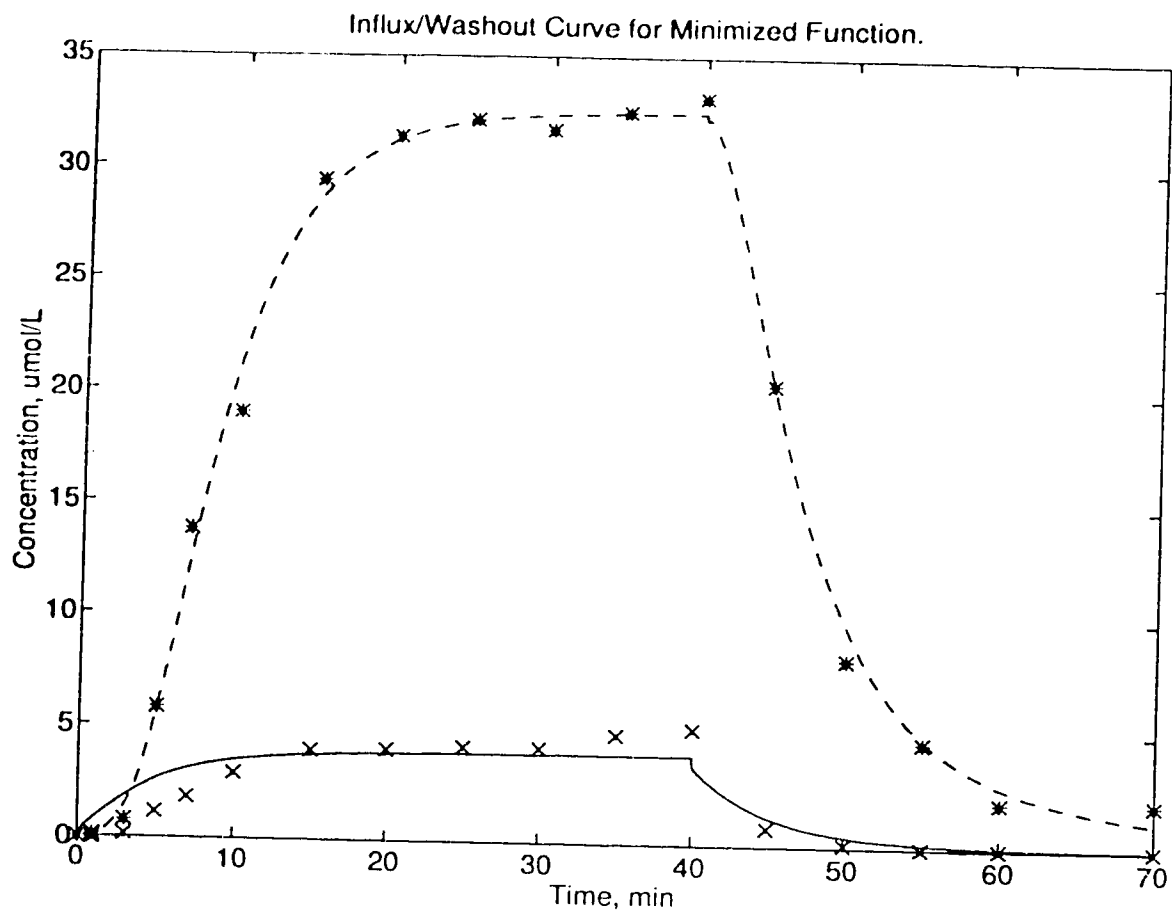


Figure E.6 Experimental (x) and simulated (—) concentration profiles for diltiazem and experimental (*) and simulated (- -) concentration profiles for total metabolites in the effluent of an isolated liver from Rat #65 with inlet diltiazem concentration of 39.79 μM . Experimental data taken from Hussain et al. (1994).

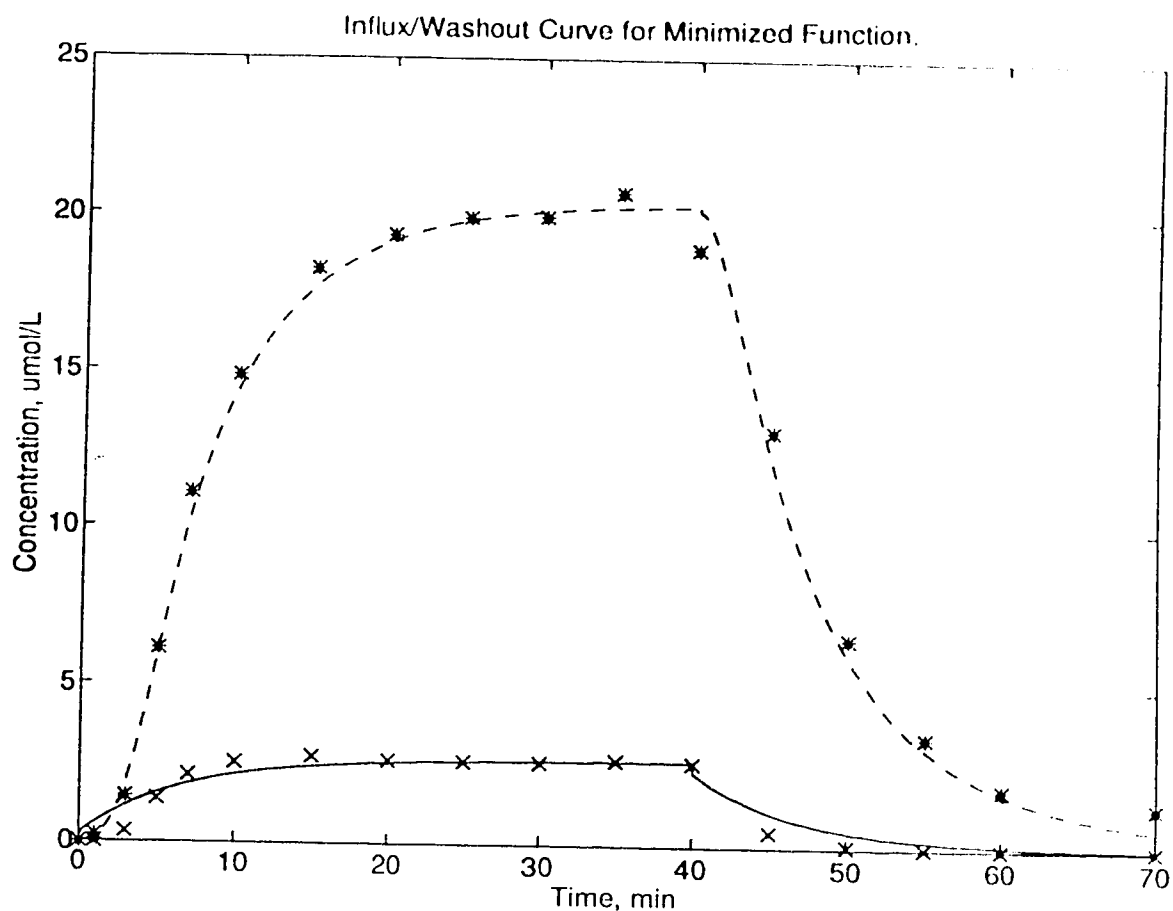


Figure E.7 Experimental (x) and simulated (—) concentration profiles for diltiazem and experimental (*) and simulated (- -) concentration profiles for total metabolites in the effluent of an isolated liver from Rat #66 with inlet diltiazem concentration of 30.89 μM . Experimental data taken from Hussain et al. (1994).

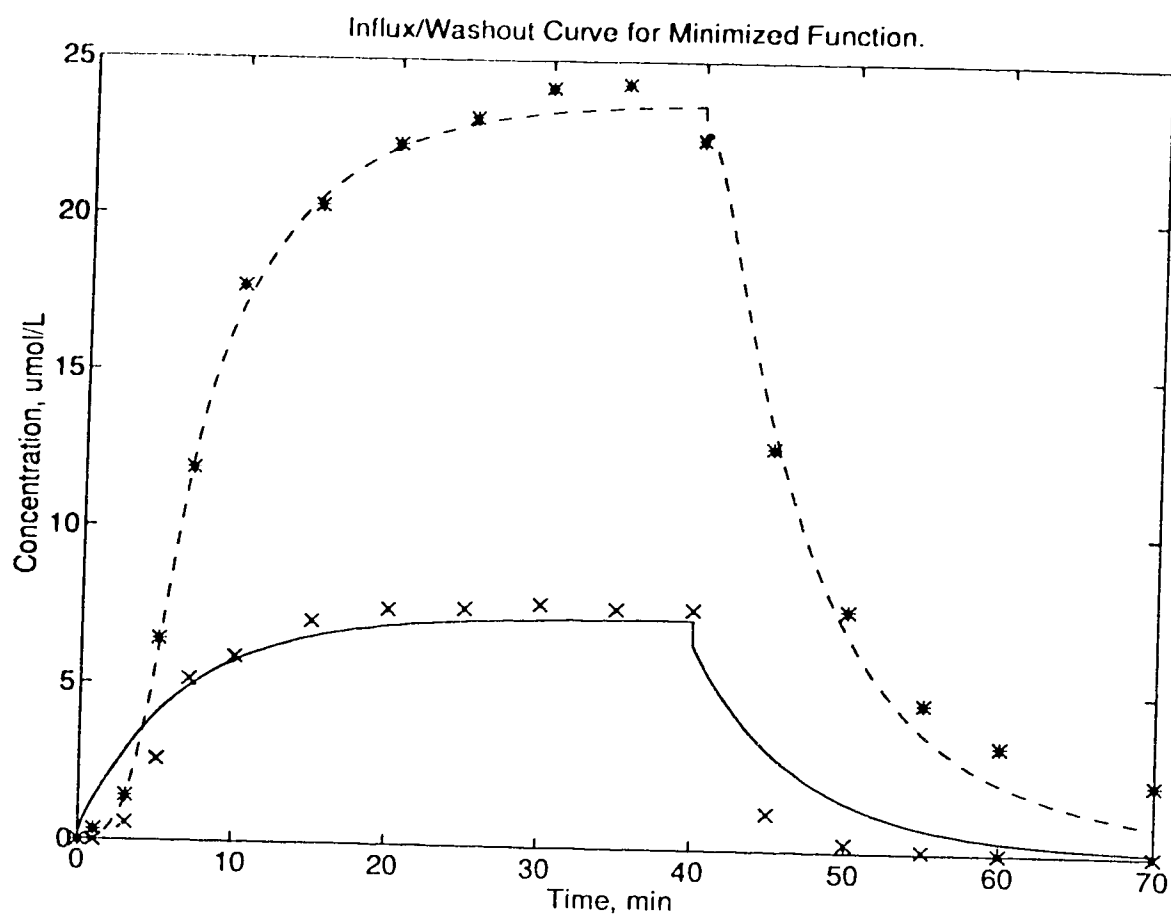


Figure E.8 Experimental (x) and simulated (—) concentration profiles for diltiazem and experimental (*) and simulated (- -) concentration profiles for total metabolites in the effluent of an isolated liver from Rat #67 with inlet diltiazem concentration of $42.87 \mu\text{M}$. Experimental data taken from Hussain et al. (1994).